NEUROMECHANICS OF LOCOMOTION: INSIGHTS FROM THE WALK-TO-RUN TRANSITION IN AMPUTEES AND PEDALING IN ABLE-BODIED INDIVIDUALS

A Thesis
Presented to
The Academic Faculty

by

Tracy Lynn Norman

In Partial Fulfillment
of the Requirements for the Degree
Doctor of Philosophy in the
School of Applied Physiology

Georgia Institute of Technology
December 2015
Copyright © Tracy L. Norman 2015

NEUROMECHANICS OF LOCOMOTION: INSIGHTS FROM THE WALK-TO-RUN TRANSITION IN AMPUTEES AND PEDALING IN ABLE-BODIED INDIVIDUALS

Approved by:

Professor Young-Hui Chang, Advisor
School of Applied Physiology
Georgia Institute of Technology

Professor Mindy L. Millard-Stafford
School of Applied Physiology
Georgia Institute of Technology

Professor T. Richard Nichols
School of Applied Physiology
Georgia Institute of Technology

Professor Richard R. Neptune
Cockrell School of Engineering
University of Texas at Austin

Professor Boris I. Prilutsky
School of Applied Physiology
Georgia Institute of Technology

Date Approved: October 14, 2015

ACKNOWLEDGEMENTS

I would like to thank my lab mates, committee members (official and honorary), friends and family for all of their advice and support throughout this process. I would also like to especially thank my husband Shawn K. Giest for his unwavering love and encouragement.

TABLE OF CONTENTS

LIST OF TABLES

LIST OF FIGURES

SUMMARY

Afferent feedback is important for modulating locomotion and maintaining stability. Studying locomotor extremes and applying perturbations to normal locomotion allows us to probe the effects of afferent feedback on the control of normal gait. Investigating the walk-to-run gait transition specifically provides a unique locomotor event to investigate the fundamental determinants of legged locomotion (walking or running) and identify the sensory inputs important to the ongoing neuromuscular control of walking and running.

The first goal of this dissertation was to investigate the contributions of plantarflexor muscles during stance (Aim 1) and flexor muscles during swing (Aim 2) to the walk-to-run transition. To accomplish this I used unilateral, transtibial amputee subjects as a means to assess the affects of unilaterally eliminating plantarflexor propulsive force production and below-knee flexor activation on the walk-to-run transition speed. The main objective of Aim 1 was to determine the preferred gait transition speeds of unilateral, transtibial amputee subjects, and the influence of kinetics on the walk-to-run gait transition speed. Unilateral, transtibial amputee subjects transition between gaits at a lower speed than able-bodied controls and are still able to generate higher propulsive forces walking at speeds above their preferred gait transition speed. This finding indicates that their walk-to-run transition is not likely dictated by the force-length-velocity characteristics of the intact plantarflexor muscles. Thus, as an experimental model, unilateral, transtibial amputee subjects can provide unique insights for decoupling the previously identified performance limit of plantarflexor muscles from the preferred gait transition speed in order to probe other

potential determinants. The main objective of Aim 2 was to quantify the muscle activation during walking and running gaits relative to the walk-to-run gait transition speed for unilateral, transtibial amputee subjects. The swing phase tibialis anterior muscle activation is a major determinant of the walk-to-run transitions in unilateral, transtibial amputee subjects. Swing phase dorsiflexion moments alone do not explain these results and additional work is necessary to probe potential mechanical and neural explanations. Furthermore, in unilateral, transtibial amputee subjects, swing-phase rectus femoris and biceps femoris long head activations and their respective joint moments are a function of changes in absolute speed and thus not indicative of their significantly lower gait transition speed.

The second goal of this dissertation was to probe the potential contributions of afferent feedback to the underlying neuromuscular mechanism ultimately responsible for the transition (Aim 3). The main objective of Aim 3 was to evaluate the effects of contralateral sensory loss on the motor output of the ipsilateral leg. Unilateral below-knee, ischemic deafferentation has significant effects on both inter- and intralimb motor output. The net effect of contralateral sensory loss below the knee is a significant decrease in ipsilateral flexor muscle activations during the transition from flexion to extension in pedaling (Q1). Due to the rapid time course of these responses, I speculate either i) contralateral below-knee afferents (most likely Ia and/or cutaneous) have a net excitatory effect on the ipsilateral flexor muscles or ii) contralateral above knee afferents (most likely Ib) have an inhibitory effect on the ipsilateral flexor muscles.

CHAPTER I

INTRODUCTION

Human locomotion is an incredibly complex task requiring the integration of descending control and afferent signals, in conjunction with intra- and interlimb coordination. The largely noninvasive nature of human locomotion control studies presents challenges from a methodological and analysis perspective. However, investigating the underlying control processes that govern locomotion in humans are paramount to our basic understanding of the neuromuscular control of gait. Two components modulating the underlying control of gait are sensory feedback (Hayes et al., 2012; Pearson, 2004) and interlimb coordination (Alibiglou et al., 2009; Stevenson et al., 2013; Ting et al., 2000). However, what type of sensory feedback is involved, and to what functional effect is not well understood.

Current gait rehabilitation strategies often focus on regaining symmetry between the limbs (Hassid et al., 1997; Hesse et al., 2013; Mauritz, 2002). Yet, we cannot appropriately strategize how to achieve symmetry in a system if we do not understand the inherent interlimb coordination strategies of said system. Furthermore, it remains to be seen if this is even the best strategy in rehabilitation. This is particularly pertinent to pathologies that manifest with unilateral deficits, such as in hemiparesis resulting from stroke, cerebral palsy, and spinal cord injury, as well as musculoskeletal trauma, such as transtibial amputation. Improving our understanding of the neuromuscular control of gait is necessary to significantly advance rehabilitation practices and assistive devices for ambulation. Recent advances in powered exoskeletons and prostheses as well as myoelectric device control are promising (Herr and Grabowski, 2012; Takahashi et al., 2015). However to increase the robustness of these systems

(i.e. across gaits and speeds) and most efficiently and effectively integrate with users we must understand the neuromuscular control of gait.

Walking and running are the most common forms of locomotion in humans, each with distinct kinematic and muscle activation patterns characteristic of the dynamics for each gait (Novacheck, 1998). At a spinal level the walk-to-run transition is most likely the result of either a change in the activation state of the same central pattern generators (a single motor program) (Cappellini et al., 2006; Labini et al., 2011; Yakovenko et al., 2005) or a switch between gait-specific central pattern generators (from one motor program to another) (Collins, 2003; Shapiro et al., 1981). Thus, the walk-to-run transition provides a unique locomotor event to investigate the fundamental determinants of legged locomotion (walking or running) and identify the sensory inputs important to the ongoing neuromuscular control of walking and running. However, the ultimate cause of the walk-to-run transition is still contested. Two leading and opposing views have emerged concerning the major determinant of the walk-to-run transition: 1. Extensor hypothesis: propulsive force production by the legs is limited by the force-length-velocity properties of ankle plantarflexors (Arnold et al., 2013; Farris and Sawicki, 2012; Neptune and Sasaki, 2005); 2. Flexor hypothesis: a sensory threshold of perceived exertion is reached when flexor muscles in the leg reach a critical level of activation during swing (Ivanenko et al., 2008; Prilutsky and Gregor, 2001) or early stance (Malcolm et al., 2009b). The aforementioned two views are not necessarily mutually exclusive, and require further investigation in terms of kinetics and muscle activations via both intra- and interlimb analysis.

The goal of this dissertation is to investigate the contributions of plantarflexor muscles during stance and flexor muscles during swing to the walk-to-run transition and probe the potential contributions of afferent feedback to the underlying neuromuscular mechanism ultimately responsible for the transition. In order to accomplish this

I employed a bipartite approach. First I sought to identify the kinetic and neuromuscular determinants of the walk-to-run transition in unilateral, transtibial, amputee subjects in comparison to able-bodied subjects (Aims 1 & 2). To my knowledge, previous gait transition studies have never imposed a unilateral perturbation, and most have focused analyses on one leg ipsilaterally. Second I investigated the likelihood of a potential underlying neuromuscular mechanism responsible for the walk-to-run transition. Specifically whether an imbalance in stance phase extensor afferent feedback and swing phase flexor muscle activations between legs at high walking speeds could be due to decreased force feedback at high walking speeds (Aim 3). This was addressed via manipulation of sensory feedback during a novel cycling paradigm in able-bodied subjects.

1.1 The walk-to-run transition

The walk-to-run transition has been investigated for nearly eight decades (Margaria, 1938). Over the years, many theories about the mechanisms responsible for this transition have evolved, which ultimately can be organized into three overarching categories: i. energetics, ii. dynamics, and iii. neuromuscular. Currently, there is significant support for the idea that some type of stress during higher than preferred walking speeds initiates the transition from walking to running in order to alleviate stress.

Most often in gait transition research, investigators are seeking to identify triggers or determinants of said transition. These words have different connotations, however are often used interchangeably in the literature. For the purposes of this thesis a trigger of the gait transition refers to the ultimate underlying mechanism responsible for the walk-to-run transition, while a determinant is any input that can significantly influence the action of the mechanism (i.e. alter the walk-to-run transition speed).

1.1.1 Energetics

Both humans and horses have been shown to prefer gaits at particular speeds in order to minimize energy expenditure or cost of transport (the amount of energy needed in order to move a unit of weight a unit of distance) (Falls and Humphrey, 1976; Hoyt and Taylor, 1981; Hreljac, 1993b; Margaria, 1938; Mercier et al., 1994; Minetti et al., 1994). The rate of oxygen consumption during walking at varying speeds is characterized by a curvilinear relationship, while a more linear relationship is indicative of running (Minetti et al., 1994). Hoyt and Taylor found a correlation between preferred type of gait in horses at different speeds and its energetic economy, leading them to conclude that horses and humans change gait and select a speed within a gait in order to be most energetically economical (Hoyt and Taylor, 1981). However, preferred transition speeds were later found to be statistically lower than the most energetically optimal speeds, suggesting something other than an energetic trigger is responsible for the walk-to-run transition in humans. Actual gait transition speeds in humans are lower than theoretical calculations of the transition speed based on metabolic energy expenditure (Ganley et al., 2011; Hreljac, 1993b; Sentija et al., 2012). Furthermore, both the theoretical and actual gait transitions speeds were not dependent on training status or aerobic capacity (Rotstein et al., 2005). Although, it is likely that energetics is the ultimate reason for the walk-to-run transition, it is not the proximate trigger.

1.1.2 Dynamics

The dynamics of the walk-to-run transition have been investigated with respect to the dynamics of the inverted pendulum model of walking, as well as the stability of the system via a dynamical systems approach.

The mechanics of walking are simplistically characterized as an inverted pendulum where kinetic and potential energy fluctuate out of phase (Cavagna et al., 1977;

McGeer, 1990b; Mochon and Mcmahon, 1980). Running gaits are modeled as springs, or spring-loaded inverted pendulums, where kinetic and potential energy fluctuations happen in phase (Blickhan, 1989; McGeer, 1990a; Mochon and Mcmahon, 1980). The exchange of kinetic and potential energy breaks down when walking at higher than preferred walking speeds, decreasing the recovery of mechanical energy, and thus increasing muscular demands. Transitioning to a run could serve as a means to conserve mechanical energy (Cavagna et al., 1977; Kram et al., 1997). The influence of the pendular dynamics of walking on the walk-to-run gait transition has been assessed by means of the Froude number (Hubel and Usherwood, 2013; Kram et al., 1997). Humans and birds consistently transition between a walk and a run at a Froude number of 0.5 (Alexander, 1977; Gatesy and Biewener, 1991; Hreljac, 1995; Thorstensson and Roberthson, 1987). The Froude number is a dimensionless number calculated using velocity of locomotion (v), acceleration due to gravity (g), and leg length (L) (Fr =v2/gL). Utilizing the Froude number to model the walk-to-run transition speed results in walk-to-run transition speeds that are consistently higher than observed walk-to-run transitions. However during increases in inclines, predicted walk-to run transition speeds decrease at the same rate as actual walk-to-run transition speeds, thus the dynamics of the inverted pendulum are predictive of walk-to-run transition speeds (Hubel and Usherwood, 2013). By reducing gravity during gait transitions, Kram et al. showed walk-to-run gait transition speeds decreased for each respective gravity condition, such that the resultant Froude number remained at approximately 0.5 (Kram et al., 1997). They concluded that the dynamics of the inverted pendulum trigger the walk-to-run transition speed in humans. However, the underlying physiological mechanism or neuromechanical determinant for the transition to occur at a Froude number of 0.5 is still unclear.

A dynamical systems approach to gait transitions, through theoretical modeling and human experiments, suggests the transition occurs to restore the stability of

the system dynamics (i.e. step frequency, stride length, kinematic variability) and consequentially reduces energetic costs (Diedrich and Warren, 1995). Walking and running are considered stable attractors. A deviation away from one of those attractors decreases stability. This stability has been likened to variability in the system and probability of a gait transition (Li, 2000). At low speeds (when walking is always the preferred gait) the probability of a gait transition is close to 0%, and thus very stable. As velocity increases, around ∼1.8 m/s, the probability of a walk-to-run transition begins to increase dramatically, consequently the stability in the locomotor system decreases dramatically. Transitioning to a running gait would then cause a subsequent drastic increase in system stability. The dynamical systems approach provides a model to assess and predict gait transitions, however it lacks the ability to assess potential afferent or other physiological inputs directly contributing to the walk-to-run transition.

1.1.3 Neuromuscular

Early investigations into potential neuromuscular determinants focused on kinematic variables, but most recently, muscular variables have been implicated as main determinants of the walk-to-run transition. Two leading and seemingly opposing views have emerged concerning the major determinant of this transition: 1. Extensor hypothesis: propulsive force production by the legs is limited by the force-velocity properties of ankle plantarflexors; 2. Flexor hypothesis: a sensory threshold of perceived exertion is reached when flexor muscles in the leg reach a critical level of activation during swing or early stance.

1.1.3.1 Critical joint loads or angles

Critical musculo-skeletal forces have been proposed as the trigger for the trot to gallop transition in horses. Evidence was found in a study where weighted horses

transitioned from trot to gallop at much lower speeds, but at the same critical mechanical stress points (peak vertical force), as when unloaded most likely to protect musculo-skeletal structures (Farley and Taylor, 1991). However, this hypothesis was not supported in humans (Hreljac, 1995). Transitioning from a walk to a run in humans results in an increase in peak force production.

Kinematic variables that decrease after transitioning to a run have been identified as potential determinants. Thigh angle has been shown to severely diminish after transitioning from walk-to-run, supporting the idea that a critical thigh angle maybe a determinant in the transition (Minetti et al., 1994). Maximum ankle angular velocity was identified as a determinant for the preferred gait transition in humans in order to prevent the overexertion of dorsiflexor muscles during fast walking (Hreljac, 1995; Hreljac et al., 2001; MacLeod et al., 2014)

1.1.3.2 Extensor hypothesis: Force-length-velocity characteristics

Impaired plantarflexor force production (propulsive force), due to the force-length-velocity characteristics of plantarflexors, as walking speed increased has been identified as a determinant of the walk-to-run transition in humans (Arnold et al., 2013; Farris and Sawicki, 2012; Lai et al., 2015; Malcolm et al., 2009a; Neptune and Sasaki, 2005). With increased walking speed, plantarflexor fascicle shortening velocities increase as well, resulting in decreased muscular force production. Transitioning to a run (at $\sim$2.0 m/s) reduces plantarflexor fascicle shortening velocities, consequently increasing propulsive force production. This has been shown by neuromuscular models (Arnold et al., 2013; Neptune and Sasaki, 2005), as well as in vivo with ultrasonography of the soleus and medial gastrocnemius muscles (Farris and Sawicki, 2012; Lai et al., 2015).

1.1.3.3 Flexor hypothesis: Perceived exertion of flexor muscles

In a 2001 study, Prilutsky and Gregor suggested that the walk-to-run and run-to-walk transitions were differentially triggered by perceived exertion related to swing phase flexors and stance phase extensors, respectively (Prilutsky and Gregor, 2001). Specifically, they identified a net effect of exaggerated swing-related activations of the tibialis anterior, biceps femoris long head, and rectus femoris muscles during walking at higher than normal speeds (i.e. at or above the gait transition speed). Whereas muscle activations during running at the same speeds were significantly lower. These results were corroborated by assessment of mapping the motor neuron activity onto the spinal cord, where walking at higher than normal speeds yielded significantly higher lumbosacral activations, than running at the same speeds (Ivanenko et al., 2008).

Rapid eccentric loading of the tibialis anterior muscle associated with heel strike has also been implicated as a major determinant of the walk-to-run transition (Malcolm et al., 2009b; Segers et al., 2007b). When dorsiflexion and thus tibialis anterior activity is resisted (via a powered exoskeleton) (Malcolm et al., 2009b) or the tibialis anterior is fatigued (Segers et al., 2007b), walk-to-run transition speeds are lower. Conversely when dorsiflexion and thus tibialis anterior motion is-aided, walk-to-run transition speeds increased (Malcolm et al., 2009b).

The aforementioned two views (extensor hypothesis & flexor hypothesis) are not necessarily mutually exclusive, and require further investigation in terms of kinetics and muscle activations via both intra- and interlimb analysis. I will attempt to reconcile these two hypotheses by proposing the underlying neuromuscular mechanism ultimately responsible for the walk-to-run gait transition is due to a release of contralateral inhibitory stance-phase extensor afferent feedback on ipsilateral flexor muscle activations at high walking speeds.

1.2 Unilateral, transtibial amputation provides a model for able-bodied perturbation

Plantarflexors are the major source of propulsive force production during walking (Anderson and Pandy, 2003; Kepple et al., 1997; Neptune et al., 2001; Neptune et al., 2004; Silverman and Neptune, 2012; Zajac et al., 2002, 2003). Loss of the ankle-foot complex (and thus effective plantarflexors) in transtibial amputees also perturbs step-to-step transitions due to their lack of active ankle actuation and diminished capacity to generate propulsive forces on the amputated side (Sanderson and Martin, 1996; Silverman et al., 2008). During able-bodied gait, it is difficult to probe interlimb coordination when the kinematic and kinetic patterns of each limb are practically identical. Traumatic and congenital unilateral, transtibial amputation provides a unique subject population to assess the intra- and interlimb effects of absent sensory feedback and motor output from plantar- and dorsiflexors on the amputated side. The use of transtibial amputees circumvents the challenges (such as adaptation periods, device customizations, and unanticipated compensations), of altering the system dynamics in able-bodied subjects with novel perturbations e.g. limb constraint or an altered environment such as split-belt treadmill walking.

It is well established that unilateral, transtibial amputees have significantly slower preferred walking speeds than able-bodied controls (Gailey et al., 1994; Snyder et al., 1995; Waters et al., 1976; Winter and Sienko, 1988). To our knowledge, their walk-to-run transition speed has never before been identified. Unilateral, transtibial amputees intact side peak anterior-posterior propulsive forces are not significantly different from controls while walking at 1.2 and 1.6 m/s (Sanderson and Martin, 1996). Furthermore, during increasing walking speeds (0.6-1.5 m/s) muscle activations of unilateral, transtibial amputees during swing phase flexors (tibialis anterior, rectus femoris, and

biceps femoris long head) were never significantly different than controls. Since able-bodied propulsive force production due to intrinsic force-length-velocity characteristics of the plantarflexors, and conversely, swing related muscles activation during walking have both been implicated as a determinants of the walk-to-run transition, unilateral, transtibial amputees provide an excellent model to further investigate these hypotheses.

1.3 The importance of afferent feedback to locomotion

Afferent feedback is important for the initiation and adaptation of locomotion. In mesencephalic cats and birds, increasing descending drive by stimulating the mesencephalic locomotor region (MLR) results in the initiation of gait (Shik et al., 1966; Shik et al., 1969; Steeves et al., 1987). Increasing stimulation leads to walk to trot to gallop and walking-to-flying (wing flapping) gait transitions, respectively. Although fictive locomotion can be induced without afferent feedback and locomotor patterns can still be recorded from ventral roots or motorneurons, that does not imply that afferent feedback is not important for locomotion (Delcomyn, 1980; Grillner and Zangger, 1984; MacKay-Lyons, 2002). In fact, MLR induced fictive locomotion can be abolished by passive movements of the limbs (Orlovsky and Feldman, 1972). Normal locomotor activations are possible after deafferentation of the cat hindlimbs, but they are very unstable (Grillner and Zangger, 1984). In humans, walking is possible after the permanent loss of large afferent fibers, however it requires visual feedback and is still severely impaired (wide base of support, decreased speed, decreased joint range of motion) (Dietz et al., 2002; Lajoie et al., 1996). Furthermore, to our knowledge, midbrain stimulation alone (without afferent feedback) has not resulted in a gait transition. Locomotor initiation and adaptation of gait is seen in spinal cats (complete transection of spinal cord), which are dependent on afferent feedback to modulate locomotion(Eidelberg et al., 1980; Giuliani and Smith, 1987; Grillner and

Zangger, 1979; Pearson and Rossignol, 1991).Ultimately, pattern generators are sensitive to afferent feedback, as only a few degrees of limb movement are necessary to entrain fictive locomotion in spinal cats (Andersson et al., 1978).

Afferent feedback affects amplitude of motor outputs within the limb. In humans, quickly decreasing stance-phase plantarflexor load, decreases feedback from group II muscle spindles and/or Ib afferents from Golgi tenson organs, and causes a subsequent drop in soleus activation (Sinkjaer et al., 2000). Ia afferents from muscles spindles also modulate activations throughout the gait cycle, but their effects are strongest in stance phase (Mazzaro et al., 2005).

Afferent feedback modulates temporal characteristics of gait. In the cat hindlimb, the semitendinosus muscle decelerates the knee extension in terminal swing to facilitate the ipsilateral transition from swing-to-stance. This is mediated by afferent feedback, as it is absent after deafferentation of the hindlimbs (Grillner and Zangger, 1984). The stance-to-swing transition also has afferent-dependent behavior, in that progression of the hindlimb from terminal stance to swing will not happen, regardless of continued contralateral stepping, until a critical thigh extension angle is reached on the ipsilateral side (most likely due to Ia length-dependent feedback) (Grillner and Rossignol, 1978). Similar results were seen in human infants (Ortqvist et al., 1984). The stance-to-swing progression only takes place if the ipsilateral limb is at the critical position, and becomes sufficiently unloaded (during double support phase) thus, illustrating the importance of afferent feedback (most likely due to Ib force-dependent feedback) to maintain interlimb coordination as well (Duysens and Pearson, 1980; Grillner and Rossignol, 1978).

Afferent feedback supports interlimb coordination during locomotion by modulating motor output timing and amplitudes. Bilateral coordination of the limbs is paramount to maintain dynamic stability during locomotion. During walking in humans displacements of the hip and knee during swing elicits a contralateral increases

in muscle activations despite body weight support (Dietz and Harkema, 2004). Increased afferent feedback during contralateral stance has an inhibitory effect on ipsilateral flexors. In walking neonatal rats, afferent feedback during contralateral stance elicits a proportional decrease in ipsilateral feedback from the ipsilateral swinging limb (Hayes et al., 2012; Hochman et al., 2013). This suggests that contralateral (donor) extensor muscle afferents (most likely force-depenedent Ib afferents from Golgi tendon organs) ultimately inhibit the ipsilateral (recipient) flexor muscles. In pedaling humans, an increase in the contralateral side extensor force elicits a decrease in muscle amplitude and change in coordination pattern on the ipsilateral side (Ting et al., 2000; Ting et al., 1998). An increase in contralateral force production from the knee and hip during extension (downstroke) results in a decrease of ipsilateral flexor motor output during the recovery phase (upstroke). This evidence leads us to believe that extensor (most likely Ib force-dependent) afferents of the contralateral side inhibits the flexor muscle activations of the ipsilateral side in humans.

Two leading and opposing views have emerged concerning the major determinant of the walk-to-run transition: 1. Extensor hypothesis: propulsive force production by the legs is limited by the force-velocity properties of ankle plantarflexors; 2. Flexor hypothesis: a sensory threshold of perceived exertion is reached when flexor muscles in the leg reach a critical level of activation. I propose the underlying neuromuscular mechanism responsible for the gait transition is due to a release of ipsilateral inhibitory force feedback from extensor muscles on contralateral flexor muscle activations at high walking speeds (reconciling the two existing hypothesis).

1.4 Ischemic nerve block as a means of deafferentation

Acute deafferentation in humans can be achieved by anesthetic agents, vibration, and ischemia. Pharmacologic nerve blocks (via anesthetic agents such as bupivacaine, ropivacaine and lydocaine) are generally used clinically to manage pain after trauma

or surgery (Black et al., 2013; Jeng et al., 2010; Kopka and Serpell, 2005). The application can be logistically arduous, requiring a physician, ultrasound, and nerve stimulator. Furthermore pharmacologic nerve blocks are extremely invasive and pose the risk of axon damage or infection in subjects (Jeng et al., 2010). Another means of deafferentation is high frequency tendon vibration. During high frequency tendon vibration, proprioceptive signals from muscle spindles (Ia) are selectively activated, distorting accurate position and velocity data, where as Type Ib and II afferences are mostly insensitive to the vibration (Rolls, 1989; Cordo, 1995). This is also referred to as the busy-line phenomenon, where the Ia fibers are overloaded due to the vibration, and thus unable to respond to changes in muscle length (Hagbarth et al., 1973). Although, high frequency vibration is a safe means of manipulating afferent feedback, it does not allow for the manipulation of Ib afferent feedback. Since previous literature regarding the inhibition of contralateral flexor muscle activations has implicated Type Ib afferent feedback (Hochman et al., 2013; Ting et al., 2000), I employed ischemia as a noninvasive means of deafferentation.

Ischemic nerve block (IB) has been shown to be a safe, reversible and reliable means of deafferentation (Baron and Irving, 2002; Christensen et al., 2007; Schlee et al., 2009; Voller et al., 2006). Standard methodology for employing an ischemic nerve block with a blood pressure cuff is detailed in the literature (McNulty et al., 2002). Inflating a blood pressure cuff to 210 mmHg to block the large diameter afferents as has been achieved in previous studies with IB (Christensen et al., 2007; Laszlo, 1967; Sinclair, 1948). Ischemic nerve block decreases feedback from large diameter afferents before the smaller efferent motor neurons are substantially affected (Christensen et al., 2007; Laszlo, 1967).

During IB of the hand and leg below the knee, muscles proximal to the IB (biceps brachii and vastus medialus, respectively) gain a larger cortical representation and increased motor evoked potentials (MEPs) during transcranial magnetic stimulation

(Brasil-Neto et al., 1993; McNulty et al., 2002). In muscles distal to the IB, MEPs are significantly lower(Brasil-Neto et al., 1993). Specifically during below-knee IB, the contralateral vastus medialus MEPs are consistent with the ipsilateral limb (increased during IB), albeit at much lower amplitudes. Contralateral muscles distal to the location of the ipsilateral IB showed no significant changes. As there was no increase in H-reflex (H/M ratio) during IB in the proximal vastus medialus muscle on either side, the increases in muscle activation during IB were not due to increases in alpha motor neuron excitability. Rather the increases in motor output has been attributed to increased cortio-spinal excitability. Interestingly in the arm, proximal to an IB, flexor muscles but not extensor muscles have increased cortico-spinal excitability (as seem in the amplitudes of motor evoked potentials)(Vallence et al., 2012).

The temporary sensory loss can be quantitatively verified by von Frey filament tests, which assesses sensation as small plastic filaments are touched to the skin of the ankle/feet (Schieppati, 1987). Aftereffects of ishchemic block include a temporary increase in proximal muscle excitability (as measured via motor evoked potentials during transcranial magnetic stimulation) (Brasil-Neto et al., 1992; Brasil-Neto et al., 1993; McNulty et al., 2002) and decrease in Ia afferent excitability (as measured via H-reflex after 5 minutes of ischemia) (Zakutansky et al., 2005). The lack of lower extremity proximal muscle and contralateral side interference as noted in previous studies, along with ease of application, noninvasive nature, and reliability, made IB the most well suited means of unilateral deafferentation for my AIM 3 protocol.

1.5 Main objective & Aims

The main objective of this dissertation is to explore the underlying mechanism responsible for the human walk-to-run transition. This objective was tacked by completing three specific aims.

1.5.1 Aim 1: To determine the preferred gait transition speeds of unilateral, transtibial amputees, and the influence of kinetics on the walk-to-run gait transition speed

In able-bodied subjects propulsive force production decreases above normal walking speeds due to high plantarflexor muscle fascicle shortening velocities. Utilizing otherwise healthy subjects with a unilateral, transtibial amputation provides an experimental model with unilateral propulsive force and afferent feedback deficits. In Aim 1, I will determine the gait transition speed in unilateral transtibial amputees and investigate the influence of propulsive force production as a determinant of the walk-to-run gait transition speed.

1.5.2 Aim 2: To quantify the muscle activation during walking and running gaits relative to the walk-to-run gait transition speed for unilateral, transtibial amputees

In able-bodied subjects increased flexor activations (tibialis anterior, biceps femoris longhead, and rectus femoris muscles) during swing/early stance have been implicated individually as determinants of the walk-to-run transition. In Aim 2 I will determine the influence increased flexor activations during swing/early stance on the walk-to-run transition in unilateral, transtibial amputees.

1.5.3 Aim 3: To evaluate the effects of contralateral sensory loss on the motor output of the ipsilateral leg

Limited plantarflexor force production during stance and increased flexor activations during swing/early stance have been implicated individually as determinants of the walk-to-run transition. Given the effects in pedaling of altered force production on ipsilateral motor output,- Could the decrease of stance phase force production at high walking speeds, cause the increase in swing/early stance phase flexor motor outputs? As a first step to answer this question, in Aim 3 I will perform an assessment of decreasing the afferent feedback at the ankle on the motor output of ipsilateral flexor muscles via temporary reversible sensory block in able-bodied subjects.

CHAPTER II

AIM 1:LOWER GAIT TRANSITION SPEEDS IN AMPUTEES ARE NOT LIMITED BY PROPULSIVE FORCE PRODUCTION

**This chapter is currently under review for publication in the Journal of Biomechanics.*

2.1 Introduction

The walk-to-run gait transition has long been studied in humans, as a means to better understand the biomechanics and neural control of locomotion. Many key determinants, or factors that appear to drive the walk-to-run transition have been identified over the years, including: metabolic energy minimization (Minetti et al., 1994), kinetics factors (Raynor et al., 2002), critical flexor muscle activations during the swing phase of gait (Hreljac et al., 2001; Malcolm et al., 2009b; Prilutsky and Gregor, 2001; Segers et al., 2007), a critical angular velocity of the ankle to protect dorsiflexors (Hreljac, 1995), and pendular dynamics of the center of mass (Kram et al., 1997). Some have also proposed the idea of a conglomeration of these factors that could contribute to the walk-to-run transition (Bartlett and Kram, 2008; Malcolm et al., 2009a). More recently, work has pointed to plantar flexor force production as a major determinant of the walk-to-run transition (Arnold et al., 2013; Farris and Sawicki, 2012; Malcolm et al., 2009a; Neptune and Sasaki, 2005). Modeling of the soleus, medial gastrocnemius, and lateral gastrocnemius, and in vivo measurement of the medial gastrocnemius have demonstrated that as walking speed increases, so do the plantar flexor fascicle shortening velocities. These increases in plantar flexor

fascicle shortening velocities result in a decrease in muscle force production, which then lead to decreases in propulsive force production by the legs. Furthermore, transitioning from a walk to a run at the preferred walk-to-run transition speed of ∼2.0 m/s greatly reduces fascicle shortening velocities in the plantar flexor muscles, and in turn increases propulsive force production (Arnold et al., 2013; Farris and Sawicki, 2012; Neptune and Sasaki, 2005). During walking, the plantar flexor muscles are the primary contributors to propulsive force production (Anderson and Pandy, 2003; Neptune et al., 2004; Silverman and Neptune, 2012; Zajac et al., 2002, 2003). Due to the plantar flexors intrinsic force-length-velocity characteristics, maximum propulsive force production of the anterior-posterior ground reaction forces during walking increases until the walk-to-run transition where it peaks, and then decreases during walking at speeds above transition speed (Neptune and Sasaki, 2005). As such, we sought to investigate the gait transition speed in persons with a unilateral, transtibial amputation, to test whether plantar flexor propulsive force production is a major determinant in their walk-to-run transition.

The effective removal of plantar flexors in a unilateral, transtibial amputation in conjunction with the use of a passive prosthesis (both passive-elastic and Solid-Ankle Cushion Heel or SACH feet) results in a diminished capacity to generate propulsive forces on the amputated side (Sanderson and Martin, 1997; Silverman et al., 2008). Walking in unilateral, transtibial amputees (using passive-elastic Flex-foot prostheses) and control subjects at speeds of 1.2 m/s and 1.6 m/s has shown that amputated side peak anterior-posterior propulsive forces are consistently and significantly lower than those of both control subjects and the intact side walking at the same speed (Sanderson and Martin, 1997). While the intact side peak anterior-posterior propulsive forces Sanderson and Martin reported were not statistically significant from controls, to our knowledge this have never been investigated at walking speeds higher than 1.6 m/s. Furthermore, the walk-to-run gait transition has not previously been

characterized in unilateral, transtibial amputees. Understanding the gait transition in an amputee population using passive devices could be helpful in the design of more robust, powered prosthetic components (to include both walking and running) as well as gait rehabilitation procedures. Previous work has shown that amputee subjects using passive prostheses have slower preferred walking speeds than able-bodied controls (Gailey et al., 1994; Snyder et al., 1995; Waters et al., 1976; Winter and Sienko, 1988). Unilateral, transtibial amputee subjects also have lower maximum sustainable walking speeds than control subjects, with ranges of $\sim$1.5-1.6 m/s and $\sim$1.9-2.0 m/s, respectively (Genin et al., 2008; Nolan et al., 2003). Consequently, otherwise healthy unilateral, transtibial amputee subjects provides an excellent experimental model to assess the effects of plantar flexor propulsive force production on the walk-to-run transition speed.

The purpose of this work was to determine the gait transition speed of unilateral, transtibial amputee subjects and assess intact side mechanical limits of the plantar flexor muscles (as indicated by peak propulsive force production) is a major determinant of the walk-to-run transition for amputee subjects. We hypothesized that unilateral, transtibial amputees would transition between gaits at a lower absolute speed than matched, able-bodied subjects serving as controls. We further hypothesized that peak propulsive force production in amputee subjects intact side, would be limited at walking speeds above the gait transition speed, thus supporting the idea that force-length-velocity characteristics of the plantar flexors are a major determinant in amputee subjects walk-to-run transitions. Alternatively, if amputees peak propulsive force production continued to increase at speeds above the gait transition speed, then the mechanical limits of the plantar flexor muscles are most likely not a major determinant of the walk-to-run transition in unilateral, transtibial amputee subjects. We employed an incremental speed protocol (Hreljac, 1993a, b; Kram et al., 1997; Prilutsky and Gregor, 2001; Raynor et al., 2002) to define each individuals

gait transition speed and assessed walking kinematics and kinetics at speeds 50-130% of that transition speed on a custom, instrumented dual belt treadmill.

2.2 Materials & methods

2.2.1 Subjects

All subjects gave informed written consent prior to completing the Georgia Institute of Technology IRB approved protocol. Subjects included 10 healthy, unilateral, transtibial amputee (AMP) subjects (5 males, 5 females; amputation: 3 elective due to congenital deformity, 7 traumatic; mean age±SD: 26.7±4.5 years; mass: 67.4±14.6 kg; sound leg length: 91.5±5.6 cm) and 10 healthy, able-bodied matched control (CON) subjects (5 males, 5 females; age: 29.6±6.9 years; mass: 67.2±10.0 kg; leg length: 91.1±5.4cm). We took great care in matching each CON subject to one of the AMP subjects for all listed characteristics. There were no significant differences in age, weight, and leg length between the two groups; in addition, subjects were also qualitatively matched on activity level, training type, and gender (Table 1).). All subjects were recreationally or competitively fit and participated in running for exercise or training at least once per week. Persons that were pregnant, diabetic, sedentary, or suffering from any cardiovascular or neurological pathologies, such as peripheral neuropathy, were excluded from the study. All CON subjects were free from musculoskeletal and neurological trauma. AMP subjects wore their own custom made, well fitting, prosthesis and commercially available passive-elastic ankle-foot component. AMP persons using SACH or powered ankle-foot devices were excluded from participating in the study, as these prosthetic feet have been shown to alter kinematics and kinetics (Herr and Grabowski, 2012; Torburn et al., 1990). Subjects refrained from exercise on testing days. Each subject completed testing over two days no more than one week apart.

Table 1: Subject Characteristics

Matched Pair #	Sex	Leg Length (cm)	Mass (kg)	Age (years)	Transtibial Amputation			Prosthesis Characteristics		
		AMP (CON)	AMP (CON)	AMP (CON)	Type	Side	Years Since	Years with Foot	Foot Component Type	Suspension
1	F	93.0 (93.5)	68.4 (70.9)	37.3 (23.5)	Traumatic	Right	5.4	1.2	Runway (Freedom)	Elevated Vacuum
2	F	87.2 (86.6)	56.0 (61.3)	28.5 (25.7)	Congenital (fibular hemilemia)	Right	28.0	1.0	Variflex (Ossur)	Supracondylar
3	F	87.3 (86.3)	53.1 (56.5)	38.2 (28.8)	Traumatic	Left	2.1	0.6	Seattle Triumph (TruLife)	Elevated Vacuum
4	F	97.5 (86.5)	69.2 (59.7)	27.9 (32.4)	Congenital (pseudoarthritis of the tibia)	Left	0.7	0.7	Accent (College Park)	Suction & Sleeve
5	F	81.5 (83.3)	65.5 (62.6)	18.3 (21.4)	Traumatic	Left	2.6	2.5	Highlander (Freedom)	Pin
6	M	101.3 (98.3)	77.4 (81.5)	60.0 (51.9)	Traumatic	Right	3.9	2.0	Renegade AT (Freedoom)	Elevated Vacuum
7	M	91.0 (94.0)	83.9 (89.3)	35.3 (36.5)	Traumatic	Right	11.9	2.0	Renegade (Freedoom)	Elevated Vacuum
8	M	88.0 (89.0)	63.5 (65.7)	21.4 (21.7)	Traumatic	Right	1.4	11.0	Renegade (Freedom)	Elevated Vacuum
9	M	102.5 (100.8)	64.5 (70.0)	21.4 (23.0)	Congenital (club foot)	Right	3.0	1.5	Variflex (Ossur)	Suction & Sleeve
10	M	94.0 (93.8)	97.8 (87.3)	42.0 (32.6)	Traumatic	Right	10.1	2.0	Trias (Ottobock)	Elevated Vacuum

2.2.2 Experimental protocol

2.2.2.1 Day 1: Determine gait transition speed

Subjects habituated to walking and running on a single belt of a custom dual-belt treadmill at self-selected speeds for 3 minutes with two-minute rest periods. The procedure to determine each individuals gait transition speed (GTS) consisted of two conditions: 1. incrementally increasing the treadmill speed; and, 2. incrementally decreasing treadmill speed, similar to what has been previously described in the literature (Hreljac, 1993a, b; Kram et al., 1997; Prilutsky and Gregor, 2001; Raynor et al., 2002). Subjects stood off of the treadmill belt while it was running. Once the belt reached the appropriate speed, we instructed subjects to step onto the moving belt. Subjects were given up to 30 seconds to both walk and run before verbally indicating which gait they preferred. Subjects rested while the moving belts speed was either increased or decreased by 0.1 m/s, and the task was then repeated at each 0.1 m/s increment. During the increasing portion, CON subjects began at 1.3 m/s and AMP at 1.0 m/s. The lowest speed where the subject preferred to run was recorded as the transition speed. For the decreasing portion, starting speeds were 2.6 and 2.3 m/s for CON and AMP subjects respectively. The highest preferred walking speed was recorded as the transition speed. The starting speeds were different to accommodate AMP subjects being uncomfortable attempting to walk above 2.3 m/s and maintaining the range of speeds tested between the two groups. Subjects repeated the procedure a total of three times with the first used as practice to familiarize themselves with the task. The second and third times completing the procedure resulted in four recorded transition speeds. The presentation of increasing or decreasing speeds was randomized for each subject. Each individuals GTS was calculated by averaging the last four transition speeds together (two from incrementally increasing the treadmill speed and two from incrementally decreasing treadmill speed).

2.2.2.2 Day 2: Instrumented dual-belt collection

Subjects habituated to walking and running on the custom dual-belt treadmill at self-selected speeds for three minutes with two-minute rest periods. Subjects walked for 30-second trials at speeds 50, 60, 70, 80, 90, 100, 110, 120, and 130% of their previously determined GTS (with 100% corresponding to each individuals GTS). Presentation of speeds was randomized for each subject. Subjects rested by sitting in a chair for at least two minutes between each trial.

2.2.3 Kinetic & kinematic analysis

We placed sixteen retroreflective markers on each subjects right and left second metatarsophalangeal joint, lateral malleolus, heel, shank segment, lateral condyle, thigh segment, anterior superior iliac spine, and posterior superior iliac spine. For AMP subjects, amputated side (AMP-Amputated) markers on the prosthetic device were placed to match those on the intact side (AMP-Intact) (Powers et al., 1998; Silverman et al., 2008). Three-dimensional positions of the lower extremity marker data were collected by a six-camera Vicon motion analysis system (120Hz, Oxford, UK). A custom built, dual-belt treadmill instrumented with two commercial force plates (1080 Hz, Advanced Mechanical Technology Incorporated, Watertown, MA, USA) simultaneously measured ground reaction force data (Kram et al., 1998). We applied a low-pass, zero-phase lag, fourth order Butterworth filter at 10 and 20 Hz to marker and force data respectively. We used custom Matlab code to calculate mean sagittal plane kinematics. Joint angles for the hip, knee, and ankle measured during a static standing trial were defined as neutral. There were no significant differences in standing joint angles between the leg types (CON, AMP-Intact, and AMP-Amputated). Peak ankle plantarflexion was defined as the peak plantarflexion angle after 50% of the gait cycle. This was done to ensure the comparisons in plantarflexion angle between

leg types were made during early swing. This distinction was made specifically because the AMP-Amputated side plantarflexion angle peaked for some subjects during loading response. A vertical ground reaction force threshold of 32 N determined foot contact events, as it was identified in our lab as the lowest threshold to yield reliable and consistent event detection (Auyang et al., 2009; Selgrade and Chang, 2015; Yen and Chang, 2010). All data were time normalized to heel strike for each respective leg. CON data presented are from the right leg. The duty factor (stance time/ stride time) for each subject-speed combination was calculated post-hoc to confirm that walking was achieved, with walking defined as having a duty factor $\geq$0.5 (Gatesy and Biewener, 1991). Every subject was able to walk at each speed tested.

2.2.4 Statistical analysis

Due to the matched design and extensive subject matching criteria, we employed paired t-tests for between subject group (CON vs. AMP) assessments of gait transition speed and neutral joint angles. Significance was defined as p-value<0.05. To assess how peak force data was affected by walking speed, separate one-factor (9 speeds: 50-130% GTS), repeated measure analysis of variances (ANOVA) were run for each leg type (CON, Amp-Intact, or Amp-Amputated). When a significant main effect was found, subsequent post-hoc analysis were conducted with significance defined as a Bonferroni corrected p-value¡0.05. To assess the differences in peak flexion and extension joint angles between leg type, separate one-factor (leg type: CON, Amp-Intact, or Amp-Amputated) repeated measure ANOVAS were run for each of the six kinematic variables at each speed (50-130% GTS). When significant main effects of leg type were found subsequent post-hoc analysis was conducted with significance defined as a Bonferroni corrected p-value<0.05.

2.3 Results

2.3.1 Gait transition speeds

AMP subjects transitioned between gaits at 1.73 ± 0.13 m/s, which was significantly lower than the CON subjects GTS of 2.09 ± 0.05 m/s ($p<0.01$) (Fig. 1). All AMP subjects transitioned between gaits at lower speeds then their matched CON. There was no significant hysteresis for CON subjects transition speeds, in that the transition speeds determined by incrementally increasing and decreasing treadmill speeds were not significantly different from one another (2.09 ± 0.10 and 2.08 ± 0.08 m/s respectively). AMP subjects transition speeds from the incrementally increasing portion of the protocol (1.75 ± 0.12 m/s) showed a small but significant difference from the

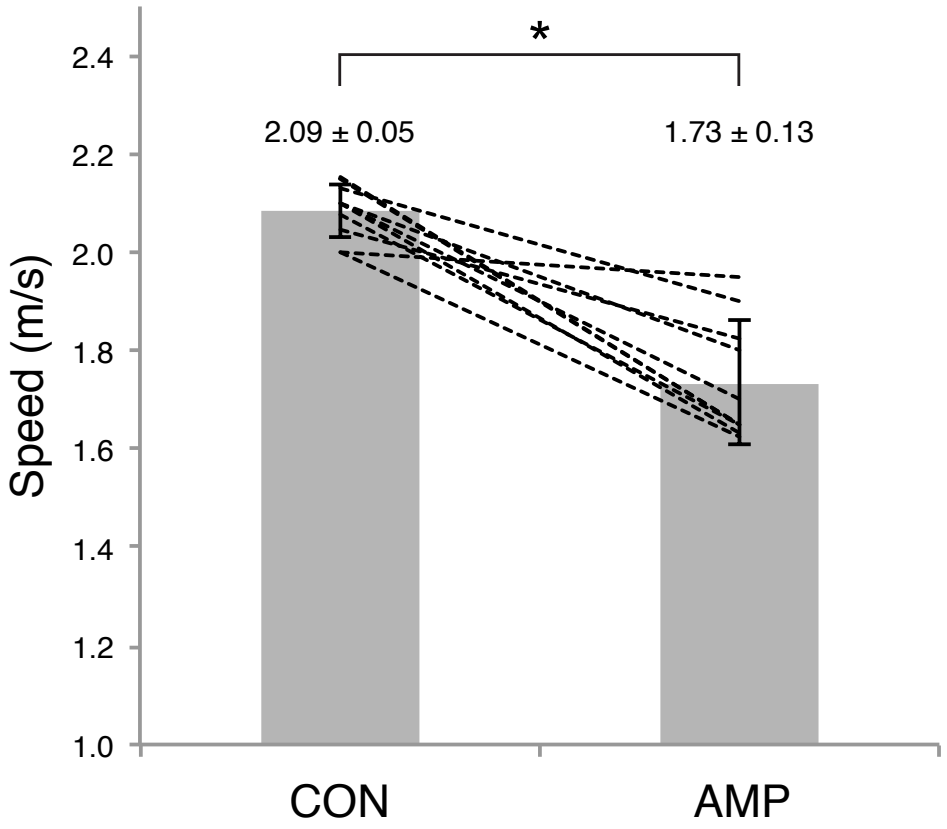

Figure 1: Unilateral, transtibial amputees (AMP) transition between gaits at significantly lower speeds than able-bodied controls (CON) (*$p<0.01$). Mean ± standard deviation. Dashed lines indicate the relationship between the AMP subjects and their matched CON.

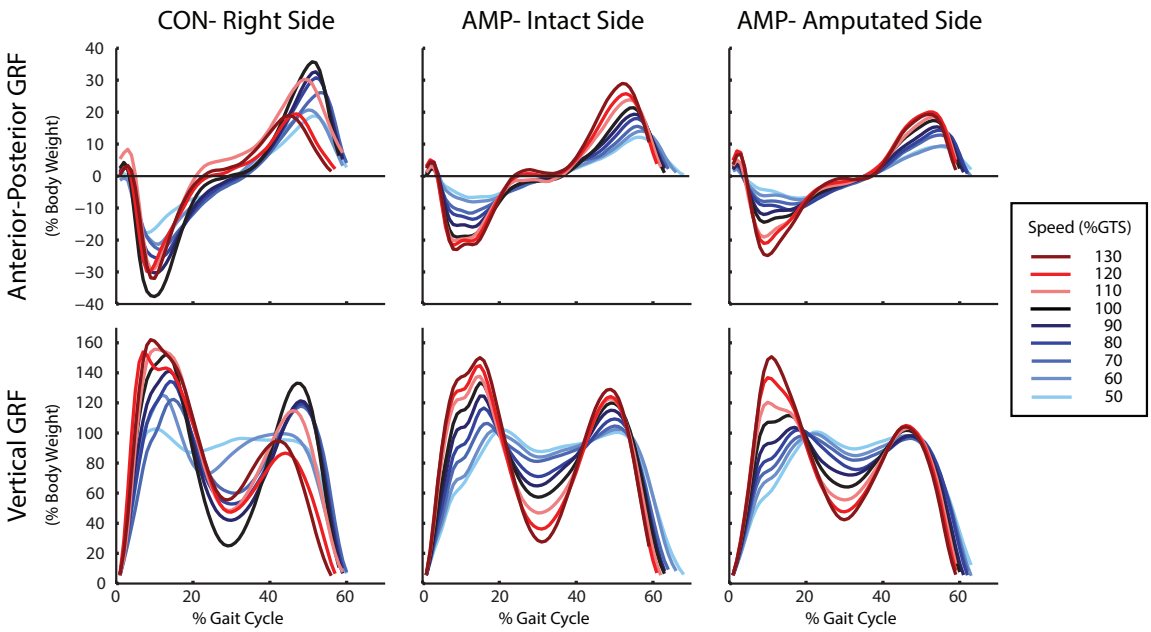

Figure 2: Representative vertical and anterior-posterior ground reaction forces during walking plotted for each relative speed 50-130% GTS from a matched control (CON) and unilateral, transtibial amputee (AMP) subject (lightest blue to darkest blue: 50-90% GTS; black: 100% GTS; lightest red to darkest red: 110-130% GTS).

incrementally decreasing portion (1.71 ± 0.13 m/s) ($p<0.01$). However, the average difference of 0.04 m/s between AMP subjects transition speeds was approximately a ∼2% difference and below the 0.10 m/s resolution used for the incremental treadmill change.

2.3.2 Ground reaction forces

Significant main effects were found for speed (50-130% GTS) in all force variables except for AMP-Amputated peak vertical propulsive force production. Representative subject data show CON subjects anterior-posterior peak propulsive force production increased with speed until 100% GTS, and decreased at speeds above the GTS (Fig. 2). CON subjects peak anterior-posterior propulsive forces significantly increased, when compared to the preceding speed at 60-80% GTS, and significantly decreased at 120% GTS (110%: 0.27±0.04 > 120%: 0.23±0.05, $p<0.05$) (Fig. 3A, Table 2). Peak anterior-posterior braking forces for CON subjects significantly increased with

Table 2: Walking Propulsive & Braking Forces

		Anterior-Posterior Ground Reaction Forces			Vertical Ground Reaction Forces		
	% GTS	CON	AMP- Intact	AMP- Amputated	CON	AMP- Intact	AMP- Amputated
Propulsion	50	0.16 ± 0.02	0.13 ± 0.02	0.10 ± 0.02	1.05 ± 0.04	0.97 ± 0.04	0.97 ± 0.03
(Body Weight)	60	0.19 ± 0.01*	0.16 ± 0.02*	0.11 ± 0.02*	1.09 ± 0.05*	1.00 ± 0.06*	0.99 ± 0.05
	70	0.23 ± 0.02*	0.18 ± 0.03*	0.13 ± 0.02*	1.16 ± 0.06*	1.04 ± 0.07*	1.01 ± 0.06
	80	0.27 ± 0.02*	0.22 ± 0.03*	0.15 ± 0.02*	1.19 ± 0.07	1.10 ± 0.10*	1.02 ± 0.07
	90	0.29 ± 0.02	0.25 ± 0.04*	0.17 ± 0.02*	1.21 ± 0.10	1.14 ± 0.12*	1.03 ± 0.09
	100	0.31 ± 0.03	0.28 ± 0.04*	0.19 ± 0.03*	1.20 ± 0.15	1.17 ± 0.13	1.05 ± 0.12
	110	0.27 ± 0.04	0.30 ± 0.04*	0.20 ± 0.05	1.12 ± 0.14	1.18 ± 0.14	1.05 ± 0.17
	120	**0.23 ± 0.05***	0.29 ± 0.05	0.21 ± 0.06	1.00 ± 0.18	1.14 ± 0.18	1.03 ± 0.24
	130	0.21 ± 0.05	0.26 ± 0.07	0.18 ± 0.06	0.98 ± 0.18	1.06 ± 0.23	0.96 ± 0.25
Braking	50	-0.13 ± 0.02	-0.09 ± 0.03	-0.08 ± 0.02	1.04 ± 0.04	1.04 ± 0.04	1.04 ± 0.04
(Body Weight)	60	-0.17 ± 0.02*	-0.12 ± 0.03*	-0.09 ± 0.01*	1.12 ± 0.07*	1.06 ± 0.06	1.05 ± 0.05
	70	-0.20 ± 0.02*	-0.14 ± 0.03*	-0.11 ± 0.02*	1.20 ± 0.08*	1.11 ± 0.08*	1.06 ± 0.07
	80	-0.24 ± 0.01*	-0.17 ± 0.03*	-0.13 ± 0.02*	1.27 ± 0.08*	1.20 ± 0.08*	1.10 ± 0.09
	90	-0.27 ± 0.02*	-0.21 ± 0.05*	-0.16 ± 0.03*	1.36 ± 0.11*	1.30 ± 0.09*	1.16 ± 0.11*
	100	-0.31 ± 0.05*	-0.24 ± 0.05*	-0.18 ± 0.03*	1.49 ± 0.09*	1.41 ± 0.12*	1.24 ± 0.11*
	110	-0.31 ± 0.06	-0.28 ± 0.06*	-0.22 ± 0.04*	1.55 ± 0.11	1.50 ± 0.11*	1.37 ± 0.10*
	120	-0.29 ± 0.09	-0.28 ± 0.06	-0.23 ± 0.06	1.63 ± 0.19	1.58 ± 0.17	1.49 ± 0.10*
	130	-0.29 ± 0.09	-0.27 ± 0.09	-0.22 ± 0.08	1.63 ± 0.18	1.60 ± 0.19	1.58 ± 0.16

Table 2: Control (CON) and unilateral, transtibial amputee intact (AMP-Intact) and amputated (AMP-Amputated) side peak anterior-posterior and vertical ground reaction forces (during braking and propulsion (mean ± standard deviation) for walking at speeds 50-130% of the gait transition speed. Paired t-tests were performed to assess whether or not each speed was significantly different from the preceding slower speed (*$p<0.05$). Bold means significantly lower than preceding slower speed.

speed from 60-100% GTS. Speeds above 100% GTS had no significant differences when compared to the speed that preceded them (Fig. 3B, Table 2).

Peak anterior-posterior propulsive force production did not significantly decrease during walking above 100% GTS in unilateral, transtibial amputees (Fig. 2 3A). In AMP-Intact and AMP-Amputated sides, peak anterior-posterior forces during the propulsive phase significantly increased with speed from 60-110% GTS and 60-100% GTS respectively (Fig. 3A, Table 2). AMP-Intact peak anterior-posterior propulsive force production during walking significantly increased at speed 110% GTS in comparison to 100% GTS (100%: $0.28 \pm 0.04 <$ 110%: 0.30 ± 0.04, $p<0.05$) (Fig. 3A, Table 2). Peak anterior-posterior braking forces significantly increased with walking speed from 60-110% GTS for AMP-Intact and AMP-Amputated sides ($p<0.05$) (Fig. 3B, Table 2). Speeds above 110% GTS for AMP subjects intact and amputated sides had no significant difference from the speed that immediately preceded them.

To assess how the peak propulsive forces changed over absolute speed rather than relative to the GTS, we applied best fit quadratic polynomial curves to data from CON ($y = -0.16x2 + 0.63x + -0.33, r^2 = 0.67$), and AMP-Intact ($y = -0.09x2 + 0.42x + -0.17, r^2 = 0.71$) (Fig. 3C). We found that changes in AMP-Intact peak propulsive force production tracked with those of CON subjects. Similar results were seen with the AMP-Amputated peak propulsive force production, however, always lower in amplitude. AMP-Amputated peak propulsive force production ranged from 3.45±2.88% body weight (50% GTS) to 9.2±4.20% body weight (110% GTS) below AMP-Intact side peak anterior-posterior propulsive force production.

2.3.3 Kinematics

There were no significant main effects of leg type (CON, Amp-Intact, or Amp-Amputated) on joint angles during dorsiflexion or peak flexion or extension angles for the knee or hip at any speed (Fig. 4, Table 3). Significant main effects for leg type

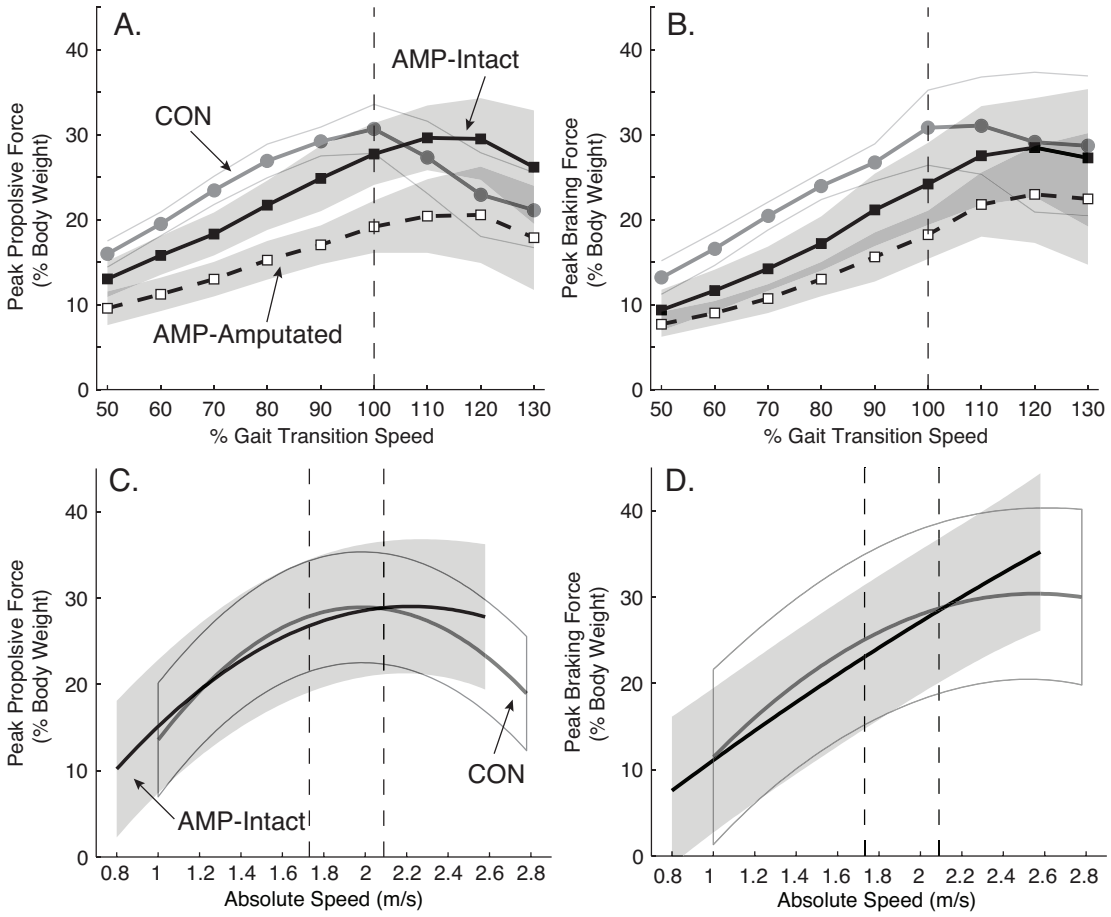

Figure 3: (A) Mean peak anterior-posterior propulsive force ± standard deviation with respect to relative speed (% GTS) for CON subjects (grey circles), AMP-Intact side (black squares), and AMP-Amputated (white squares). (B) Mean peak anterior-posterior braking force ± standard deviation with respect to % GTS for CON subjects (grey circles), AMP-Intact side (black squares), and AMP-Amputated (white squares). (C) Peak propulsive force with respect to absolute speed (m/s) plotted as quadratic polynomial curves to with the 95% confidence interval of the data for each group; CON (grey line, white 95% confidence interval) ($y = -0.16x2 + 0.63x + -0.33, r^2 = 0.67$), AMP-Intact (black line, grey 95% confidence interval) ($y = -0.09x2 + 0.42x + -0.17, r^2 = 0.71$). (D) Peak braking force with respect to absolute speed (m/s) plotted as quadratic polynomial curves to with the 95% confidence interval of the data for each group; CON (grey line, white 95% confidence interval) ($y = -0.08x2 + 0.40x + -0.21, r^2 = 0.61$), AMP-Intact (black line, grey 95% confidence interval) ($y = -0.01x2 + 0.20x + -0.08, r^2 = 0.76$).

were found at every speed for peak ankle plantarflexion. Post-hoc analysis revealed that there was a difference in peak plantarflexion angle at every speed (50%-130%

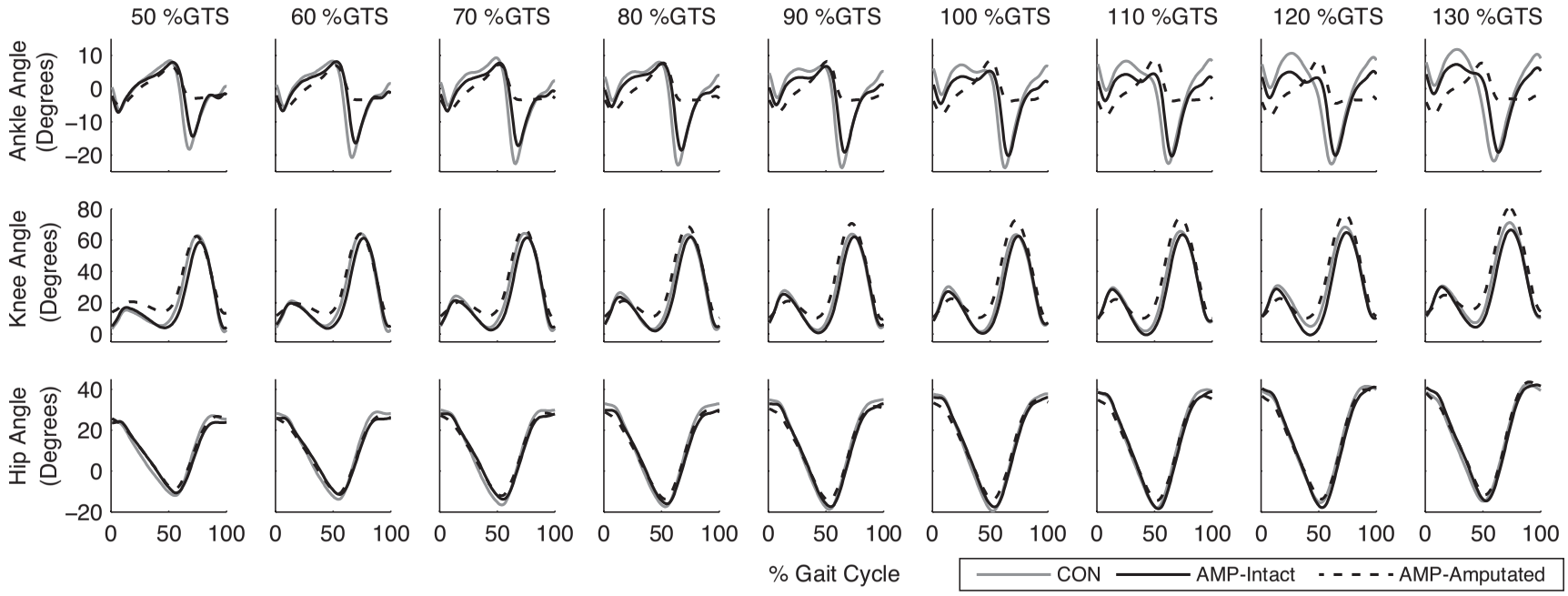

Figure 4: Mean kinematics of all subjects walking at speeds relative to the gait transition speed. CON (grey line), AMP-Intact (black solid line), AMP-Amputated (black dashed line).

GTS) when comparing CON or AMP-Intact to AMP-Amputated ($p < 0.05$). Post-hoc analysis also showed there was no significant difference between CON and AMP-Intact side peak plantarflexion angle at any speed. No significant differences between CON and AMP-Intact were found for peak flexion or extension angle at the ankle, knee, or hip at any speed. Thus, verifying Amp-Intact kinematics are similar to those of CON subjects (Fig. 4). Maucheys test of sphericity was satisfied for comparisons of ankle plantarflexion and dorsiflexion and knee flexion and extension. Maucheys test of sphericity was violated for hip flexion at speeds of 60-110% GTS and hip extension at 120% GTS, therefore degrees of freedom were corrected using Greenhouse-Geisser estimates of sphericity. Regardless, we found no main effects of leg type on peak hip flexion or extension.

Table 3: Peak Kinematics

		% Gait Transition Speed								
		50	60	70	80	90	100	110	120	130
Ankle Plantarflexion	CON	-20.0 ± 6.3	-22.3 ± 5.7	-23.1 ± 5.1	-23.5 ± 5.5	-24.3 ± 5.2	-24.1 ± 4.8	-23.0 ± 5.4	-23.2 ± 5.8	-22.4 ± 5.9
	AMP-Intact	-15.4 ±6.1	-16.9 ± 5.8	-17.7 ± 5.5	-18.9 ± 5.8	-19.6 ± 6.0	-20.6 ± 6.0	-20.6 ± 6.0	-20.5 ± 6.5	-19.6 ± 7.0
	AMP-Amputated	-3.5 ± 2.4*†	-4.0 ± 2.9*†	-4.0 ± 2.9*†	-4.3 ± 2.9*†	-4.3 ± 2.9*†	-4.5 ± 2.7*†	-4.4 ± 2.7*†	-5.1 ± 3.2*†	-4.5 ±2.5*†
Ankle Dorsiflexion	CON	9.3 ± 3.5	9.4 ± 3.1	9.6 ± 2.8	8.8 ± 3.9	8.8 ± 4.0	9.0 ± 4.2	10.2 ± 4.4	11.9 ± 5.9	13.3 ± 6.4
	AMP-Intact	8.5 ± 4.4	8.5 ± 5.1	8.1 ± 5.1	8.1 ± 4.9	7.6 ± 5.3	7.3 ± 5.1	7.3 ± 5.4	7.8 ± 5.8	10.4 ± 5.6
	AMP-Amputated	6.8 ± 2.4	7.1 ± 2.9	7.4 ± 3.0	7.9 ± 3.2	8.4 ± 3.5	8.7 ± 3.5	9.2 ± 3.8	8.9 ± 3.9	8.4 ± 4.1
Knee Flexion	CON	63.4 ± 5.9	64.4 ± 5.7	64.6 ± 5.0	63.8 ± 4.8	64.1 ± 4.7	63.8 ± 5.3	65.8 ± 4.7	68.5 ± 5.0	71.4 ± 5.9
	AMP-Intact	59.3 ± 7.2	61.6 ± 7.0	61.9 ± 6.5	62.3 ± 6.4	62.6 ± 6.4	62.8 ± 6.2	63.9 ± 6.3	65.4 ± 6.5	67.1 ± 7.2
	AMP-Amputated	63.0 ± 11.0	64.6 ± 11.9	67.7 ± 11.2	69.2 ± 11.9	71.0 ± 11.9	72.9 ± 11.9	74.5 ± 12.2	77.1 ± 13.4	80.7 ± 14.1
Knee Extension	CON	0.6 ± 5.7	0.5 ± 5.4	0.5 ± 5.4	0.9 ± 5.2	1.1 ± 5.3	1.1 ± 5.8	1.6 ± 5.7	3.0 ± 6.2	4.6 ± 7.0
	AMP-Intact	2.5 ± 4.0	2.4 ± 3.4	1.4 ± 3.7	0.9 ± 3.5	-0.1 ± 3.1	-0.1 ± 3.5	-0.8 ± 3.7	-0.9 ± 3.6	2.8 ± 5.7
	AMP-Amputated	10.9 ± 13.0	9.2 ± 13.5	8.7 ± 12.8	7.9 ± 12.6	6.8 ± 12.4	7.1 ± 12.2	6.6 ± 12.5	6.6 ± 12.8	10.4 ± 15.6
Hip Flexion	CON	27.7 ± 3.9	29.9 ± 3.5	31.0 ± 4.1	33.7 ± 4.4	35.9 ± 4.0	38.7 ± 3.2	40.9 ± 2.5	42.4 ± 3.6	42.8 ± 3.8
	AMP-Intact	25.5 ± 6.9	27.1 ± 7.3	29.1 ± 7.7	30.9 ± 8.1	34.1 ± 9.0	37.5 ± 9.0	39.8 ± 9.6	42.4 ± 9.0	43.9 ± 9.4
	AMP-Amputated	27.1 ± 3.6	27.5 ± 3.9	29.1 ± 4.0	30.7 ± 4.0	32.6 ± 4.0	35.7 ± 5.0	37.8 ± 5.5	41.0 ± 5.8	44.3 ± 7.2
Hip Extension	CON	-12.1 ± 4.2	-14.0 ± 3.9	-16.6 ± 3.6	-17.5 ± 3.2	-18.8 ± 3.9	-19.7 ± 4.1	-18.1 ± 2.4	-15.5 ± 3.2	-15.0 ± 3.0
	AMP-Intact	-10.9 ± 6.7	-11.6 ± 6.0	-13.9 ± 6.0	-16.2 ± 6.4	-17.6 ± 6.7	-17.8 ± 7.3	-18.8 ± 8.0	-18.1 ± 8.1	-14.9 ± 10.5
	AMP-Amputated	-9.6 ± 4.1	-11.6 ± 4.9	-12.7 ± 4.9	-14.4 ± 5.0	-15.1 ± 5.5	-14.7 ± 5.5	-15.2 ± 6.3	-14.2 ± 6.8	-11.8 ± 8.9

Table 3: Peak kinematic joint angles in degrees (mean ± standard deviation) for CON, AMP-Intact, and AMP-Amputated. Significance presented from Bonferroni post-hoc testing when significant main effects were present after one-way repeated measures ANOVA. * Significantly different from CON; † Significantly different from AMP-Intact ($p<0.05$, Bonferroni corrected).

2.4 Discussion

This study aimed to determine the GTS of AMP subjects and assess whether intact side propulsive force production (indicative of intrinsic mechanical limits of the plantar flexor muscles) is a major determinant of their walk-to-run gait transition. Consistent with our first hypothesis, AMP subjects transition between gaits at a significantly slower absolute speed than CON subjects (1.73±0.13 m/s and 2.09±0.05 m/s respectively). The CON subjects gait transition speeds were consistent with previous work that has defined able-bodied gait transition speeds ranging from 1.89 and 2.16 m/s (Diedrich and Warren, 1995, 1998; Hreljac, 1993a, 1995; Hreljac et al., 2001; Hreljac et al., 2008; Kram et al., 1997; Li and Ogden, 2012; Mercier et al., 1994; Prilutsky and Gregor, 2001; Raynor et al., 2002; Segers et al., 2006; Sentija et al., 2012; Thorstensson and Roberthson, 1987; Turvey et al., 1999; Van Caekenberghe et al., 2010). Although the gait transition speeds were determined using different ranges of speeds for CON and AMP subjects (CON: 1.3-2.6 m/s; AMP: 1.0-2.3 m/s), we believe this had no bearing on the difference found between the two groups. This is supported by the fact that Prilutsky and Gregor previously reported an able-bodied GTS of 2.1±0.2 m/s, which is consistent with our findings of 2.09±0.05 m/s, even though they utilized a different range of speeds to determine that GTS (1.4-3.0 m/s) (2001). The higher variability in AMP subject gait transition speeds were not surprising given the nature of pathologic gait. AMP subjects using passive-elastic prostheses also have increased variability in preferred walking speeds (Houdijk et al., 2009). Furthermore, despite the hysteresis between the AMP subjects increasing and decreasing gait transition speeds, we were confident that collecting data relative to the averaged GTS (1.73±0.13 m/s), which is only ±0.02 m/s from the average transition speeds achieved during the increasing and decreasing protocols, would allow for a more versatile dataset to make walk-to-run and run-to-walk comparisons in the future without affecting our main conclusions.

Although the ankle-foot componentry worn by the AMP subjects was not standardized, allowing subjects to wear their own passive-elastic ankle-foot components have yielded meaningful and consistent results of both muscle activations and walking mechanics within previous studies (Adamczyk and Kuo, 2014; Fey et al., 2010; Silverman et al., 2008). Providing a standardized ankle-foot component would require an adaptation period to the novel components and potentially affect the subjects level of comfort with the protocol. Given the consistent decrease in GTS across all AMP subjects with respect to their matched CON, and similar variability in AMP-subject outcome measures compared to CON, we are confident that our inclusion criterion of testing only AMP subjects with passive-elastic ankle-foot components was sufficient to maintain the group homogeneity. Minimal differences in kinematics between CON subjects and the AMP-Intact side verified amputee subjects were not using a different walking strategy. This difference in ankle kinematics compared to the AMP-Amputated side was not surprising due to the prosthetic foot-ankle complex lacking actuation.

Contrary to our second hypothesis, AMP subjects were able to continue generating higher peak propulsive forces on both their intact and amputated sides at speeds beyond their preferred GTS. Results from CON subjects exhibiting limited peak propulsive force production above GTS were consistent with previous work (Neptune and Sasaki, 2005). The limited propulsive force production at higher than normal walking speeds found in CON subjects, supports previous findings implicating the plantar flexors and their unique force-length-velocity characteristics as a major determinant of the walk-to-run gait transition in able-bodied subjects (Arnold et al., 2013; Farris and Sawicki, 2012; Malcolm et al., 2009a; Neptune and Sasaki, 2005). Conversely, the AMP subjects abilities to increase propulsive force production at walking speeds above their preferred GTS suggest the force-length-velocity characteristics of the plantar flexors are not a major determinant of the walk-to-run transition in

unilateral, transtibial, amputees. In assessing the effects of absolute speed changes on propulsive force production, we observed the polynomial fits of CON and AMP-Intact anterior-posterior propulsive forces tracked together. Additionally, the 95% confidence intervals of the data almost completely overlay one another. Since AMP subjects had significantly lower GTS, these findings support that propulsive force production is a function of changes in absolute speed rather than relative to the preferred walk-to-run transition speed. Thus, there must be another variable or variables primarily responsible for the gait transition in the AMP population.

These findings do not rule out previous explanations for the determination of the GTS that feature a conglomeration of determinants (Bartlett and Kram, 2008; Malcolm et al., 2009b). Bartlett and Kram found that selectively perturbing the demand on dorsiflexors, plantarflexors, and hip flexors resulted in altered walk-to-run transition speeds, however perturbing multiple muscle groups at once did not produce a summative effect (2008). They introduced the theoretical framework that a critical threshold of influence must be met in order for the walk-to-run transition to occur, in which an ultimate, underlying trigger can be influenced by various muscle groups, whose impact can change with walking conditions (e.g. incline walking). The weakest link concept, introduced by Malcolm et al., is another theoretical framework supporting the idea that there are multiple determinants or factors affecting the walk-to-run transition speed, and whichever one is stressed to a critical point first, ultimately determines the speed of the transition (2009). Most likely the impaired nature of AMP subject walking amplifies another determinant of the walk-to-run gait transition to a level in which it becomes the limiting factor. However, there is also the possibility that the same determinant of the walk-to-run gait transition is responsible for the CON and AMP subject transitions, and the plantar flexor force-length-velocity characteristics associated with the gait transition in CON subjects is correlative rather than causal. As we did not directly measure muscle fascicle

force, fascicle shortening velocity, or fascicle length changes, future investigation of AMP subject gait transitions would benefit from using ultrasound to directly measure AMP-Intact plantar flexor force-length-velocity characteristics.

To our knowledge, this is the first investigation of gait transitions in persons with a lower limb amputation. Identifying the average walk-to-run and run-to-walk transition speeds in otherwise healthy unilateral, transtibial amputees, provides unique foundational information for future studies. Potential applications of this research include expanding the use of a single powered prosthetic device for both walking and running. Presently, prosthesis design is migrating toward powered biomimetic components, which have been shown to decrease oxygen consumption as compared to passive-elastic prosthesis during walking (Herr and Grabowski, 2012). However, these powered prosthetic foot-ankle components only allow for walking, which is not surprising since the gait transition has long been a challenge in the field of legged robotics (Aoi et al., 2012). Characterizing the gait transition speed in amputees and identifying key variables underlying the transition, provides important foundational data for both the control and gait versatility of future powered prosthetic foot-ankle devices, powered exoskeletons, and legged robots.

In conclusion, since unilateral, transtibial amputees transition between gaits at a lower speed than able-bodied controls and are still able to generate higher propulsive forces walking at speeds above their preferred gait transition speed, their walk-to-run transition is not likely dictated by the force-length-velocity characteristics of the intact plantar flexor muscles. This suggests that, as an experimental model, unilateral, transtibial amputees can provide unique insights for decoupling the previously identified performance limit of plantar flexor muscles from the preferred gait transition speed in order to probe other potential determinants.

CHAPTER III

AIM 2: TIBIALIS ANTERIOR IS THE MAIN FLEXOR MUSCLE ASSOCIATED WITH THE WALK-TO-RUN TRANSITION IN UNILATERAL, TRANSTIBIAL AMPUTEES

**This chapter is currently in preparation for submission to the Journal of Experimental Biology*

3.1 Introduction

An important facet of understanding human locomotion is the control of the transition between gaits. Consequentially, the walk-to-run transition has been an active topic of debate and investigation for the better part of the past century (Margaria, 1938). Global variables such as metabolic energy minimization (Minetti et al., 1994) and pendular dynamics (Hubel and Usherwood, 2013; Kram et al., 1997), have been identified as factors that ultimately determine the optimal walk-to-run gait transition speed. It is suggested that the nervous system via sensory feedback, however, plays a more immediate role in the online step by step determination of the walk-to-run transition speed (Harischandra et al., 2011; MacLeod et al., 2014; Thorstensson and Roberthson, 1987).

These sensory afferent signals can provide rapid feedback on a variety of biomechanical parameters that have been identified as potential determinants or triggers of the walk-to-run transition, which include: force-length-velocity limits of plantarflexor muscles in propulsive force production (Arnold et al., 2013; Farris and Sawicki, 2012a;

Lai et al., 2015; Malcolm et al., 2009a; Neptune and Sasaki, 2005); minimizing swing-phase ankle and stance phase hip joint loads (Farris and Sawicki, 2012b; Pires et al., 2014); an increased sense of exertion specifically from the tibialis anterior muscle activation associated with heel strike (Malcolm et al., 2009b; Segers et al., 2007b); and the increased activation and stress of swing-related flexor muscles (tibialis anterior, rectus femoris and biceps femoris long head) (Hreljac, 1995; Hreljac et al., 2001; MacLeod et al., 2014; Prilutsky and Gregor, 2001). With all of these variables exhibiting correlations with the walk-to run transition speed, it has been difficult to identify which among these are most strongly associated with the transition and may play more of a causative role in determining the gait transition. Furthermore experiments perturbing able-bodied locomotion to probe these variables via selective muscle fatigue (Segers et al., 2007b), assisting and resisting movements (Bartlett and Kram, 2008; Malcolm et al., 2009a; Malcolm et al., 2009b), changes in incline (Minetti et al., 1994) or acceleration (Li, 2000; Segers et al., 2007a; Thorstensson and Roberthson, 1987; Van Caekenberghe et al., 2010) have yielded significant but relatively small changes in the walk-to-run transition speed ($\sim$0.10 m/s). This has made it difficult to selectively decouple the previously identified variables from the walk-to-run transition speed to assess their potential contributions to the change in gait.

In able-bodied subjects, limits in propulsive force production during walking due to muscle fascicle shortening dynamics, appear to coincide with the walk-to-run transition speed; however, this is not the case in unilateral, transtibial amputee subjects (Aim 1). The ability of plantarflexor muscles to generate propulsive force as a determinant of the able-bodied walk-to-run transition is supported by the observation that force-length-velocity dynamics of these muscles limit propulsive force production at walking speeds greater than the preferred walk-to-run transition speed (Neptune and Sasaki, 2005). Transitioning from a walk to a run at the preferred transition speed

greatly reduces fascicle-shortening velocities in the plantarflexor muscles, resulting in increased propulsive force production (Farris Sawicki, 2012; Arnold, 2013). Our recent investigations of walk-to-run transitions in unilateral, transtibial amputees revealed that amputee subjects transition between gaits at a preferred speed on average 0.36 m/s lower than their matched, able-bodied controls (1.73 ± 0.13 and 2.09 ± 0.05 m/s respectively) (Aim 1). This lower transition speed occurs despite the fact that amputee subjects are able to continue generating higher propulsive forces at speeds beyond their preferred gait transition speed. This suggests any limit of the intact-side plantarflexor muscles force production is a function of absolute walking speed rather than indicative of the walk-to-run transition speed. Thus, studying unilateral, transtibial amputees provides a unique opportunity to decouple propulsive force production from the walk-to-run transition to further probe the contributions of muscle activations on the transition speed.

The criterion we used for determining if a variable was a determinant of the walk-to-run transition speed was similar to the previously described undesirable variable by Prilutsky and Gregor (2001). That is, we sought to test whether a hypothesized undesirable variable became significantly larger at or near the gait transition speed (i.e. 90, 100, or 110% GTS) compared to when running at the same speed, and maintained this significant different between gaits at each subsequent speed (i.e. up to 130% GTS). Thus identifying a 'critical divergent point' prior to the gait transition where walking activations become larger than running activations. If this critical divergent point for an undesirable variable coincided with the preferred walk-to-run transition speed, it would support the idea that one function of the gait transition is to reduce this undesirable variable (Hreljac, 1993a, 1995; MacLeod et al., 2014; Pires et al., 2014; Prilutsky and Gregor, 2001). If walking activations visually became higher than running activations, but significant differences were not found at 90, 100, or 110% GTS and maintained to 130% GTS, the point at which walking activations

visually become higher than running were termed non-critical divergent points.

The goal of this work was to examine whether muscle activations are a function of changes in absolute walking speed or a major determinant of the walk-to-run gait transition speed in unilateral, transtibial amputees. We hypothesized that the lower gait transition speed in unilateral, transtibial amputees, would coincide with the critical divergent point where 1) swing- phase tibialis anterior, rectus femoris, and biceps femoris long head muscles and 2) stance phase tibialis anterior muscles would show much greater activation during walking as compared to running at the same speeds. To test these hypotheses we studied unilateral, transtibial amputees and their matched, able-bodied controls while walking and running at speeds of 50-130% of each subjects individual gait transition speed on a custom, instrumented dual belt treadmill. Ground reactions forces, marker location, and electromyographic (EMG) data were simultaneously recorded.

3.2 Materials & methods

3.2.1 Subjects

Ten unilateral, transtibial amputee (AMP) subjects (5 males, 5 females; age: 26.7 $\pm$ 4.5 years; mass: 67.4 $\pm$ 14.6 kg; intact leg length: 91.50 $\pm$ 5.58 cm) and ten, matched, able-bodied control (CON) subjects (5 males, 5 females; age: 29.6 $\pm$ 6.9 years; mass: 67.2 $\pm$ 10.0 kg; leg length: 91.08 $\pm$ 5.41cm) gave written informed consent to participate in the Georgia Institute of Technology IRB approved protocol. The subjects discussed in Aim 2 are the same subjects used in the Aim 1 investigation. Each CON subject was rigorously selected to best match the sex, age, weight, leg length, activity level, and training type of each corresponding AMP subject. There was no significant difference in age, weight, and leg length between the two groups (Table 1, Aim 1). All CON subjects were free of previous musculoskeletal trauma. Both CON and AMP persons were excluded from participating in the study if they were pregnant, diabetic,

sedentary, or suffering from a cardiovascular or neurological pathology. AMP persons were excluded from participating in the study if their prosthesis included a Solid-Ankle Cushion Heel (SACH) or powered ankle foot. Seven of the amputations were due to trauma while three were elective amputations due to congenital deformity. All AMP subjects wore their own custom made, well fitting, prosthesis, which were all categorized as typical passive elastic energy storage and return commercial devices.

3.2.2 Experimental protocol

The locomotion protocol was completed over two days no more than one week apart, with subjects refraining from exercise before testing. On each day, subjects habituated to walking and running on the treadmill at self-selected speeds for three minutes with two-minute rest periods. Day 1 collection consisted of an incremental speed protocol completed on a single treadmill belt to determine each subjects individual gait transition speed. Subjects were asked to both walk and run at speeds of 1.3-2.6 m/s for CON subjects and 1.0-2.3 m/s for AMP subjects. After a maximum of 30 seconds at each speed, subjects verbally indicated whether they preferred to walk or run. The incremental protocol consisted of two parts: (i) increasing speeds by 0.1 m/s (walk-to-run); and, (ii) decreasing speeds by 0.1 m/s (run-to-walk). The transition speeds were defined as the lowest preferred running speeds and highest preferred walking speeds, for the increasing and decreasing portions respectively. The first iteration of this procedure, both increasing and decreasing speeds, was used as practice. It was completed twice more with the presentation of speed direction randomized, resulting in four transition speeds (two walk-to-run, two run-to-walk). These four transition speeds were averaged to determine the overall gait transition speed (GTS). A more detailed account of the protocol can be found in Aim 1 and is similar to those used in previous gait transition investigations (Hreljac, 1993b; Kram et al., 1997; Prilutsky and Gregor, 2001).

On day 2 each subject completed a total of 18 randomized conditions: 2 gaits x 9 speeds. Subjects were instructed to walk and run on a custom, instrumented, dual-belt treadmill at speeds 50, 60, 70, 80, 90, 100, 110, 120, and 130% of their previously determined GTS (100% to each individuals GTS). Data were collected for 30-seconds at each gait-speed combination. Subjects rested a minimum of two minutes between each condition. Simultaneous acquisition of all marker, ground reaction force, and electromyographic data was all accomplished with Vicon Motion Analaysis Software (Workstation 5.2.4). Data analysis was completed using custom Matlab code (Mathworks, 2013b).

3.2.3 Kinematics and kinetic recording & analysis

Sixteen retroreflective markers were placed bilaterally on each subjects second metatarsophalangeal joint, lateral malleolus, heel, shank segment, lateral condyle, thigh segment, anterior superior iliac spine, and posterior superior iliac spine. For AMP subjects, marker placement on the prosthetic limb was matched to the intact side. We applied a low-pass, zero-phase lag, fourth order Butterworth filter at 10 Hz to marker data. Three-dimensional lower extremity marker data were collected by a six-camera Vicon motion analysis system (120Hz, Oxford, UK).

Mechanically isolated force plates embedded beneath each treadmill collected bilateral ground reaction force (GRF) data (1080 Hz, Advanced Mechanical Technology Incorporated, Watertown, MA, USA (see (Kram et al., 1998). A vertical ground reaction force threshold of 32 newtons was used to define foot contact events. A 20 Hz low-pass, zero-phase lag, fourth order Butterworth filter was applied to all GRF data. We calculated sagittal plane joint moments for CON subjects and AMP subjects using inverse dynamics and segment inertial characteristics (Winter, 2005). Body weight normalized means of 10 steps for each leg of interest (CON, AMP-Intact, AMP-Amputated) during each condition (gait x speed combination) were analyzed.

3.2.4 Electromyographic recording & analysis

Surface electromyographic data (EMG) (1080Hz, Noraxon 16-channel) were collected from tibialis anterior (TA), soleus (SO), medial gastrocnemius (MG), vastus medialis (VM), rectus femoris (RF), and biceps femoris long head (BF). All muscles were collected bilaterally on CON subjects. AMP subject residual TA, SO, and MG were not collected on the amputated side due to occlusion by the prosthetic socket. Data were bandpassed 20-450Hz, demeaned, rectified, and 10 Hz lowpass filtered. A 40 ms shift in the EMG data was applied to account for electromechanical delay to align the activation data with the mechanical action of the muscles (Caldwell and Li, 2000; Prilutsky and Gregor, 2001; Prilutsky et al., 1998). For each condition (gait x speed combination), data from 10 steps were normalized to the 130% walking trial peak for each subject (Burden, 2010; Shiavi et al., 1998).

3.2.5 Amputated side mass analysis

In order to assess potential discrepancies between amputee intact leg and amputated leg mass, prosthetic limb weights as well as body composition data and was obtained for 7 of the 10 amputee subjects (Table 4). The subset of amputees received dual-energy x-ray absorptiometry (DEXA) scans without their prosthetic limbs using a Lunar Prodigy whole body scanner and software (GE Medical Systems, Madison, WI). Most amputee subjects were scanned the same week they completed the locomotion protocol (five of the seven amputee subjects), while one subjects scan was three months post, and two amputee subjects scans were within three years. Using Lunar Prodigy software, for each subject, virtual transections were made at the femoral neck on each limb in order to calculate the overall mass of the intact side and amputated sides separately. All subjects wore their own, standard running shoes.

Table 4: Amputated & intact side leg masses

	Masses (kg)				
	Amputated Side			Intact Side	**Amputated Side- Intact Side**
AMP Subject #	Residual Limb	Prosthetic Limb	Total		
1	8.93	3.23	12.16	11.31	**0.85**
2	6.63	1.14	7.77	10.29	**-2.52**
3	5.32	2.32	7.64	8.13	**-0.49**
5	7.22	2.09	9.31	10.84	**-1.53**
7	10.55	3.16	13.71	13.41	**0.30**
8	7.08	3.41	10.49	10.05	**0.44**
9	7.96	2.45	10.41	10.13	**0.28**
Subtotal	7.67 ± 1.69	2.54 ± 0.80	10.21 ± 2.22	10.59 ± 1.59	**-0.38 ± 1.22**

3.2.6 Statistical analysis

Due to the matched design and extensive subject matching criteria, we employed a within-subject statistical design to perform paired t-tests for between subject group comparisons (CON vs. AMP). To assess relative speed differences in moments and muscle activations between gait type (walk vs. run), we ran separate two-way repeated measures analysis of variance (2 gaits x 9 speeds), for each leg type (CON, Amp-Intact, vs. Amp-Amputated) to test for significant gait-speed interactions. If Maucheys test of sphericity was violated degrees of freedom were corrected using Greenhouse-Geisser estimates of sphericity. When a significant interaction effect of gait and speed was found, post-hoc, Bonferroni-corrected, pairwise comparisons for each gait-speed combination were employed for a simple main effects analysis. Significance was defined as a Bonferroni adjusted alpha level of 0.05 (p-value < 0.0056). To assess absolute speed changes in moments and muscle activations between gait type (walk vs. run), quadratic polynomials were fit to the data and 95% confidence intervals of the scatter were denoted.

3.3 Results

3.3.1 Gait transition speed

As we have previously published, the gait transition speed of AMP subjects (n=10) was significantly lower than that of matched CON subjects (n=10) (1.73 ± 0.13 m/s and 2.09 ± 0.05 m/s respectively, $p<0.01$) (Aim 1). The subset of AMP subjects (n=7) that underwent additional body composition analysis also had significantly lower gait transition speeds then their respective matched controls (n=7) (1.77 ± 0.14 m/s and 2.06 ± 0.05 m/s respectively, $p<0.01$).

3.3.2 Muscle activations: Swing phase at relative speeds

Muscle activation envelops for walking (solid) and running (dashed) were similar between CON and AMP subjects (Fig. 5). Normalized amplitudes per respective relative speeds and gaits were similar between CON and AMP-Intact side muscles, however AMP-Amputated side activation amplitudes were generally slightly lower. Mean AMP-Amputated side biceps femoris long head activation at 120% GTS (Fig. 5, light pink) had a notably different envelope than other relative speeds. This was due to early swing-phase bursting in one subject. There were significant gait-speed interactions (within subject groups) for every muscle during stance and swing phase, except stance phase biceps femoris long head and vastus medialis.

Mean swing phase activations with respect to relative speed changes between walking and running for tibialis anterior were consistent between CON and AMP subjects (Fig. 6A). Tibialis anterior walking activations became significantly larger than running activations at 110% GTS for both subject groups, and the critical divergent points for each were prior to the GTS. Although swing-phase rectus femoris and biceps long head activations showed a similar crossing of walking and running data, a critical divergent point was only identified in CON subjects. Tibialis anterior muscle activations during the swing phase of the walking gait cycle were significantly

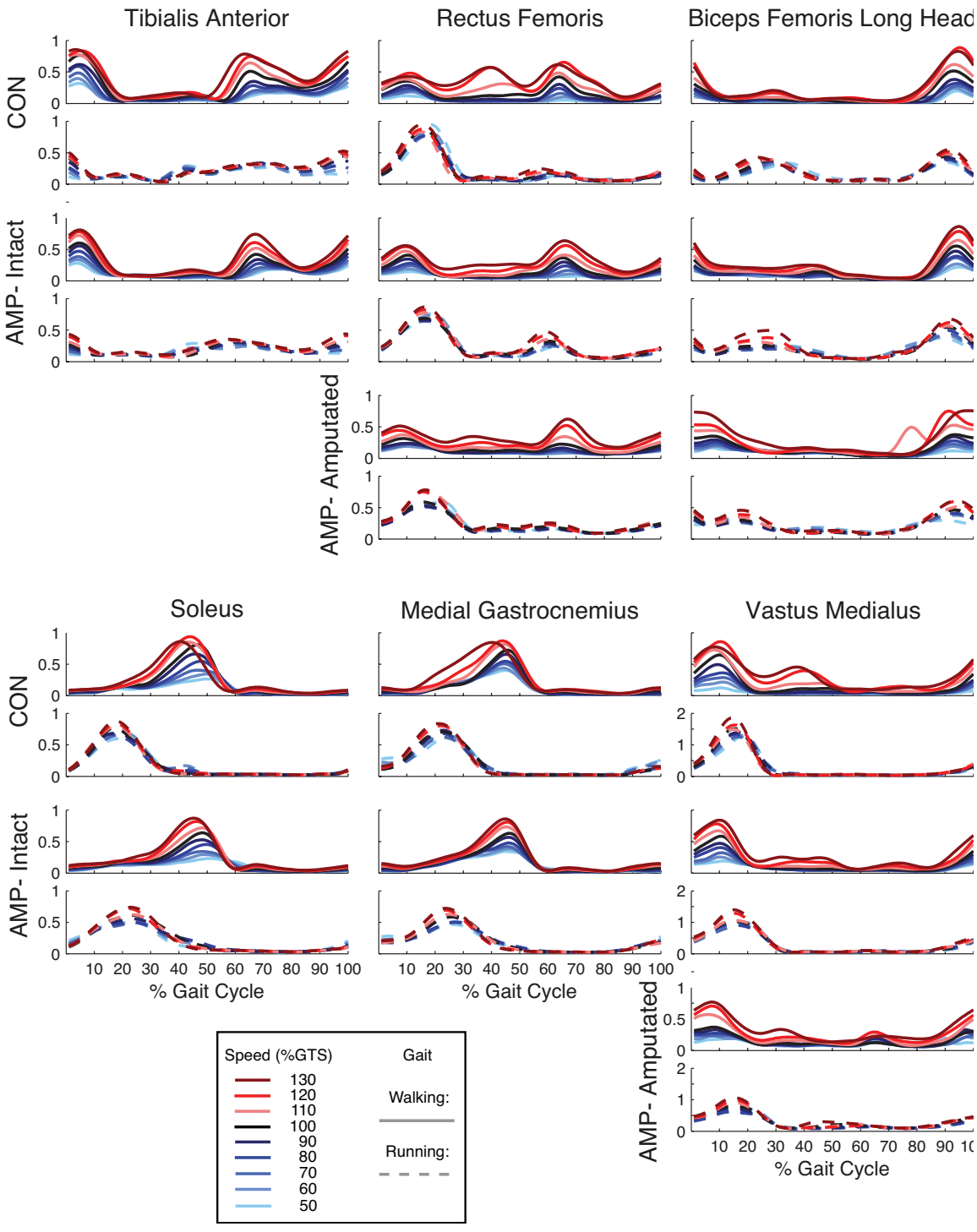

Figure 5: Mean electromyographic (EMG) traces during walking (solid lines) and running (dashed lines) at relative speeds 50-130% of the gait transition speed. All data was normalized to peak activation during walking at 130% GTS, and traces represent the mean across 10 steps for 10 subjects in each of the respective groups: CON (right leg data), AMP-Intact, and AMP- Amputated. 50-90% GTS: lightest blue to darkest blue; 100% GTS: black; 110-130% GTS: lightest red to darkest red.

higher than running activations at 110-130% GTS for both CON and AMP-Intact. In contrast, the relative speeds in which swing phase rectus femoris muscle activations were significantly higher for walking than running were not consistent between CON and AMP subjects (CON at 100-130% GTS, AMP-Intact at 110 & 120% GTS, and AMP-Amputated at 130% GTS). Furthermore, rectus femoris activations were significantly lower than running activations for AMP-Intact at 50-70% GTS, and AMP-Amputated at 50-80% GTS, but never for CON subjects. Significantly lower swing phase walking activations for biceps femoris long head were also seemingly staggered between subject groups (CON at 50 & 60% GTS, AMP-Intact at 50-80% GTS, and AMP-Amputated at 50-100% GTS), while activations during walking were significantly higher than running only for CON at 120 & 130% GTS.

Only non-critical divergent points were identified for swing-phase soleus, medial gastrocnemius, or vastus lateralis muscles in CON or AMP subjects (Fig. 6B). Few significant differences were found in comparing mean walking and running activations, and walking muscle activations never became higher than running activations at 90, 100, or 110% GTS and maintained significantly higher activations though 130% GTS. Not surprisingly, the activation magnitudes of the soleus, medial gastrocnemius, and vastus lateralis muscles during swing phase were noticeably lower than those of the tibialis anterior, rectus femoris, and biceps femoris long head. We observed significantly lower swing phase soleus muscle activations on the intact limb of amputee subjects (AMP-Intact) in walking compared to running only at 50 and 60% GTS. Soleus muscle activations in walking were significantly higher than running activations for CON at 120 and 130% GTS, and AMP-Intact at 130%GTS (Fig. 6B). There were no significant differences between walking and running for swing phase medial gastrocnemius muscle activations in CON or AMP-Intact subject groups. In the swing phase of walking, vastus medialus muscle activations were significantly lower compared to running for CON at 50% GTS, AMP-Intact at 50-90% GTS, and AMP-Amputated

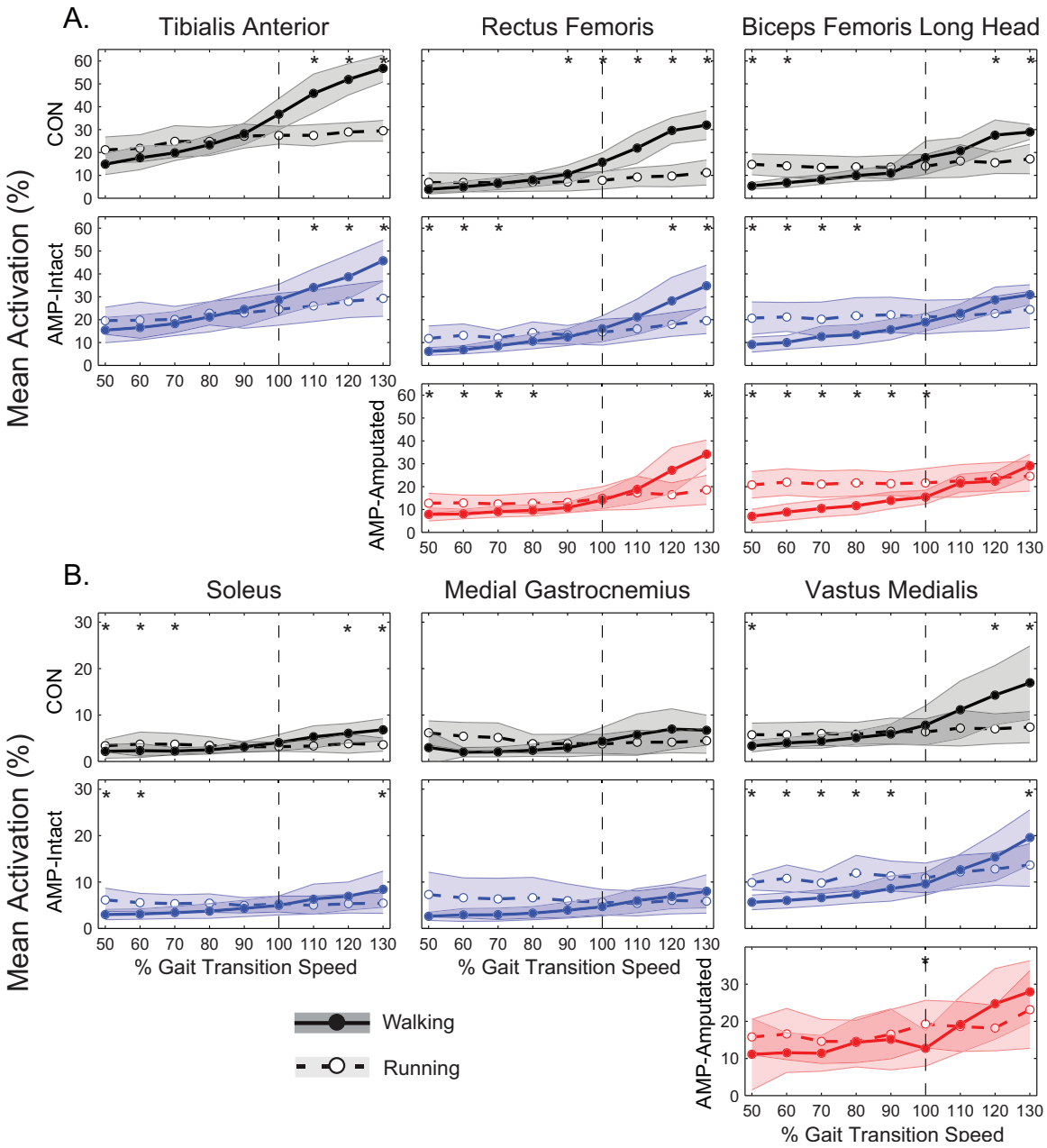

Figure 6: Average mean swing phase activation for walking and running relative to % gait transition speed (GTS). Electromyographic (EMG) activity (mean ± std) of peak stance phase activations for walking and running across speeds relative to the %GTS for A) primarily flexors and B) primarily extensors during walking. 100% GTS refers to 2.09 ± 0.05 m/s for CON subjects and 1.73 ± 0.13 m/s for AMP subjects (vertical grey dashed line). Control (CON, n=10) subject right leg data, and unilateral, transtibial amputee data (AMP-Intact & AMP-Amputated, n=10) are depicted during walking (solid circles, solid line) and running (open circles, dashed line). Data presented for tibialis anterior, rectus femoris, biceps femoris long head, soleus, medial gastrocnemius, and vastus medialis was normalized to peak activation during walking at 130% GTS and meaned across the swing phase of 10 steps. Paired t-tests compared % activation during walking vs. running within subjects at each speed relative to the GTS (*Bonferonni corrected α-level of 0.05, $p < 0.0056$).

at 100% GTS. Walking activations were significantly higher running for CON at 120 and 130% GTS, AMP-Intact at130 % GTS, and never for the AMP-Amputated side.

3.3.3 Muscle activations: Stance phase at relative speeds

During stance phase, tibialis anterior was the only muscle we identified as having a critical divergent points (CON and AMP-Intact) (Fig 7A). where walking activations became higher than running near the GTS. Stance phase, tibialis anterior critical divergent points were identified at 100% GTS for CON and 110% GTS for AMP subjects. Stance phase tibialis anterior activations were significantly higher than running activations at 100-130% GTS for CON subjects and 110-130% GTS for AMP-Intact.

No divergent points (critical or non-critical) were found for rectus femoris, biceps femoris long head soleus, medial gastrocnemius, or vastus lateralus (Fig. 7A-B). Stance phase walking activations were never significantly higher than running activations for rectus femoris (CON at 50-100% GTS, AMP-Intact at 50-120% GTS) (Fig. 7A). No significant gait-speed interaction was found for rectus femoris on the AMP-Amputated side or any of the subject groups for biceps long head activation to warrant a pairwise analysis. (Fig. 7A).

At all speeds, mean stance phase activations during walking never surpassed those of running for the soleus, medial gastrocnemius, or vastus lateralus (Fig. 7B). Stance phase soleus activations were significantly lower than running activations for CON at 50-90% GTS and AMP-Intact at 50-130% GTS. Medial gastrocnemius activations were similar, with significantly lower walking activations for CON at 50-110% GTS and AMP-Intact at 50- 110% GTS. No significant gait-speed interaction was found any of the subject groups vastus medialus activations.

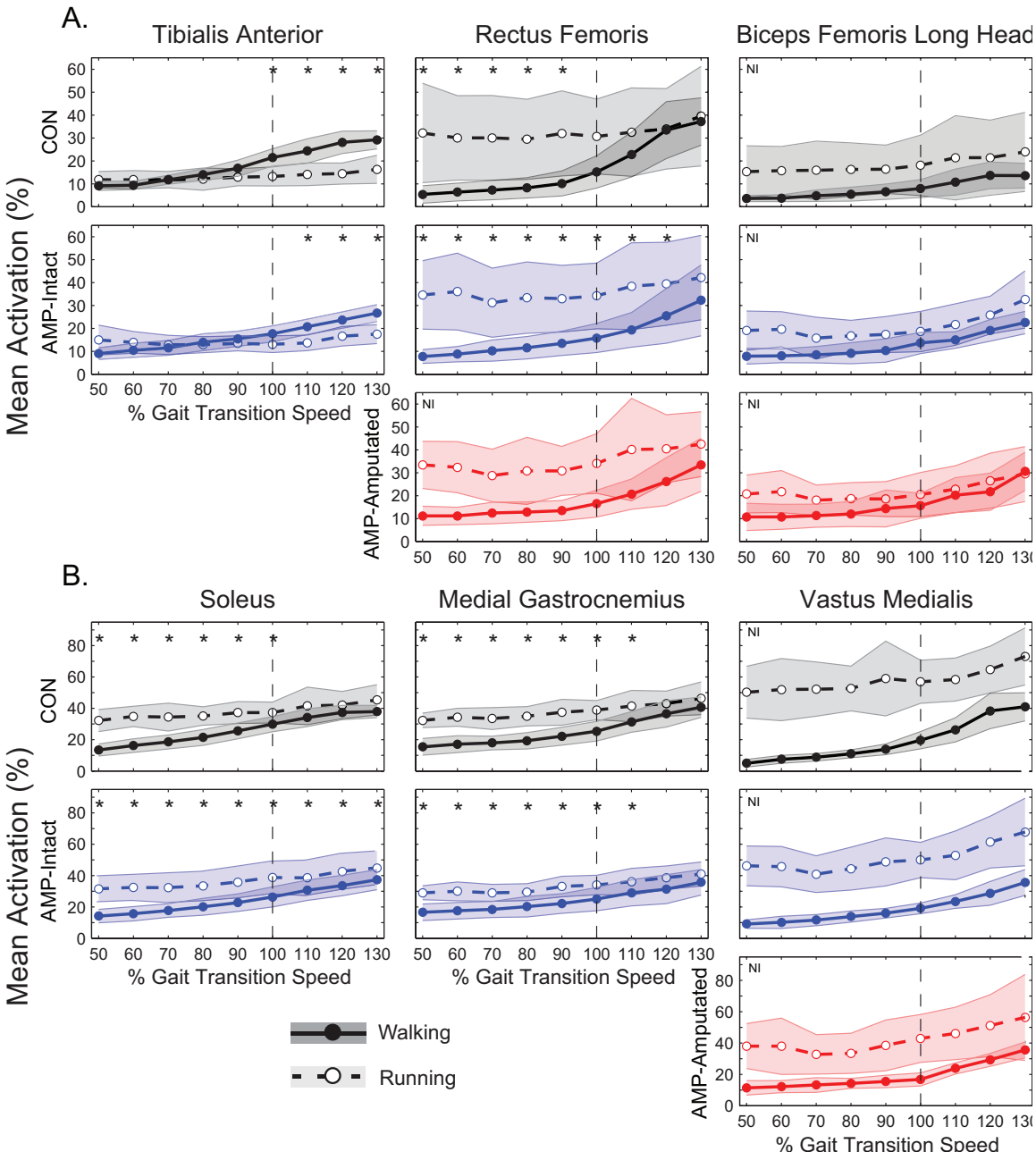

Figure 7: Average mean stance phase activation for walking and running relative to % gait transition speed (GTS). Electromyographic (EMG) activity (mean±std) of peak stance phase activations for walking and running across speeds relative to the %GTS for A) primarily flexors and B) primarily extensors during walking. 100% GTS refers to 2.09 ± 0.05 m/s for CON subjects and 1.73 ± 0.13 m/s for AMP subjects (vertical grey dashed line). Control (CON, n=10) subject right leg data , and unilateral, transtibial amputee data (AMP-Intact & AMP-Amputated, n=10) are depicted during walking (solid circles, solid line) and running (open circles, dashed line). Data presented for tibialis anterior, rectus femoris, biceps femoris long head, soleus, medial gastrocnemius, and vastus medialis was normalized to peak activation during walking at 130% GTS and meaned across the stance phase of 10 steps. Paired t-tests compared % activation during walking vs. running within subjects at each speed relative to the GTS (*Bonferonni corrected α-level of 0.05, $p < 0.0056$).

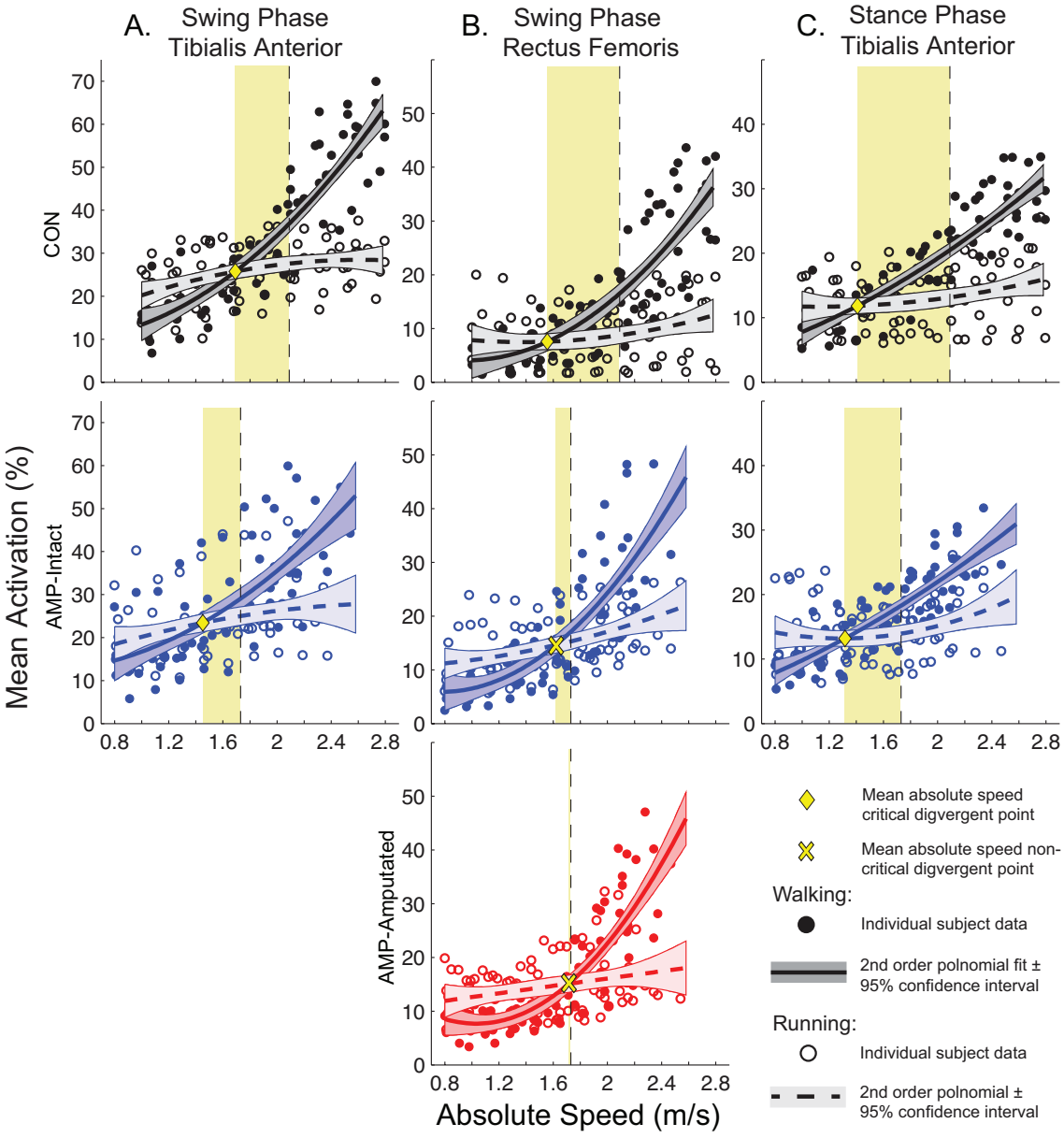

Figure 8: Individual swing-phase mean EMG at absolute speeds. (Caption next page.)

Figure 8: Individual swing-phase mean EMG at absolute speeds. Swing-phase mean EMG as a % of maximum activation for each subject during walking (solid circles) and running (open circles) are plotted with respect to absolute speed. The vertical black dashed line denotes the average gait transition speed (GTS) for CON and AMP subjects at 2.09 and 1.73 m/s respectively. Second order polynomial line fits are denoted for walking (solid line) and running (dashed line) with 95% confidence intervals of the data shaded in dark and light respective colors. Yellow boxes superimposed over the plots highlight the the area between the divergent points (where the walking activations become higher than the running activations) and the gait transition speed.Critical diverget point: Yellow diamond; Non-critical divergetnt point: Yellow "X". A) Swing Phase Tibialis Anterior: CON (walking: $r^2 = 0.66$; running: $r^2 = 0.93$); AMP-Intact (walking: $r^2 = 0.80$; running: $r^2 = 0.92$); B) Swing Phase Rectus Femoris: CON (walking: $r^2 = 0.51$; running: $r^2 = 0.75$); AMP-Intact (walking: $r^2 = 0.30$; running: $r^2 = 0.84$); AMP-Amputated (walking: $r^2 = 0.41$; running: $r^2 = 0.88$); C) Stance Phase Tibialis Anterior: CON (walking: $r^2 = 0.73$; running: $r^2 = 0.89$); AMP-Intact (walking: $r^2 = 0.73$; running: $r^2 = 0.90$).

3.3.4 Muscle activations: Absolute speeds

To further illustrate the statistical findings of the relative speed analysis, for muscles exhibiting a divergent point in their activations (swing and stance phase tibialis anterior, and swing phase rectus femoris), the walking and running mean EMG amplitudes were plotted with respect to absolute speed for all subject groups. We compared the absolute speeds at which the respective critical divergent points and non-critical divergent points of these muscles, occurred in CON or AMP subjects (Fig 8A-C). The swing phase tibialis anterior activation critical divergent point for CON was 1.69 m/s, approximately 0.40 m/s below the CON GTS of 2.07 m/s, while AMP-Intact side was 1.45 m/s, approximately 0.28 m/s below the AMP GTS of 1.73 m/s (Fig. 8A, critical divergent point: yellow diamonds; difference between critical divergent point and GTS: shaded yellow). The critical divergent point for swing-phase tibialis anterior mean EMG appeared to track with each groups respective gait transition speed. Conversely, changes in walking and running amplitudes for swing phase rectus femoris activations for AMP subjects appear to be a function of absolute speed changes rather than the GTS (Fig. 8B, critical divergent point: yellow diamond;

non-critical divergent point: yellow X). The swing phase rectus femoris mean EMG critical divergent point occurred at approximately the same absolute speed in both CON and AMP-Intact side at 1.56 m/s, and 1.62 m/s respectively. AMP-Amputated side occurred at approximately the same speed as the AMP GTS at 1.72 m/s (Fig 8B, difference between divergent points and GTS: shaded yellow). Absolute speed plots of mean stance phase tibialis anterior activity showed mean critical divergent points 1.40 m/s for CON subjects and 1.32 m/s for AMP subjects with larger differences between the critical divergent points and GTSs of 0.67 and 0.41 m/s (Fig. 8C, critical divergent point: yellow diamond; difference between divergent points and GTS: shaded yellow).

3.3.5 Joint moments

Data from a representative pair of matched subjects show the changes in joint moments across speed and between gaits (Fig. 9). Generally peak joint moments increased with speed in both walking and running. For all subjects, extensor moments became more positive and flexor moments became more negative at greater speeds, with the exception of the stance phase peak ankle moments during walking (Fig. 10). Instead, stance phase peak plantarflexion moments (positive) peak at 90% GTS in CON subjects and at 110% GTS in AMP subjects (intact and amputated sides) (Figure 10). CON subjects peak stance phase dorsiflexion moments (negative) during walking peak is at 100% GTS while AMP-Amputated side peaks at 120% (intact and amputated sides) (Figure 10, Table 5).

Almost all joint moment comparisons (within subject group: flexion or extension) had significant gait-speed interactions (Table 5). For all subject groups, no interaction effect between gait (walking and running) and speed (50-130% GTS) was found for the ankle during peak ankle plantarflexion moment during swing. AMP-Amputated did not have a significant interaction during stance phase peak ankle plantarflexion

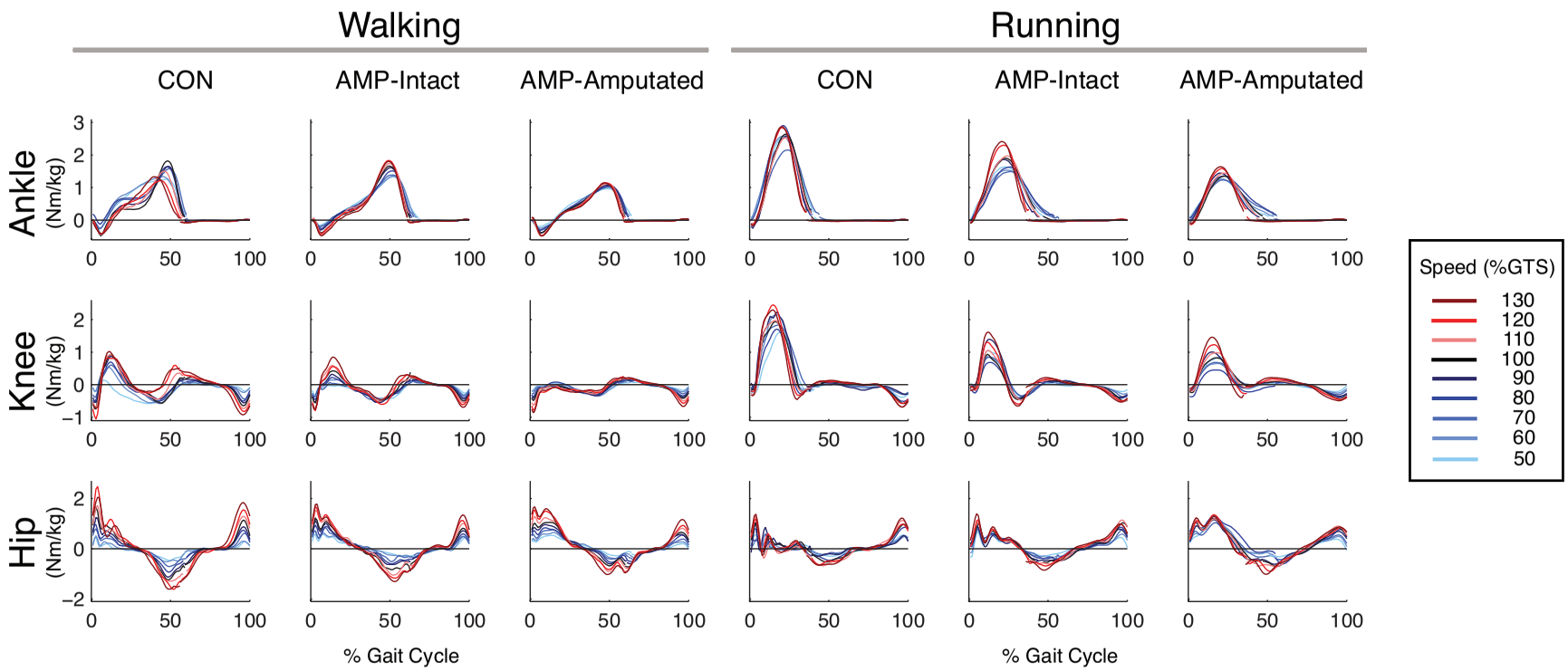

Figure 9: Representative joint moments (Nm/kg) during walking and running at speeds 50-130%GTS. Representative joint moments from one CON and AMP subject matched pair at the ankle, knee, and hip during walking and running for each relative speed 50-130% GTS. 50-90% GTS: lightest blue to darkest blue; 100% GTS: black; 110-130% GTS: lightest red to darkest red. Positive value indicate extension moments and negative values indicate flexion moments.

Table 5: Peak joint moments: Two-way ANOVA statistics

		Ankle				Knee				Hip			
		Stance		Swing		Stance		Swing		Stance		Swing	
	Two-Way ANOVA	Plant. Flex. (+)	Dorsi. Flex. (-)	Plant. Flex. (+)	Dorsi. Flex. (-)	Ext. (+)	Flex. (-)	Ext. (+)	Flex. (-)	Ext. (+)	Flex. (-)	Ext. (+)	Flex. (-)
CON	Gait	0.003	<0.001	0.011	<0.001	<0.001	<0.001	<0.001	0.001	0.003	<0.001	0.037	0.125
	Speed	<0.001	<0.001	0.400	<0.001	<0.001	<0.001	<0.001	<0.001	<0.001	<0.001	<0.001	<0.001
	Interaction	**0.001**	**0.012**	0.643	**<0.001**	**0.001**	**0.008**	**<0.001**	**<0.001**	**<0.001**	**<0.001**	**<0.001**	**<0.001**
AMP-Intact	Gait	0.002	<0.001	0.642	<0.001	<0.001	<0.001	0.003	0.241	0.097	<0.001	0.002	0.144
	Speed	<0.001	<0.001	0.056	<0.001	<0.001	<0.001	<0.001	<0.001	<0.001	<0.001	<0.001	<0.001
	Interaction	**<0.001**	**<0.001**	0.787	**<0.001**	**0.015**	**0.003**	**<0.001**	**<0.001**	**<0.001**	**<0.001**	**<0.001**	**0.001**
AMP-Amputated	Gait	0.004	<0.001	0.119	<0.001	0.001	0.020	0.006	0.070	0.323	<0.001	0.011	0.386
	Speed	<0.001	<0.001	0.375	<0.001	<0.001	<0.001	<0.001	<0.001	<0.001	<0.001	<0.001	<0.001
	Interaction	0.091	**0.048**	0.320	**<0.001**	0.163	**0.012**	**0.001**	**<0.001**	**<0.001**	**<0.001**	**<0.001**	**0.002**

or peak knee extension. Instances where peak moments became significantly larger during walking than running at relative speeds near the gait transition speed (i.e. 90, 100, or 110% GTS) were during swing phase peak dorsiflexion (negative) in AMP-Amputated (90-130% GTS), swing phase peak knee flexion (negative) in CON (90-130% GTS), AMP-Intact (110-130% GTS) and AMP-Amputated (110 & 130% GTS), stance phase peak hip extension (positive) in CON (100-130% GTS).

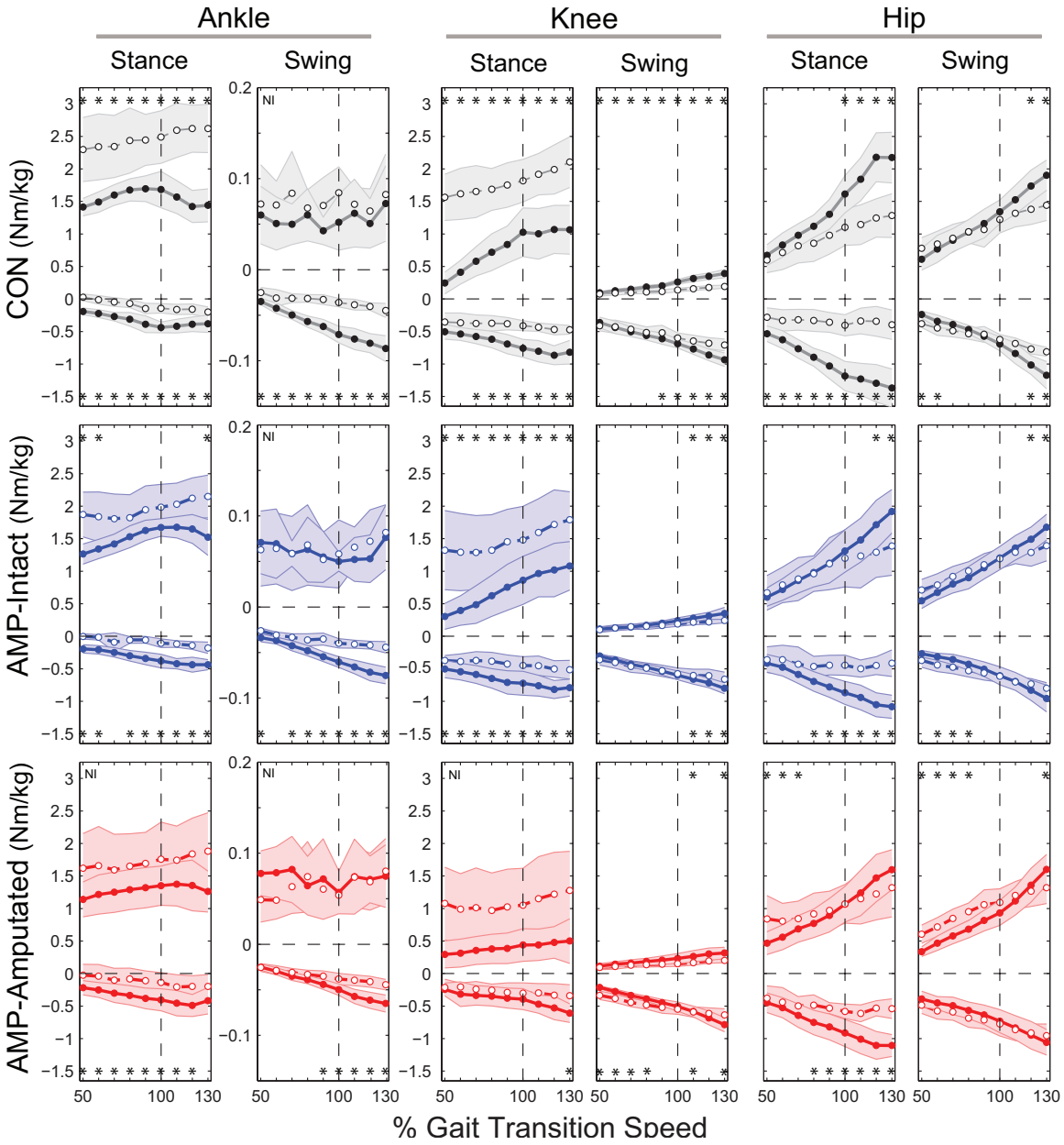

Figure 10: Peak extension and flexion joint moments (Nm/kg) during stance and swing phase of walking and running at speeds 50-130%GTS. Positive value indicate extension moments and negative values indicate flexion moments. Peak moments (mean±std) of stance and swing phase for walking and running across speeds relative to the %GTS. 100% GTS refers to 2.09 ± 0.05 m/s for CON subjects and 1.73 ± 0.13 m/s for AMP subjects (vertical grey dashed line). Control (CON, n=10) subject right leg data, and unilateral, transtibial amputee data (AMP-Intact & AMP-Amputated, n=10) are depicted during walking (solid circles, solid line) and running (open circles, dashed line). Positive value indicate extension moments and negative values indicate flexion moments. Paired t-tests compared % activation during walking vs. running within subjects at each speed relative to the GTS (*Bonferonni corrected α-level of 0.05, $p<0.0056$).

3.4 Discussion

We determined tibialis anterior muscle activation to be an important determinant of the walk-to-run transition in unilateral, transtibial, amputees, just as it is in their matched controls. The tibialis anterior muscle exhibits critical divergent points (in swing and stance phase) indicating that switching to a running gait would lead to reduced muscle activation at or above the preferred gait transition speed in both amputees and controls. In amputee subjects, the critical divergent points for the tibialis anterior muscle activation is the only muscle we observed to track with the significantly lower gait transition speed compared to able-bodied control subjects.

3.4.1 Tibialis anterior muscle is a determinant in CON and AMP subject walk-to-run transitions

Muscle activation results suggest that the tibialis anterior is the main flexor muscle, of those tested, determining the walk-to-run transition in unilateral, transtibial amputee subjects. Tibialis anterior activations during walking significantly increase above those of running (i.e., the critical divergent point) at the same relative speed (110% GTS) (Fig. 6A). Despite the significantly lower gait transition speed in AMP subjects, the swing phase tibialis anterior activations during walking were significantly higher than the activations during running at the same relative speeds in both CON and AMP subjects (110-130% GTS). This suggests that the preferred walk-to-run transition speed for both CON and AMP subjects is similarly influenced by swing phase tibialis anterior activation. Plotting the muscle activations with respect to absolute speed further supported these results (Fig. 8A). The critical divergent points (Fig. 8A, yellow diamonds, CON: 1.69 m/s, AMP: 1.45 m/s) maintained a consistent relationship with respect to the transition speeds (Fig. 8A, shaded yellow) when plotted on an absolute speed scale. AMP and CON swing-phase tibialis anterior data, are consistent with previous work in able-bodied subjects. Our results support the hypothesis that tibialis anterior is a determinant of the walk-to-run transition,

due to the increased mechanical demands during swing phase at high walking speeds (Bartlett and Kram, 2008; Hreljac, 1995; Hreljac et al., 2001; Prilutsky and Gregor, 2001).

Stance phase tibialis anterior activation also showed significantly higher walking activations compared to running for controls and amputee subjects (100-130%GTS and 110-130%GTS respectively, Fig. 7A) These findings are consistent with previous work in able bodied subjects that have implicated stance phase tibialis anterior activation as a determinant of the walk-to-run transition speed due to the rapid plantarflexion and eccentric loading of the muscle during early stance (Malcolm et al., 2009b; Segers et al., 2007b). However, unlike the tibialis anterior swing phase activations, the evidence that stance phase activations are indicative of the walk-to-run transition is not as strong. Although the critical divergent point occurs at 100% GTS in controls and 110% GTS in amputee subjects (Fig 7A), the absolute speed plots (Fig 8C) show the mean critical divergent points are very similar in absolute speed (1.40 m/s and 1.32 m/s). Thus we are unable to conclude if stance phase tibialis anterior activation have a stronger association with absolute speed changes of the walk-to-run transition speed.

3.4.2 Rectus femoris and biceps femoris long head muscle activations are a function of absolute speed changes

Previous work has also indicated contributions of swing phase rectus femoris and biceps femoris long head activations as determinants of the gait transition (Prilutsky and Gregor, 2001). Although our data from AMP subjects do not corroborate these findings, we do not refute that swing phase rectus femoris and biceps femoris long head activations may be important for the walk-to-run transition of the able-bodied system. Only non-critical divergent points were identified in AMP subject for rectus femoris and biceps femoris long head muscles activations during swing phase (Fig. 3A). The relative speeds where significant differences for femoris and biceps femoris long

head activations appeared to be staggered when comparing within a muscle, across groups (CON, AMP-Intact, and AMP-Amputated). For the rectus femoris, running activations continued to be significantly higher than walking activations at faster relative speeds in AMP-Intact (RF: 50-70% GTS), and AMP-Amputated (50-80% GTS) than CON. Conversely, walking activations began to be significantly higher than running activations at slower relative speeds in CON (90-130% GTS) than in AMP-Intact (120-130% GTS), and AMP-Amputated (130% GTS). We observed a similar pattern for swing phase biceps femoris long head activations. Swing phase rectus femoris and biceps femoris long head activations appear to be a function of changes in absolute speed rather than indicative of the walk-to-run transition speed. This finding is even more apparent when comparing swing phase rectus femoris activations in walking and running with respect to changes in absolute speed (Fig. 5B). As speed increases, rectus femoris activations during walking increase above those of running at similar absolute speeds for all subject groups, irrespective of the gait transition speed (CON: 1.56 m/s, AMP-Intact: 1.62 m/s, AMP-Amputated: 1.72 m/s).

Critical divergent points were not identified for swing phase soleus, medial gastrocnemius, or vastus medialus muscles (Fig. 6B) or stance phase rectus femoris, biceps femoris long head, soleus, medial gastrocnemius, and vastus medialus muscles (Fig. 7A & B). Hence none are considered determinants of the walk-to-run transition for controls of amputees.

Data for control subjects alone during swing are consistent with the prior findings of Prilutsky and Gregor (2001) and corroborate the idea that the increased joint moments at higher walking speeds during swing phase, and the subsequent muscle activations of the tibialis anterior, rectus femoris, and biceps femoris long head contribute to the walk-to-run transition However, given this hypothesis, our data from unilateral, transtibial amputees, indicate the main determinant of their walk-to-run transition increased activation level of the intact side tibialis anterior muscle.

3.4.3 Joint moments

Inertial characteristics for the amputated side were calculated using the intact side parameters (center of mass location, radius of gyration and, and segment mass). This decision was made due to the lack of normative data in the literature for amputee subjects (Sagawa et al., 2011). Inertial characteristics for amputees have previously been characterized by one study, however on average the amputated leg weighed 42.3% less than the intact leg (Mattes et al., 2000). The amputated leg of subjects who received DEXA scans was only -0.38 $\pm$ 1.22 kg lighter than the intact side on average (Table 4). Thus, we felt that the more accurate representation of inertial characteristics would be to use those of the intact side. Furthermore, we used a within-subject statistical analysis for all subject peak moments, with comparisons made between walking and running gaits at each speed. Hence, any potential discrepancy in the inertial characteristics used to calculate the amputated leg joint moments would not affect our general conclusions.

Consistent with electromyographic data, peak joint moments for running data remained approximately the same or increased with speed (i.e. extensor moments became more positive and flexor moments became more negative at greater speeds)(Fig. 10). Peak joint moments for walking were also consistent with EMG in the knee and the hip, and plantarflexion moments of the ankle.

3.4.4 Explanation of peak ankle flexion moments and tibialis anterior activation magnitude discrepancy

Taken alone, peak dorsiflexion moments for stance and swing do not explain the disproportionate increase in tibialis anterior activation during walking compared to running at speeds above 100% GTS. Mechanically, these seemingly attenuated peak dorsiflexion moments could be explained by an increase in coactivation at the ankle (stance and swing phase) or increased passive plantarflexion contributions from

a lengthened gastrocnemius (swing phase). A passive plantarflexion moment counteracting the active dorsiflexion, is supported by the significantly higher swing phase peak knee flexion moments during fast walking in both CON and AMP subjects, which would lengthen the gastrocnemius ultimately causing an antagonistic passive plantarflexion moment (Fig. 10). Alternatively, the disproportionate increase in walking tibialis anterior activation compared to running (in stance and swing phase), could be indicative of an independent neural response due to intra or interlimb coordination.

3.4.5 Implications of study

The results presented here provide a unique insight into our basic understanding of the human walk-to-run gait transition. Investigating locomotor deficits and extremes offer a means of probing underlying mechanisms regarding the control of normal gait. Examining gait transitions in unilateral, transtibial amputees, allows us to investigate the fundamental determinants of legged locomotion and underlying neuromuscular controls. Furthermore, this research shows that unilateral, transtibial amputees provide an in vivo model for decoupling mechanical limits (i.e. architectural limits of plantarflexors) from neural responses (i.e. tibialis anterior muscle activations) when walking at high walking speeds.

Additionally this study provides foundational data for the development of more robust transtibial prosthetic devices. Currently, the field of prosthetics is attempting to advance technology and design of lower extremity prosthetic devices to most accurately and efficiently mimic human gait. However, it does this with limited information due to the paucity of scientific knowledge regarding gait transitions. Running- and walking-specific prosthetic design would greatly benefit from an increased understanding of the able-bodied and amputee gait transition. There is also the potential for a more versatile leg that could be used for both running and walking gaits, if the control systems underlying gait transition can be isolated and then implemented in

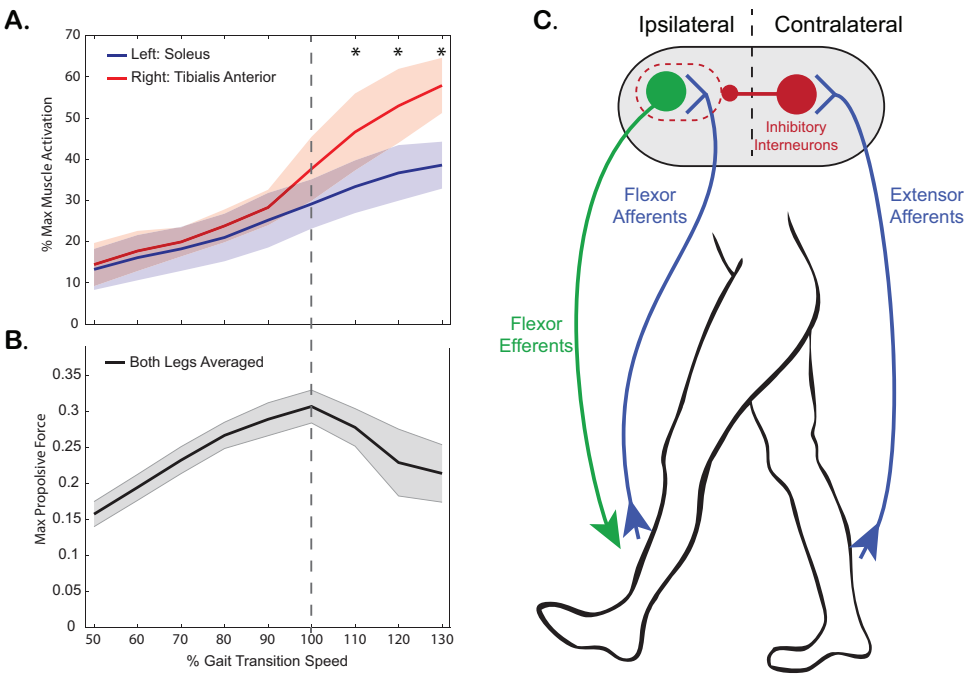

Figure 11: A) Walking muscle activations for tibialis anterior (blue) and soleus (red) muscles in able-bodied controls. B) Able-bodied control propulsive force production during walking. C) Proposed theoretical circuitry that could cause an imbalance in the stance phase extensor afferent feedback and swing phase flexor muscle activations between the legs at high walking speeds.

such a device.

3.4.6 Potential mechanism for the walk-to-run transition

Our investigation of walk-to-run transitions in unilateral, transtibial amputees provides interesting insights into the effects of a unilateral perturbation on the gait transition. Although, this study does not explicitly investigate an underlying neuromuscular mechanism responsible for the walk-to-run transition, we have posited a potential mechanism based on our results.

We suspect that a release of contralateral inhibitory stance-phase extensor afferent feedback on ipsilateral flexor muscle activations at high walking speeds is ultimately responsible for the gait transition. In walking rats, force-dependent afferent feedback during ipsilateral stance elicits a proportional decrease in sensory feedback from the contralateral swinging limb (Hayes et al., 2012; Hochman et al., 2013). This suggests

that ipsilateral extensor muscle afferents (e.g., force-depenedent Ib afferents from Golgi tendon organs) presynaptically inhibit the contralateral flexor muscles (Hayes et al., 2012; Hochman et al., 2013). In humans, ipsilateral sensory inputs affecting contralateral motor output has also been observed in stationary pedaling studies (Ting et al., 2000; Ting et al., 1998). This evidence leads us to believe that extensor (most likely Ib force-dependent) afferents of the ipsilateral side inhibits the flexor muscle activations of the contralateral side in humans. Previous findings show plantarflexor force production becomes limited at high walking speeds (Neptune and Sasaki, 2005). We found similar results in Aim 1 (Fig. 11B). We propose both the extensor an flexor muscles are implicated in the walk-to-run transition rather than solely changes in force feedback directly onto the central pattern generator. Previous work showed targeted fatiguing of the tibialis anterior muscle (Segers, 2007) and selectively increasing and decreasing the swing phase activations (Bartlett Kram, 2008) can also alter the walk-to-run transition speed.

We suspect decreases in ipsilateral force feedback could lead to a disinhibition of contralateral flexor efferents and subsequent motor output. We propose a release in inhibition leads to an imbalanced increase in contralateral flexor muscle activations, surpassing that of the ipsilateral extensor muscle activations. This imbalance between the limbs, ultimately triggering the walk-to-run transition. The disproportionate increases we observed in tibialis anterior activations during walking at speeds above the gait transition speed in comparison so plantarflexor activations supports this idea (Fig. 11A). Figure 11C illustrates a simplistic schematic of the proposed theoretical circuitry underlying the contralateral inhibition as set by the ipsilateral extensor afferent feedback. Further investigations should seek to apply a controlled assessment of the effects of extensor sensory feedback on contralateral flexors.

3.5 Conclusion

We concluded that in unilateral, transtibial amputees, swing phase activations or at least the tibialis anterior are a major determinant of their walk-to-run transitions. Swing phase dorsiflexion moments alone do not explain these results and additional work is necessary to probe potential mechanical and neural explanations. Furthermore, swing-phase rectus femoris and biceps femoris long head activations and their respective joint moments, are a function of changes in absolute speed and thus not indicative of the significantly lower gait transition speed in unilateral, transtibial amputees.

CHAPTER IV

AIM 3: THE EFFECTS OF CONTRALATERAL BELOW-KNEE ISCHEMIC BLOCK ON IPSILATERAL MOTOR OUTPUT

4.1 Introduction

The spontaneous gait transition is an example of afferent feedback modulating locomotion in humans (unpublished work by Graham Brown as described by Lundberg and Phillips, 1973; Hagio et al., 2015). Afferent feedback is well regarded as important to the control and adaptation of locomotion. In animal models, increasing descending drive by stimulating the mescenphalic locomotor region of the brain can elicit walk-to-run gait transitions (Shik et al., 1966; Shik et al., 1969; Steeves et al., 1987). However, to our knowledge, brain stimulation alone (without afferent feedback) has never been shown to result in a gait transition. Muscle activations during locomotion are modulated via ipsilateral (Hoogkamer et al., 2012; Mazzaro et al., 2005b; Sinkjaer et al., 2000; Zehr et al., 2001b; Zehr et al., 1997) and contralateral (Hayes et al., 2012; Hochman et al., 2013; Hohne et al., 2012; Hoogkamer et al., 2012; Zehr et al., 2001a) afferent feedback. These modulations support interlimb coordination to maintain dynamic stability. To date, the vast majority of gait transition literature has focused on legs ipsilaterally, neglecting the possibility of afferent contributions to interlimb coordination as a major determinant of the walk-to-run transition.

Recent work in rats suggests a contralateral force dependent afferents could presynaptically inhibit ipsilateral flexor muscles. Investigations during walking in a rat spinal cord-hindlimb preparation show afferent feedback during contralateral stance

(limb loading and toe contact) which elicits a proportional decrease in sensory feedback from the ipsilateral swinging limb, as measured from ipsilateral dorsal root potentials (Hayes et al., 2012; Hochman et al., 2013). This work suggests that contralateral extensor muscle afferents (most likely force-dependent Ib afferents from Golgi tendon organs) could decrease ipsilateral flexor muscle output during swing phase via presynaptic inhibition.

This interlimb pathway is corroborated by human pedaling studies. Ting, et al. showed ipsilateral tibialis anterior and rectus femoris activation decrease during flexion phase (mid-upstroke of the pedaling cycle), when high rhythmic extensor force is generated concomitantly on the contralateral side (mid down stroke, due to anti-phasing of two-legged pedaling), in comparison to when the contralateral limb is held static (1998, 2000). This ipsilateral decrease in flexor muscle activation was only present when the contralateral limb was moving out of phase with the ipsilateral limb (as is indicative of normal pedaling), hence this interlimb coordination response appears to be locomotor-dependent. Furthermore, there is no change in tibialis anterior or rectus femoris activation when compared to a static contralateral limb, when the contralateral limb generates a low rhythmic extensor force. This evidence leads us to believe that extensor (most likely Ib) afferents of the contralateral side inhibits the flexor muscle activations of the ipsilateral leg in humans.

This interlimb coordination could have implications to the underlying neural mechanism responsible for the walk-to-run transition. We suspect that a release of contralateral inhibitory stance-phase extensor afferent feedback on ipsilateral flexor muscle activations at high walking speeds is ultimately responsible for the gait transition. Previous findings in able-bodied individuals show plantarflexor force production decreases at high walking speeds (near the gait transition speed) (Neptune and Sasaki, 2005). If a contralateral reduction in force production leads to a subsequent reduction in force feedback, given the interlimb circuitry seen in walking rats and pedaling

humans, then a subsequent facilitation of ipsilateral flexor motor output would be expected. The natural release in inhibition at high walking speeds would lead to an imbalanced increase in contralateral flexor muscle activations, surpassing that of the ipsilateral extensor muscle activations (as seen in Aim 2). Thus, an imbalance in the stance phase extensor afferent feedback and swing phase flexor muscle activations of the limbs may be triggering the spontaneous transition from walking to running. The purpose of this work is to quantify the effects of contralateral, below-knee deafferentation on ipsilateral limb flexor motor output during locomotion. This is a necessary first step toward understanding a potential interlimb neuromuscular mechanism present during human locomotion, and potentially responsible for the walk-to-run transition. We hypothesize that diminished afferent feedback from the contralateral extensor muscles below the knee will cause an increase in flexor muscle activation of the ipsilateral side due to contralateral extensor afferents normally having a net inhibitory effect on the ipsilateral flexor muscles.

To accomplish this, we imposed a below-knee ischemic nerve block as a means of deafferentation. Ischemic nerve block (IB) is a safe, reversible and reliable means of deafferentation (Baron and Irving, 2002; Christensen et al., 2007; Schlee et al., 2009; Voller et al., 2006). Due to the locomotion-dependent nature of the proposed pathway, we must assess the effects of contralateral afferent feedback on ipsilateral motor output during rhythmic locomotor movement. Furthermore, the task mechanics, especially of the ipsilateral side, must be well controlled despite the imposed unilateral afferent perturbation to prevent confounding influences on the muscle activations. As changes in balance, step lengths and stance/swing times have been noted in walking studies utilizing ischemia as a perturbation (Dickey and Winter, 1992), cycling is a preferable paradigm to perturb the able-bodied locomotor system and minimize potential confounders, which can alter task mechanics. We used a cycle ergometer with mechanically decoupled cranks.

4.2 Materials & methods

4.2.1 Subjects

Nine able-bodied subjects (8 males, 1 female) gave written informed consent to participate in the Georgia Institute of Technology IRB approved protocol. One subject was unable to maintain appropriate crank phasing during the ischemic block portion of the protocol and was excluded. The results presented here are from the remaining 8 subjects, (7 males, 1 female; age: 29.69 $\pm$ 5.21 years; mass: 82.60 $\pm$ 6.77 kg; leg length: 91.43 $\pm$ 3.84 cm). All subjects were free of previous major musculoskeletal and neuromuscular trauma. Potential subjects were excluded from participating in the study if they were pregnant, diabetic, sedentary, or suffering from a cardiovascular or neurological pathology. All subjects had at least some experience with cycling prior to enrollment.

4.2.2 Experimental protocol

To test the effects of contralateral ischemic deafferentation (donor leg- right side) on the ipsilateral leg (recipient leg- left side) we developed a custom modified cycle ergometer with mechanically decoupled cranks (Fig. 12) and custom instrumented pedals (Broker and Gregor, 1990). Pedaling on a mechanically decoupled cycle ergometer is an appropriate paradigm to severely perturb the able-bodied locomotor system without the confounding influence of balance or changes in stance-swing times. Decoupled cranks loaded with constant resistance on separate flywheels ensures that each leg will pedal against the same bilateral load for all conditions as we manipulate the afferent feedback unilaterally. Constant-torque springs applied to the independent cranks will resist extension and aid in flexion as would happen in a regular coupled cycle ergometer, as previously done by Ting et al. (2000). This ensures the task mechanics of the decoupled set up are equivalent to regular cycling, and more closely mimics walking, as gravity and inertia aids the flexion phase of walking gait.

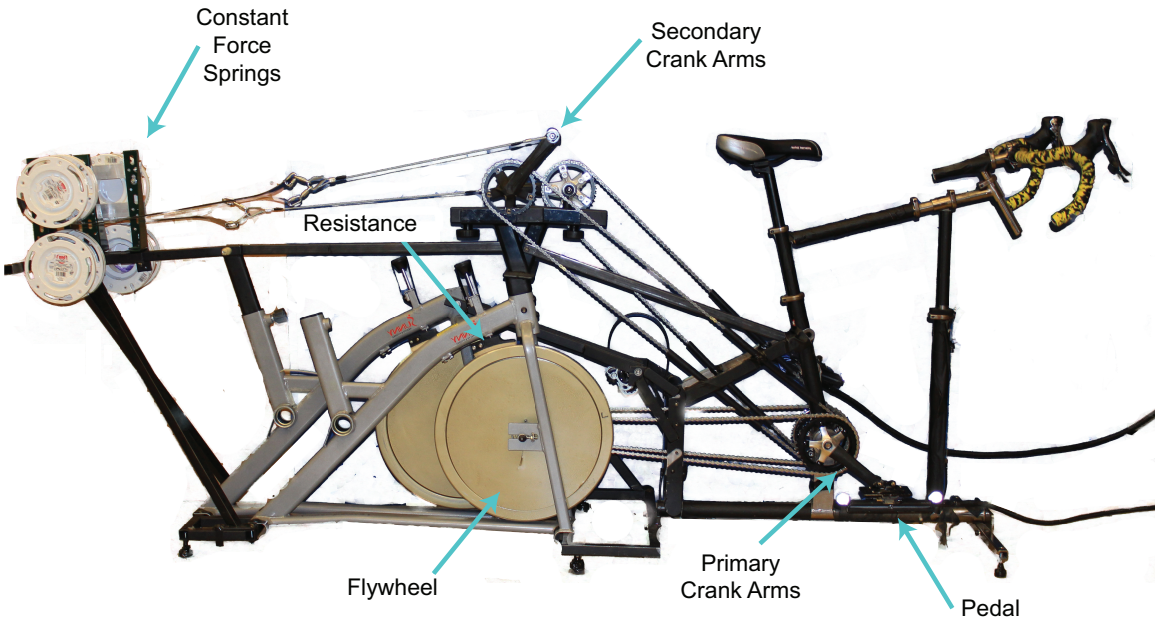

Figure 12: Custom mechanically decoupled cycle ergometer.

The protocol was completed on two consecutive days: Day 1- Training; Day 2- Ischemic Deafferentation. Subjects refrained from exercise before testing each day. Saddle height was set to 95% of mean leg length, followed by fine adjustments based on subject feedback regarding comfort. The same saddle height was used on both days of collection. Clip-in pedals and a standard set of cycling shoes (Fig. 13) were utilized to keep the subjects feet in contact with the pedals at all times. Subjects were instructed to concentrate on three things during pedaling: 1. maintaining a constant cadence of 120 rpm with the aide of a metronome, 2. maintaining normal pedal phasing (i.e. 180° offset), and 3. minimizing pelvis and torso motion. The average load on each crank of the mechanically decoupled cycle ergometer was measured to be 78.33 ± 14.91 watts and held constant between each collection day for each subject. Although the load varied between subjects, there was no difference in load within a subject. Decoupling the cranks and having separate flywheels for each crank ensures that each leg will pedal against the same load during all conditions.

Day 1 consisted of a training session to familiarize the subjects with the custom mechanically decoupled cycle ergometer. Seven subjects completed five 5-minute

Figure 13: Cycling Shoes

training trials (25 minutes total pedaling). The eighth subject only completed four 5-minute training trials due to time restraints. Subjects were allowed unlimited rest in between trials.

On Day 2, subjects completed the ischemic deafferentation portion of the protocol. Marker, pedal force, and electromyographic (EMG) data were collected during each 45-second trial. Subjects warmed up on the cycle ergometer for 5 minutes while data were collected at minutes 0, 2, and 4. Subjects then completed a series of 45-second pedaling trials of bilateral pedaling under two conditions: 1. wearing an un-inflated blood pressure cuff on their right leg, below the knee (Baseline), and 2. under ischemic nerve block, with the blood pressure cuff on the right leg, below the knee, inflated to 220mmHg (IB). The blood pressure cuff was placed below the knee as to not affect knee flexion. During these trials, the subjects would begin pedaling and then verbally indicate when they felt they were on the cadence and had correct pedal phasing (180° offset) to start the collection. Subjects were given a minimum of 3 minutes rest before and after the Baseline trial. During the IB condition rest was limited to 3 minutes between each trial. Data was analyzed at minutes 0, 4, 12, and 20 (IB0, IB4, IB12, IB20 respectively). Approximately 15-20 minutes of ischemic block is documented as the duration at which subjects loose substantial tactile and proprioceptive sensation

Figure 14: Dermatome locations drawn on subjects ankle for von Frey filament testing.

(Berger et al., 1984; Dickey and Winter, 1992; Dietz et al., 1979; Laszlo, 1967).

Deafferentation was verified by von Frey filament tests (Sinclair, 1948) at the S1 (lateral aspect of the foot/ankle), L4 (dorsum of the foot, frontal aspect of the ankle), and L5 (medial aspect of the foot/ankle) dermatomes (Fig. 14) prior to each IB condition. The S1 dermatome is associated with plantarflexor nerves and the L5 dermatome is associated with of dorsiflexor nerves (Netter et al., 2002). Von Frey filament testing was conducted at the ankle. Each subjects ankle was shaved to prevent extraneous stimulation and location of the dermatomes was conservatively estimated based on Bates Guide to Physical Examination and History Taking (Bickley, 2009).

4.2.3 Cycling analysis

All data were crank angle normalized (0-360°) (Fig. 3). Pedal cycle begins at 0°, which is set even with the seat post. This orients maximum flexion and extension to crank angles of 0 and 180° respectively. The pedaling cycle was further broken into four quadrants (Q) for analysis: Q1- flexion to extension transition, Q2- extension, Q3- extension to flexion transition, and Q4- flexion. Additionally, vastus medialus and gluteus maximus electromyographic data were analyzed during the crank angles corresponding to 0-180° (Fig 15, "Ex"), as these muscles are mainly active for the duration of extension and are graphically presented this way in the results. Since

the cranks are mechanically decoupled, maintaining a 180° phase difference between the cranks falls on the subjects to stay in time with the metronome. A 180° phase difference between the cranks indicates a 0° crank offset (goal). The cycles that did not maintain a crank offset of 0°±30° were excluded from analysis, to minimize the effect on leg phasing on changes in motor output (Alibiglou et al., 2009). Data were analyzed using custom Matlab code (Mathworks, 2013b).

4.2.4 Kinematics and kinetic recording & analysis

Three-dimensional lower extremity marker data were collected by a six-camera Vicon motion analysis system (120Hz, Oxford, UK). Retro-reflective markers were placed bilaterally on each subjects second metatarsophalangeal joint, lateral malleolus, heel, shank segment, lateral condyle, thigh segment, anterior superior iliac spine, and posterior superior iliac spine, as well as on the tenth thoracic vertebrae and seventh cervical vertebrae. A permanent bracket on each pedal held two retroreflective markers (one at each end) in order to calculate pedal angle. We applied a low-pass, zero-phase lag, fourth order Butterworth filter at 10 Hz to marker data. Peak flexion and extension angles over the pedal cycle for each joint were analyzed. Force data was analyzed within each functional quadrant of the pedal cycle.

4.2.5 Electromyographic recording & analysis

Surface electromyographic data (EMG) (1080Hz, Noraxon 16-channel) were collected bilaterally from tibialis anterior (TA), soleus (SO), medial gastrocnemius (MG), vastus lateralis (VL), rectus femoris (RF), biceps femoris long head (BF), and gluteus maximus (GM) muscles. Data were bandpassed 20-450Hz, demeaned, rectified, and 10 Hz lowpass filtered. Data were bandpass filtered 10-450 Hz, demeaned, rectified, and 10 Hz lowpass filtered. For each trial, EMG data from 10 pedal cycles were normalized to the peak value during the Baseline trial for each subject (Shiavi, 1998; Burden, 2003). Changes to motor output on the deafferented right side (with IB)

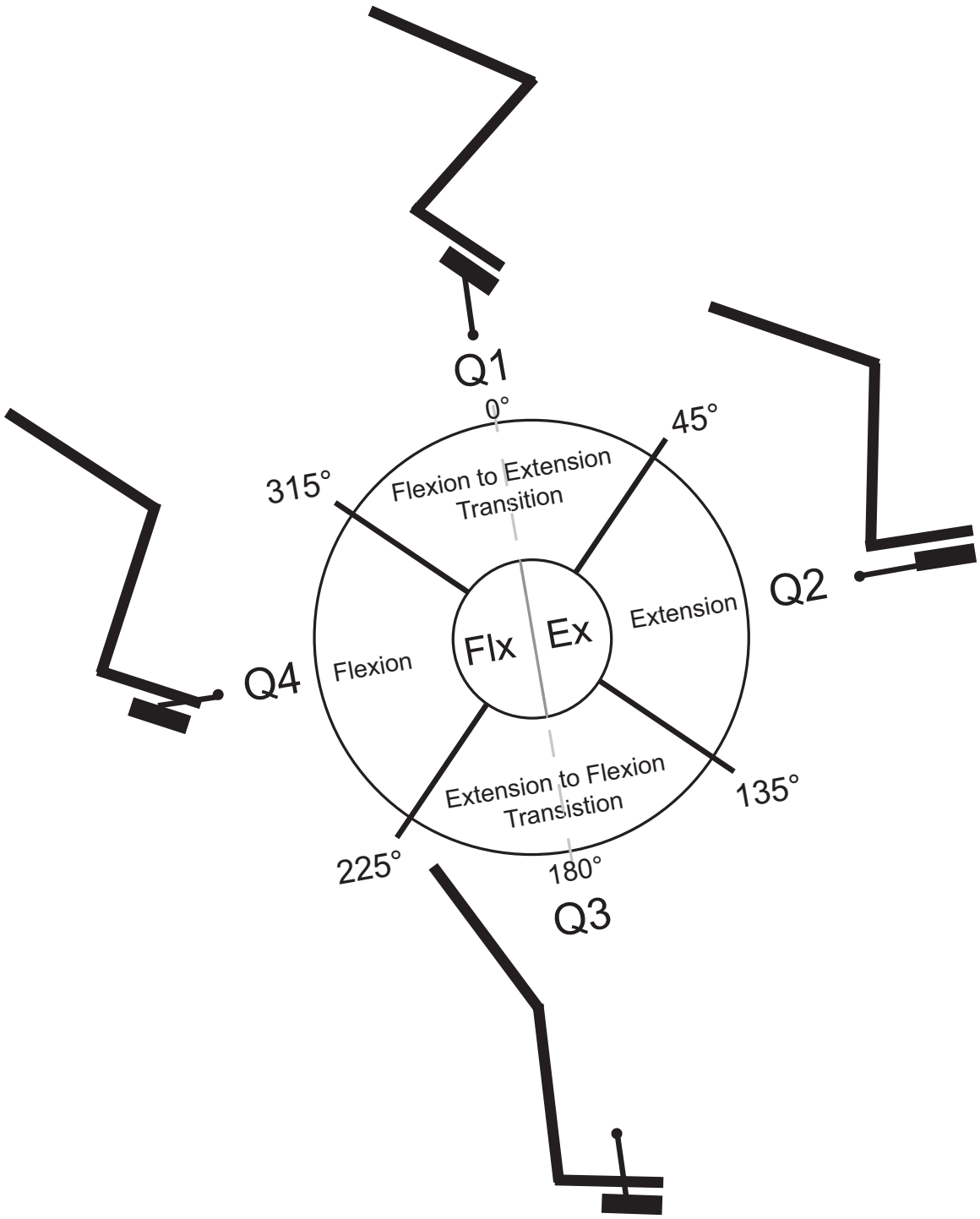

Figure 15: Schematic of functional cycling quadrants (Flx: flexion, Ex: Extension)

were quantified with integrated EMG (iEMG) for each functional quadrant (Q1-Q4) of the pedaling cycle.

4.2.6 Statistical analysis

Due to the within-subject repeated measures design, we performed a one-way repeated measures analysis of variance (ANOVA) to assess detect main effects across trials (Baseline, IB0, IB4, IB12, IB20) ($p < 0.05$). If Maucheys test of sphericity was violated degrees of freedom were corrected using Greenhouse-Geisser estimates of sphericity to prevent Type II error (Geisser and Greenhouse, 1959). When a significant main effect was found, Holm-Bonferroni corrected, pairwise comparisons were made post-hoc to compare each IB trial to Baseline for a simple main effects analysis (Holm, 1979). Significance was defined as a Holm-Bonferroni adjusted alpha level of 0.05.

4.3 Results

4.3.1 Deafferentation

Loss of cutaneous afferent feedback was confirmed by von Frey filament testing with significant main effects for all dermatomes: S1 ($F(3,21) = 23.82$, $p < 0.001$), L4 ($F(1.34,9.38) = 8.84$, $p = 0.011$), and L5 ($F(3,21) = 12.14$, $p < 0.001$) (Fig. 4). Increases in filament size correspond logarithmically with reductions in afferent feedback. Afferent feedback was significantly lower beginning at ∼12 minutes of ischemic block for S1 and L4 dermatomes (pre-IB12, pre-IB16, and pre-IB20) and at ∼4 minutes of ischemic block in the L5 dermatome (pre-IB4, pre-IB12, pre-IB16, and pre-IB20). Data presented is mean ± standard deviation for all 8 subjects. Increases in filament size correspond to increases in cutaneous sensory loss. Baseline refers to the testing period after the Baseline cycling trial, and before the IB0).

4.3.2 Crank offset

There were no significant main effects for mean crank offset ($F(4,28) = 1.958$, $p = 0.128$) or average maximum negative crank offset ($F(4,28) = 1.669$, $p = 0.185$) (Fig.

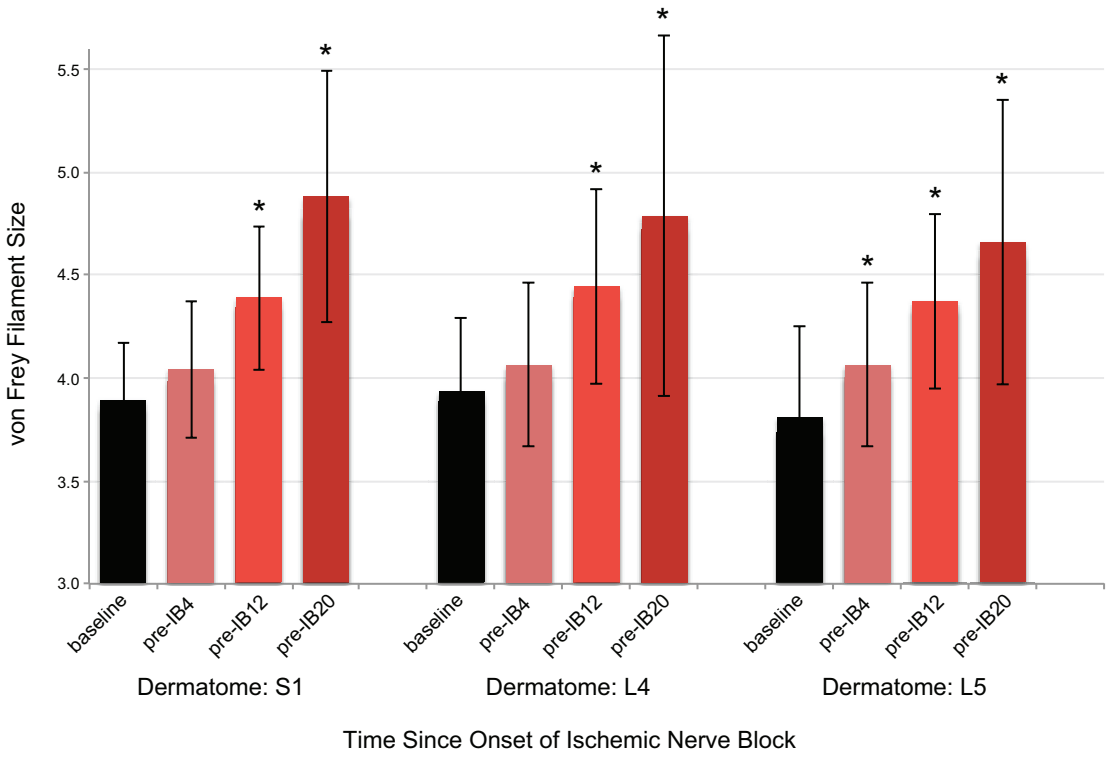

Figure 16: von Frey filament testing during onset of deafferentation. Mean ± standard deviation von Frey filament size for dermatomes, S1, L4, and L5 (as measured at the ankle). Higher filament size indicates greater sensory loss. For reference filament sizes 3.22 and 5.46 correspond to 0.16 and 26.0 newtons, respectively. Baseline measurement was taken after the baseline cycling trial, and directly before minute 0 of ischemic block. (*p<0.05, Holm-Bonferroni corrected).

17A, grey bars and white bars respectively). There was a significant main effect for average maximum positive crank offset ($F(2,24.04) = 4.707$, $p = 0.027$), however pairwise comparisons revealed no significant differences from Baseline for any IB trials (Fig. 17A, black bars). A positive crank offset indicated that the pedal crank on the contralateral donor side was lagging behind where it should be with respect to the ipsilateral crank arm. In contrast a negative crank offset indicated that the pedal crank on the contralateral donor side was ahead of where it should be with respect to the ipsilateral crank arm. During Baseline, the maximum positive and negative crank offsets were about even (11.16° ± 4.11 and -8.89° ± 3.11 respectively) (Fig. 17A).

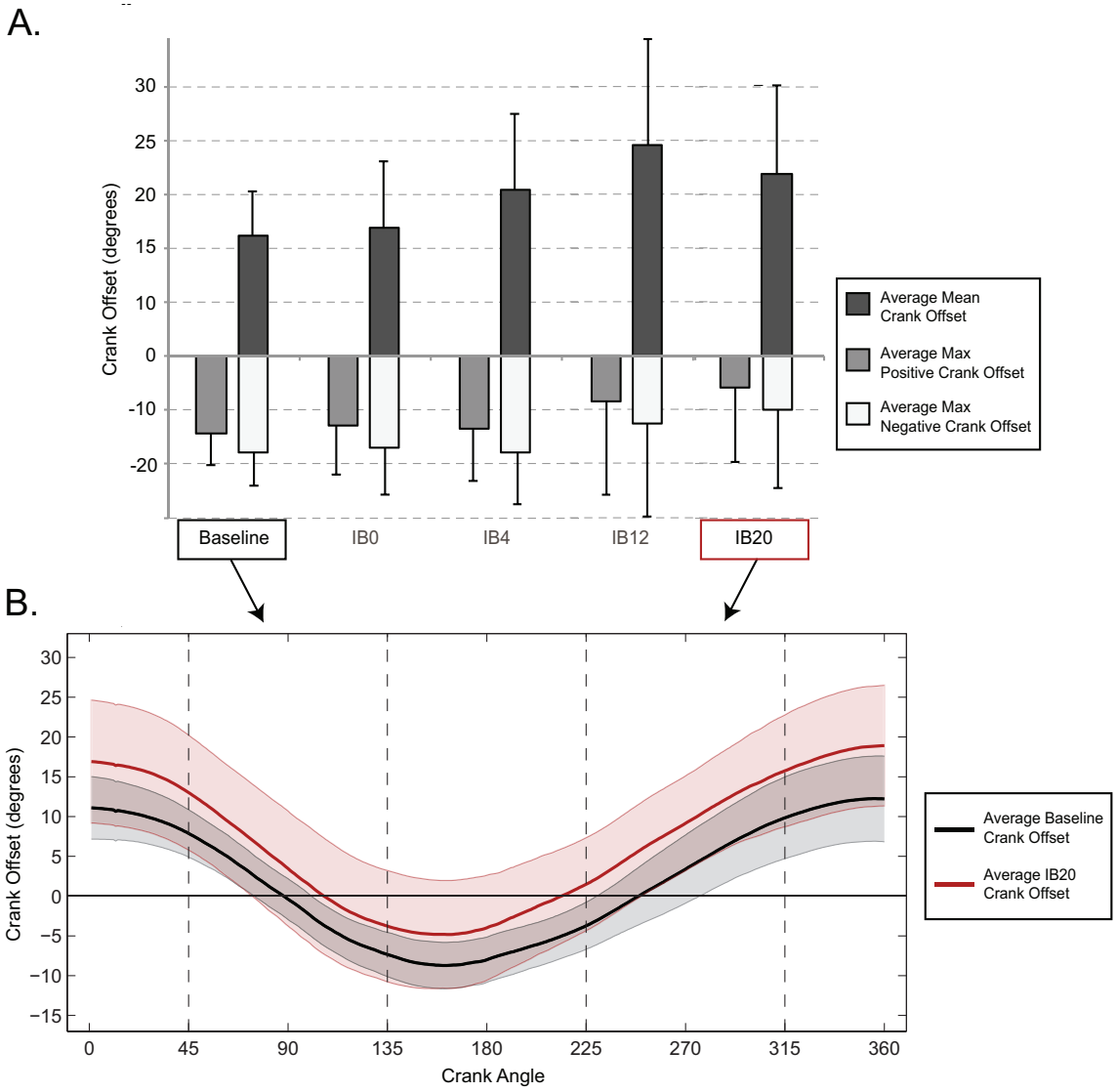

Figure 17: Crank offsets A) Mean ± standard deviation (grey), maximum positive ± standard deviation (dark grey), and maximum negative ± standard deviation (white) crank offsets during baseline and after 0, 4, 12, and 20 minutes of ischemic block (IB0, IB4, IB12, and IB20 respectively). No significant main effects were found across any condition. B) Mean ± standard deviation crank offset trace with respect to crank angle for Baseline (black) and IB20 (dark red). Data represents the mean across 10 cycles for 8 subjects for panel A. and B.

This indicates that with respect to the ipsilateral crank position, the magnitude of contralateral crank angle fluctuations were relatively even above and below the goal (being 0° crank offset). The mean crank offset however being negative (-7.15° ± 2.95), indicates that for the majority of crank cycle, the contralateral crank position was below the 0° goal (Fig 5B). After 20 minutes of ischemic block (IB20), the maximum positive crank offset increased and maximum negative crank offset increased (less negative) (16.93° ± 8.22 and -4.92° ± 7.29 respectively, NS). The mean crank offset also increased, but was still negative (-2.91° ± 6.88, NS).

4.3.3 Electromyographic results

Ipsilateral and contralateral average EMG traces (mean ± standard deviation) in general show consistent onsets of all muscle activations between the Baseline trial and IB trials (Fig. 18 & 19). All p-values for main effects analysis reported in Table 6. For the ipsilateral limb, significant main effects were only found in quadrant 1 (Q1) of the ipsilateral tibialis anterior and rectus femoris activations ($F(4,28) = 6.551$, $p = 0.001$ and $F(4,28) = 6.180$, $p = 0.001$ respectively) (Fig. 18A). Horizontal black bars spanning the quadrant indicate quadrants containing significant main effects. Quadrants highlighted in yellow indicate post-hoc pairwise analyses yielded significant decreases from baseline. The iEMG pairwise analyses are illustrated in bar plots directly beneath the EMG trace plots, also highlighted in yellow. It is important to note that Q1, indicative of the transition from flexion to extension, spans from 315-360° and 0-45°. Post-hoc pairwise comparisons revealed significantly lower muscles activations from Baseline in the ipsilateral tibialis anterior at IB4 (41.92% lower), IB12 (39.12% lower), and IB20 (36.65% lower) during Q1 ($p = 0.036$, $p = 0.028$, $p = 0.040$, respectively). Ipsilateral rectus femoris muscle activations were significantly lower than baseline for all IB trials during Q1: IB0 (21.61% lower), IB4 (41.11% lower), IB12 (37.29% lower), and IB20 (41.03% lower) (IB0: $p = 0.046$, IB4: $p =$

0.016, IB12: p = 0.022, IB20: p = 0.006). No other muscles in the ipsilateral limb exhibited significant differences in any quadrant (soleus, medial gastrocnemius, lateral gastrocnemius, vastus lateralis, biceps femoris long head or gluteus maximus) (Fig. 6 B). Although not significant, the ipsilateral gluteus maximus muscle activations markedly increased during Q2 and the first half of Q3 during IB4, IB12, and IB20, (Q2: $F(1.547,10.829) = 3.367$, $p = 0.082$ and Q3: $F(1.258,8.804) = 6.551$, $p = 0.112$).

In the contralateral limb, only Q3 of biceps femoris long head muscle activations and Q4 of lateral gastrocnemius muscle activations showed significant main effects ($F(4,28) = 5.397$, $p = 0.002$ and $F(4,28) = 8.987$, $p < 0.001$, respectively) and subsequent differences in post-hoc pairwise comparisons (Fig. 7A). Activations were significantly reduced in the biceps femoris long head muscle during every IB trial compared to Baseline in Q3: IB0 (31.23% lower), IB4 (47.05% lower), IB12 (36.92% lower), and IB20 (39.31% lower) (IB0: p = 0.014, IB4: p = 0.004, IB12: p = 0.012, IB20: p = 0.020). Lateral gastrocnemius muscle activations showed a similar pattern in Q4: IB0 (54.17% lower), IB4 (66.31% lower), IB12 (44.02% lower), and IB20 (50.60% lower) (IB0: p = 0.030, IB4: p = 0.012, IB12: p = 0.016, IB20: p = 0.028). Lateral Gastrocnemius muscle activations also had significant main effects in Q3 ($F(4,28) = 3.603$, $p = 0.017$), however, there were no significant differences between Baseline and IB trials upon post-hoc pairwise comparisons. The same was true for the Q4 of the gluteus maximus muscle ($p = 0.031$). No other muscles in the contralateral limb exhibited significant differences in any quadrant (Fig. 20B) or during extension phase (Fig. 21).

4.3.4 Kinematics

Kinematics trajectories were well maintained across conditions for all joints except the contralateral ankle (Fig. 22). There were no significant differences on the ipsilateral side peak flexion (positive) or peak extension (negative) angles at the ankle, knee,

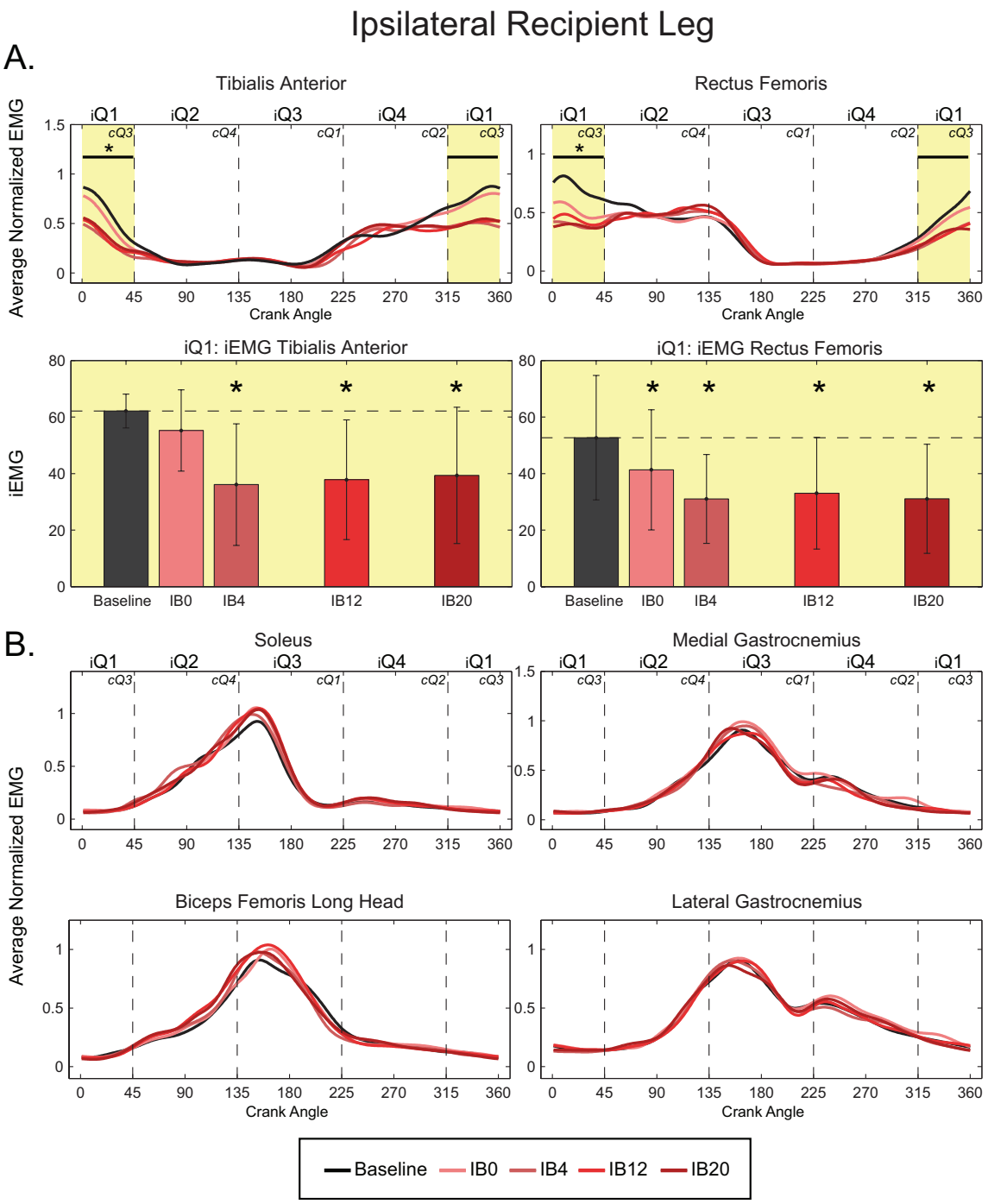

Figure 18: Ipsilateral recipient leg electromyographic (EMG) traces by functional quadrant. Mean ± standard deviation EMG traces during cycling at baseline (black line) and after 0, 4, 12, and 20 minutes of ischemic block (IB0, IB4, IB12, and IB20 respectively) (pink to dark red lines). All data was normalized to peak activation during the baseline trial, and traces represent the mean across 10 cycles for 8 subjects. Vertical dashed lines represent quadrant boundaries (Q1-Q4). Significant main effects in iEMG are denoted by: * and horizontal black bar spanning the quadrant, (*$p<0.05$). Quadrants where post-hoc analysis revealed significant differences between baseline and any IB trial are colored yellow. The subsequent pairwise post hoc analysis of iEMG values comparing each IB trial to baseline is found directly underneath, also with a yellow background. Horizontal black dashed lines indicate the mean value at Baseline. (*$p<0.05$, Holm-Bonferroni corrected, significant difference from baseline condition).

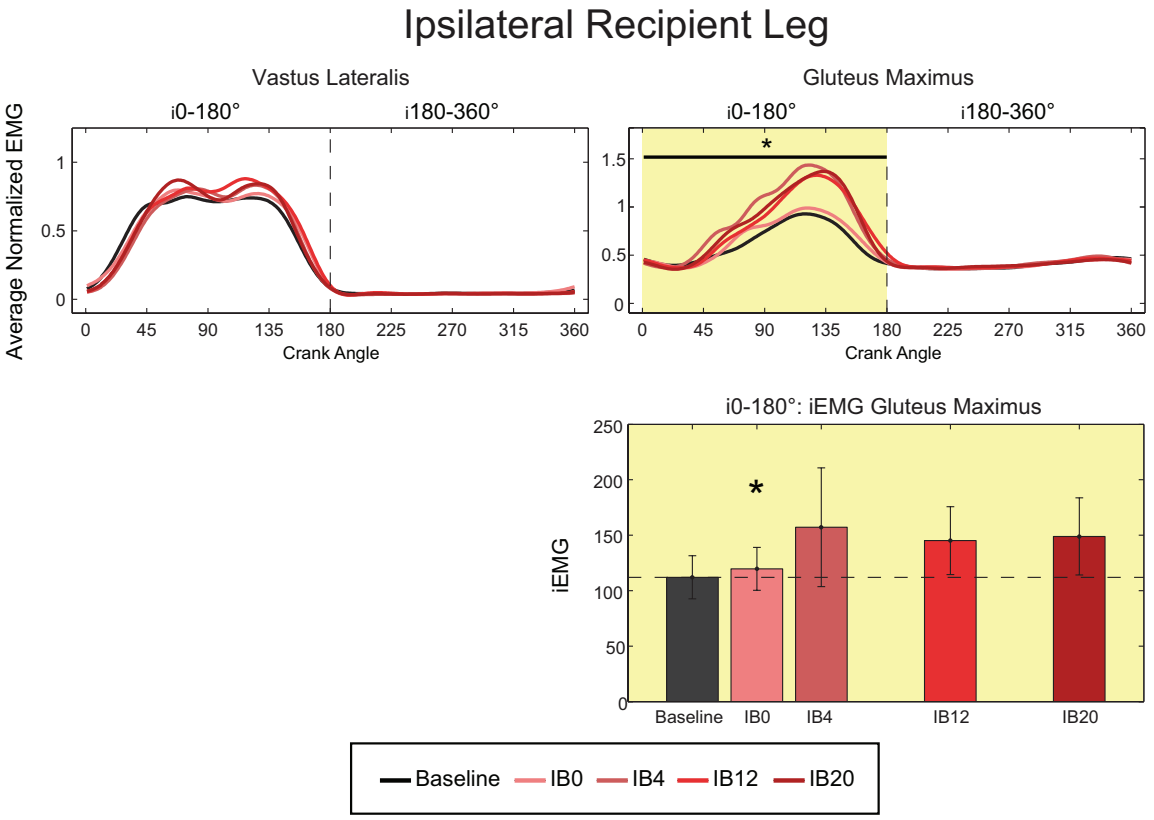

Figure 19: Ipsilateral recipient VM and GM electromyographic (EMG) traces. Mean ± standard deviation EMG traces during cycling at baseline (black line) and after 0, 4, 12, and 20 minutes of ischemic block (IB0, IB4, IB12, and IB20 respectively) (pink to dark red lines). All data was normalized to peak activation during the baseline trial, and traces represent the mean across 10 cycles for 8 subjects. Vertical dashed line represents the end of flexion phase (180°). Significant main effects in iEMG are denoted by: * and horizontal black bar spanning the flexion phase, (*$p<0.05$). Post-hoc analysis revealed significant differences between baseline and any IB trial are colored yellow. The subsequent pairwise post hoc analysis of iEMG values comparing each IB trial to baseline is found directly underneath, also with a yellow background. Horizontal black dashed lines indicate the mean value at Baseline. (*$p<0.05$, Holm-Bonferroni corrected, significant difference from baseline condition).

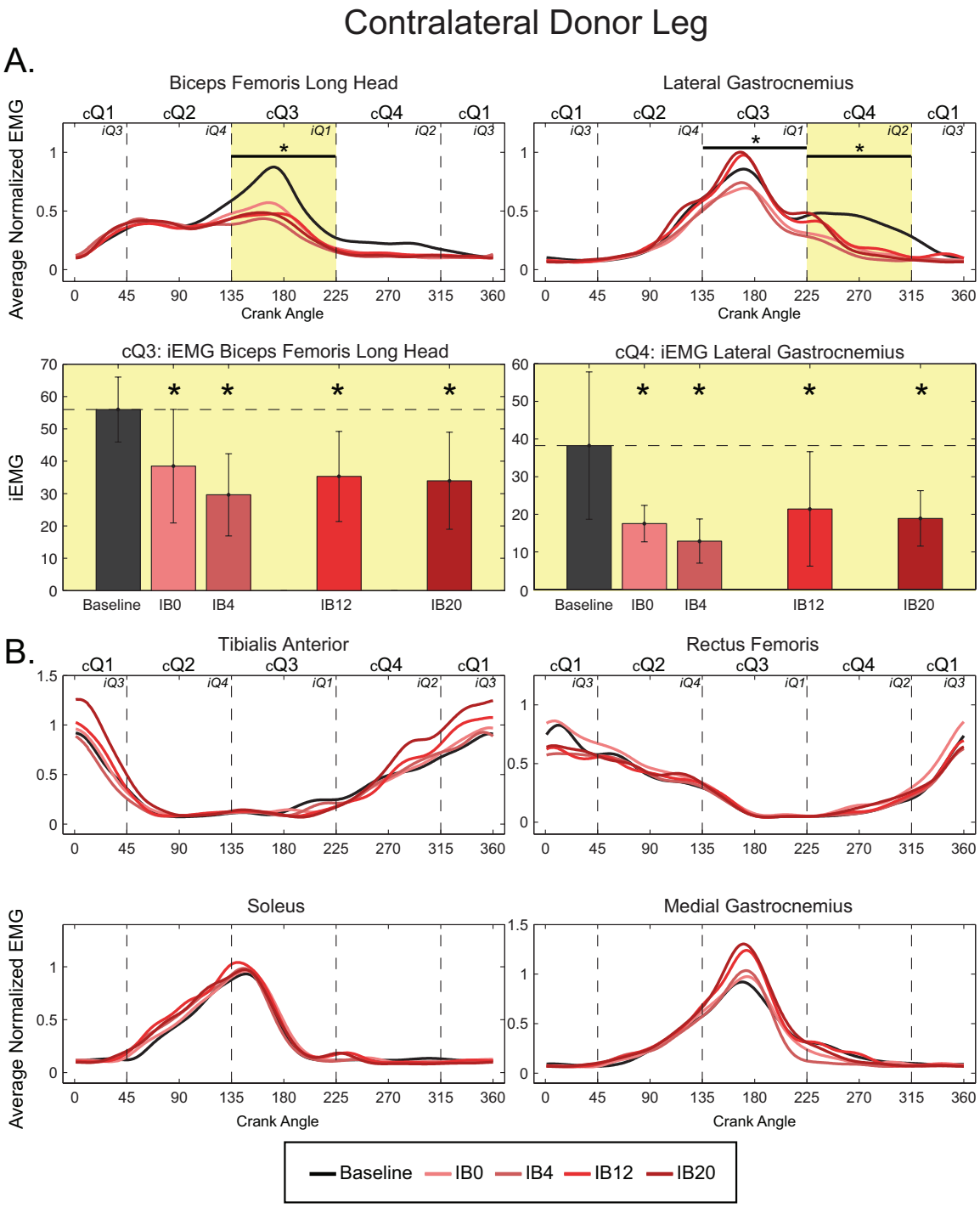

Figure 20: Contralateral donor leg electromyographic (EMG) traces. Mean ± standard deviation EMG traces during cycling at baseline (black line) and after 0, 4, 12, and 20 minutes of ischemic block (IB0, IB4, IB12, and IB20 respectively) (pink to dark red lines). All data was normalized to peak activation during the baseline trial, and traces represent the mean across 10 cycles for 8—subjects. Vertical dashed lines represent quadrant boundaries (Q1-Q4). Significant main effects in iEMG are denoted by: * and horizontal black bar spanning the quadrant, (*$p<0.05$). Quadrants where post-hoc analysis revealed significant differences between baseline and any IB trial are colored yellow. The subsequent pairwise post hoc analysis of iEMG values comparing each IB trial to baseline is found directly underneath, also with a yellow background. Horizontal black dashed lines indicate the mean value at Baseline. (*$p<0.05$, Holm-Bonferroni corrected, significant difference from baseline condition).

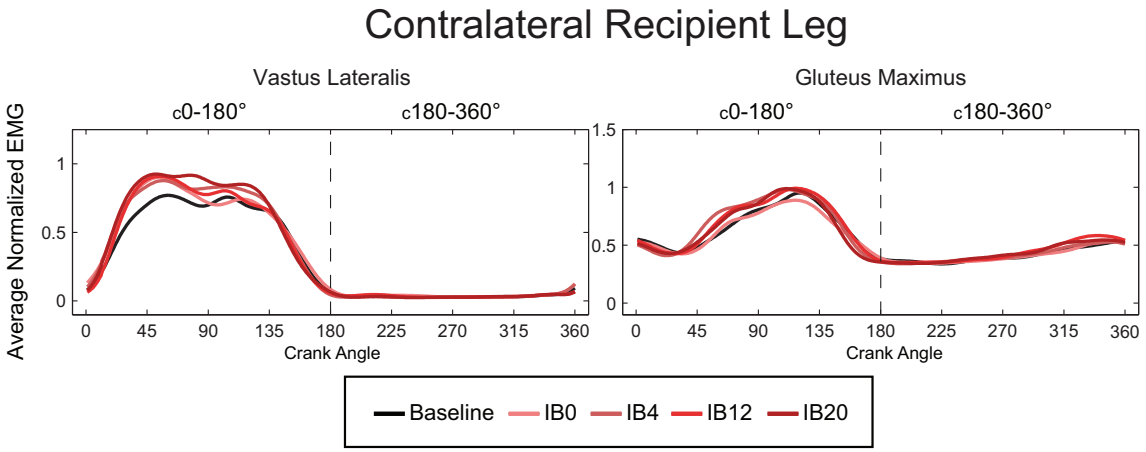

Figure 21: Contralateral recipient VM and GM electromyographic (EMG) traces. Mean ± standard deviation EMG traces during cycling at baseline (black line) and after 0, 4, 12, and 20 minutes of ischemic block (IB0, IB4, IB12, and IB20 respectively) (pink to dark red lines). All data was normalized to peak activation during the baseline trial, and traces represent the mean across 10 cycles for 8 subjects. Vertical dashed line represents the end of flexion phase (180°). No significant main effects were found.

Table 6: Repeated measures ANOVA main effects analysis results comparing iEMG within each quadrant across all speeds. Significant main effects bolded.

	Ipsilateral Recipient Leg				Contralateral Donor Leg			
	Q1	Q2	Q3	Q4	Q1	Q2	Q3	Q4
TA	**0.001**	0.554	0.190	0.478	0.296	0.489	0.507	0.549
SO	0.594	0.440	0.290	0.382	0.637	0.058	0.582	0.389
MG	0.098	0.867	0.490	0.241	0.161	0.762	0.099	0.199
LG	0.330	0.914	0.856	0.431	0.053	0.366	**0.017**	**<0.001**
RF	**0.001**	0.689	0.362	0.544	0.095	0.324	0.457	0.336
BF	0.380	0.152	0.918	0.596	0.497	0.684	**0.002**	0.087
VL	0.331	0.566	0.371	0.646	0.109	0.167	0.748	0.231
GM	0.405	0.082	0.112	0.307	0.387	0.355	0.398	**0.031**

	0-180		0-180
VL	**0.041**		0.175
GM	0.792		0.609

or hip (Fig 22 A-C). On the contralateral side ankle trajectory variability increased and mean range of motion decreased. Both peak dorsiflexion (positive) and peak plantarflexion (negative) had significant main effects ($F(4,28) = 3.598$, $p = 0.017$ and $F(4,28) = 8.831$, $p > 0.001$ respectively) (Fig. 22A). Due to high variability of the ankle trajectories between subjects, pairwise analysis revealed no significant differences between Baseline and any of the IB trials for peak dorisflexion angles in the contralateral ankle. Peak contralateral ankle plantarflexion angle, was significantly decreased from Baseline (-10.64° ± 6.80) at IB4 (-7.91° ± 7.17, $p = 0.022$), IB12 (-4.03° ± 6.57, $p = 0.004$), and IB20 (-3.77° ± 6.94, $p = 0.006$). There were no significant differences in peak flexion or extension angles in the contralateral knee or hip (Fig. 22B & C).

4.3.5 Forces

In order to get a full picture of force production and application, crank torques, resultant forces (Fig. 23), effective force (Fig. 24) and index of effectiveness (Appendix A) were all quantified. All comparisons were made between Baseline and the IB trials. There were significant main effects for ipsilateral crank torques during IB trials in Q1 (spanning 315-360° and 0-45°) ($F(4,28) = 3.077$, $p = 0.032$), however there were no significant differences in pairwise comparisons of Baseline to IB trials (Fig. 23A). There were no differences between ipsilateral crank torques in Q2-4 or contralateral crank torques in any quadrant (Q1-4).

Resultant force is the total force applied to the pedal (as calculated from vertical and anterior-posterior components). Resultant forces in the ipsilateral leg had significant main effects in Q2 and Q3 ($F(4,28) = 3.492$, $p = 0.020$ and $F(4,28) = 6.451$, $p = 0.001$, respectively) (Fig. 23B, line plot). Post-hoc pairwise comparisons indicated significantly higher integrated resultant force from Baseline in Q2 during IB4 (7.77% higher, $p = 0.045$) and IB12 (7.07% higher, $p = 0.028$) (Fig. 23B, bar plot). Pairwise

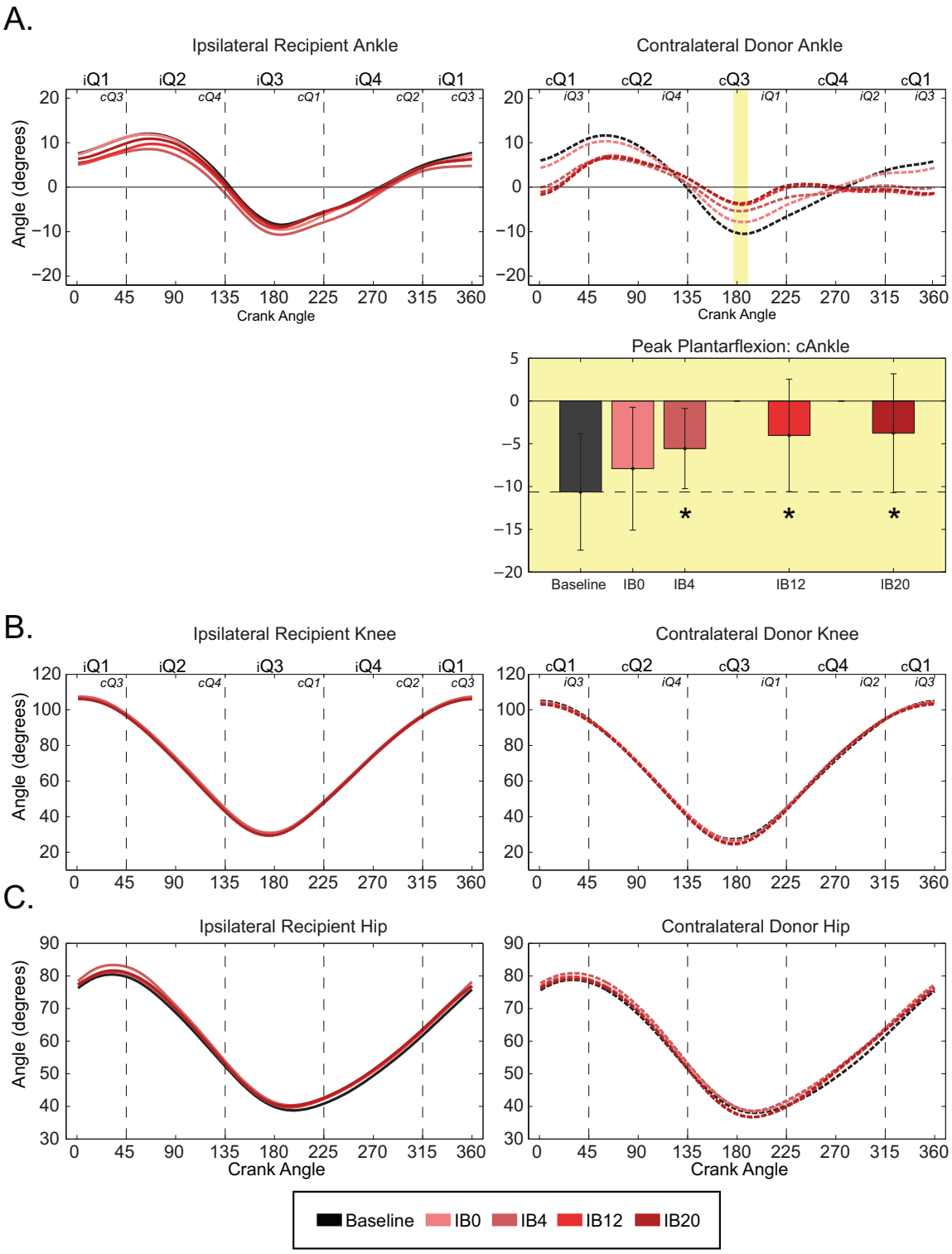

Figure 22: Mean kinematics ± standard deviations. (Caption next page.)

Figure 22: Mean kinematics ± standard deviations of all subjects for the A.) ankle, B) knee, and C) hip. Higher angles indicate flexion and lower angles indicate extension. Ipsilateral and contralateral limbs are denoted by a solid lines and dashed lines respectively. Data is presented from baseline (black line) and after 0, 4, 12, and 20 minutes of ischemic block (IB0, IB4, IB12, and IB20 respectively) (pink to dark red lines). All data was normalized to neutral during standing as 0, and traces represent the mean across 10 cycles for 8 subjects. Vertical dashed lines represent quadrant boundaries (Q1-Q4). Significant main effects in mean peak extension or flexion are denoted by:*$p<0.05$ for peak extension and flexion angles. Post-hoc analysis revealed significant differences between baseline and IB trials in peak contralateral plantarflexion only (A. shaded yellow). The subsequent pairwise post hoc analysis of iEMG values comparing each IB trial to baseline is found directly underneath, also with a yellow background. Horizontal black dashed lines indicate the mean value at Baseline. (*$p<0.05$, Holm-Bonferroni corrected, significant difference from baseline condition).

analysis for Q3 showed significantly higher integrated resultant forces from Baseline during IB12 (14.70% higher, $p = 0.039$) and IB20 (11.37% higher, $p = 0.020$) (Fig. 23B, bar plot). There were no significant differences in Q1 or Q4 in resultant force of the ipsilateral leg.

Resultant forces in the contralateral leg had significant main effects in Q1 and Q2 $F(4,28) = 12.020$, $p < 0.001$ and $F(4,28) = 3.072$, $p = 0.0032$, respectively) (Fig. 23B, line plot). Pairwise comparisons indicated significantly higher integrated resultant forces from Baseline in Q1 during all IB trials: IB0: 38.79% higher ($p = 0.002$), IB4: 35.64% higher ($p = 0.002$), IB12: 26.16% higher ($p = 0.003$), IB20: 38.14% higher $p = (0.005)$ (Fig. 23B, bar plot). Pairwise analysis for Q2 indicted no significant differences for any IB trial with compared to Baseline (Fig. 23B, bar plot). The bar plot was included to further illustrate these findings. No significant differences were found in resultant forces in Q3 or Q4 for the contralateral limb.

Effective force is the amount of force applied tangential to the crank arm. The timing of average contralateral minimum and maximum effective force applications with respect to the ipsilateral limb appeared unchanged between Baseline and IB20 (Fig. 24).

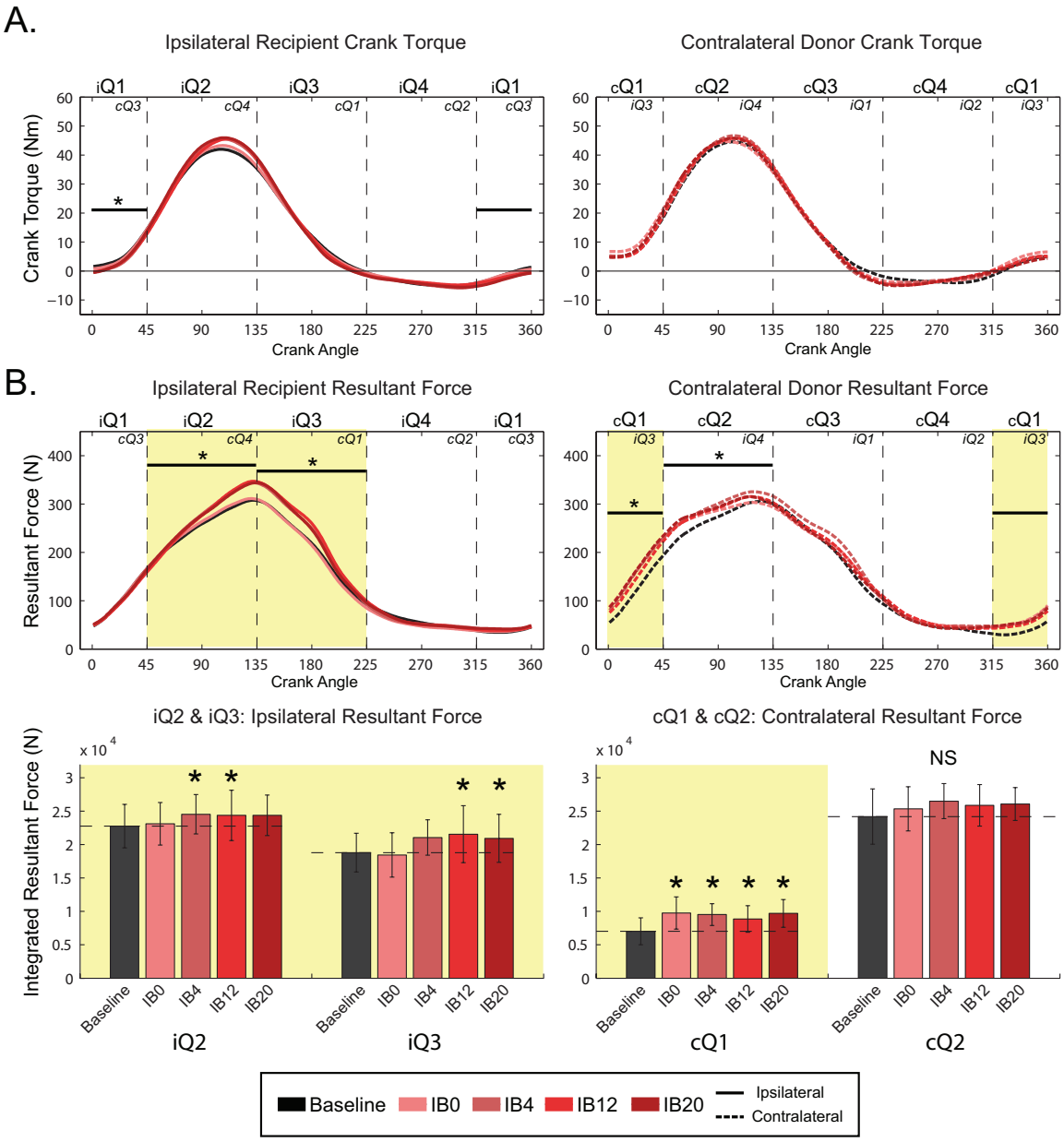

Figure 23: A.) Crank torque and B). Resultant forces (mean ± standard deviation) during cycling at baseline (black line) and after 0, 4, 12, and 20 minutes of ischemic block (IB0, IB4, IB12, and IB20 respectively) (pink to dark red lines). Data represents the mean across 10 cycles for 8 subjects. Vertical dashed lines represent quadrant boundaries (Q1-Q4). Significant main effects of integrated forces are denoted by: * and horizontal black bar spanning the quadrant, (*$p<0.05$). Quadrants where post-hoc analysis revealed significant differences between baseline and any IB trial are colored yellow. The subsequent pairwise post hoc analysis of iEMG values comparing each IB trial to baseline is found directly underneath, also with a yellow background. Horizontal black dashed lines indicate the mean value at Baseline. (*$p<0.05$, Holm-Bonferroni corrected, significant difference from baseline condition; NS: no significance)

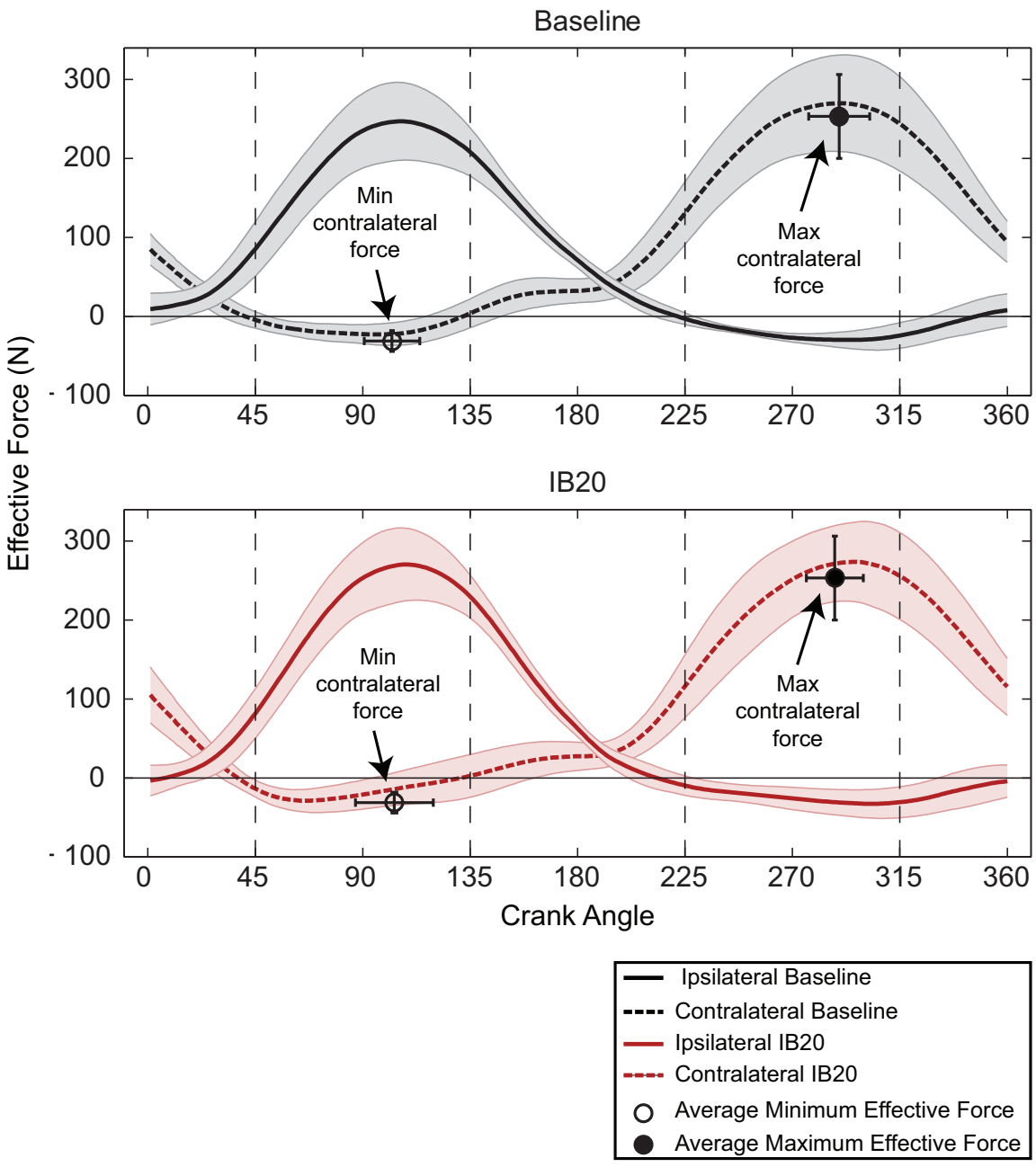

Figure 24: Effective force (mean ± standard deviation) traces for for the ipsilateral (solid lines) and contralateral limbs (dashed lines) during cycling at baseline (black) and IB20 (dark red). Timing and amplitude of minimum and maximum contralateral effective force application is denoted by open and closed circles respectively on each plot.

4.4 Discussion

Previous cycling work shows that contralateral afferent feedback during extension (most likely Ib afferents from Golgi-tendon organs) have an inhibitory effect on the ipsilateral flexor motor output (Ting et al., 2000; Ting et al., 1998). We hypothesized that contralateral deafferentation below the knee by way of ischemic nerve block would cause disinhibition of these interlimb pathways and subsequent increase in ipsilateral flexor activations. In the pursuit of testing this hypothesis we achieved, at a minimum, unilateral, partial deafferentation below the knee and were successful in maintaining the task mechanics of cycling in the ipsilateral leg, despite this neural perturbation. This hypothesis, however, was not supported by our results, and in fact the ipsilateral flexor motor out put instead decreased. Parsimoniously speaking, our results can most likely be explained by the summed affect of all below-knee contralateral afferents normally having a net facilitory effect on ipsilateral flexors rather than an inhibitory one. Alternatively, increases in contralateral afferent feedback proximal to the knee may have had an inhibitory effect on the ipsilateral flexors, however, this is less likely due to the inconsistency in the timing of the response with previous work.

4.4.1 Verifying ischemic deafferentation

At minimum we achieved a partial below-knee deafferentation. The von Frey filament testing quantified cutaneous perceptual thresholds and verified a significant degradation of afferent feedback for dermatomes S1 (associated with the plantarflexor nerves), L4, and L5 (associated with the dorsiflexor nerves), beginning at minute 12 of the ischemic nerve block (Fig. 4). Specifically, the sural nerve, which branches from the tibial nerve, innervates the S1 dermatome (Netter et al., 2002). The tibial nerve branches in the popliteal fossa to innervate the medial and lateral gastrocnemii, and soleus muscles. The superficial peroneal (fibular) nerve innervates the L5 dermatome. The superficial peroneal (fibular) nerve is a branch of the common peroneal

nerve which, along with the deep peroneal (fibular) nerve, innervates the tibialis anterior. The saphenous branch of the femoral nerve innervates the L4 dermatome. The branches of the femoral nerve do not innervate any muscles below the knee. Previous work shows that cutaneous sensation is degraded earlier than proprioceptive afferent sensation, which is degraded earlier than motor output and control (Christensen et al., 2007; Laszlo, 1967; Sinclair, 1948). Anecdotally contralateral ankle dorsiflexion and plantarflexion decreased immediately following the application of the IB (Fig. 22, minute 0), indicating deficits in control of the ankle joint. Due to the immediate effects of changes observed both in the contralateral and ipsilateral limbs, we speculate that the responses were due to degradation of cutaneous and/or Ia afferent feedback. We observed significant decreases in cutaneous feedback per von frey filament testing following the IB0 trial, before IB4 (Fig. 22). By limiting plantarflexor action, Ia afferent feedback can be immediately decreased via the application of a blood pressure cuff below the knee (Leukel et al., 2009).

4.4.2 Maintaining task mechanics

It was important to maintain the mechanics between Baseline and IB20, especially on the ipsilateral side, in order to rule out mechanical contributions to changes in the ipsilateral motor output. Despite contralateral deafferentation, the task mechanics of the ipsilateral side were well maintained. This is not surprising given the lower limbs abilities to perform well coordinated yet varied locomotor tasks such as hybrid walking (legs moving in different directions) and split belt treadmill walking (Choi and Bastian, 2007).

Minimizing deviations in crank offset from the goal (being 0° crank offset) was important to maintain task mechanics. Interlimb pathways can be affected by deviations in crank offset (Alibiglou and Brown, 2011; Alibiglou et al., 2009). Studies systematically altering and locking in crank offset show changes in muscle activity

and onset/offset timing. For this reason, we only analyzed cycles where the maximum crank offset was no more than ± 30°, however the mean crank offset was far less during Baseline (-7.12° ± 2.95) and IB20 (-2.91° ± 6.89) (Fig. 5A). Since EMG amplitude was expected to change with the onset of ischemic block, we visually inspected the onset/offset timing of our EMG signals (Fig. 18-21) to verify whether there was an effect of the deviations in crank offset. Our signals showed no notable changes between onset/offset timing between the Baseline and IB20 trial. Perhaps more importantly, the timing of contralateral maximum and min effective force application with respect to ipsilateral limb angle remained consistent between Baseline and IB20 (Fig. 24). This further supports that the small temporal changes in crank offset from Baseline to IB20, did not markedly affect the task mechanics of bilateral pedaling or confound the motor output results of the ipsilateral leg.

Overall kinematic trajectories remained consistent between Baseline and IB20 for all joints except the contralateral ankle (Fig. 22). In the contralateral limb, maximum ankle plantarflexion was significantly different during IB20 from Baseline (Fig. 22A-B). Deficits in motor control of the joint distal to the IB (contralateral ankle) were expected due to loss of proprioception and cutaneous feedback (Laszlo, 1967). Furthermore, the deficits in ankle range of motion further limit the Ia afferent feedback from below the knee thats integrated at a spinal level (Weiss et al., 1986).

4.4.3 Below-knee contralateral afferents have a net facilitory effect of the ipsilateral flexors

We determined that contralateral, below-knee, ischemic deafferentation during cycling results in in a selective decrease in ipsilateral flexor motor output (iEMG of tibialis anterior and rectus femoris in Q1) (Fig. 21). These results were contrary to our hypothesis, and suggest the below-knee, contralateral extensor afferents may have a net facilitory effect on the ipsilateral flexors rather than an inhibitory one. This net facilitory effect suggests that, during the cycling task under Baseline conditions,

the contralateral afferents below the knee may either excite or disinhibit the ipsilateral flexors. Since the below-knee ischemic nerve block resulted in at least partial deafferentation of the plantarflexors, dorsiflexors, and cutaneous afferents, we cannot decipher their individual contributions to the net excitatory effect on the ipsilateral flexors, nor the level of the central nervous system in which they occur (i.e. cortical or spinal).

There is precedence for crossed limb facilitory effects onto ipsilateral flexors during walking. In humans, increasing contralateral plantarflexor feedback shows a concurrent increase in ipsilateral dorsiflexor muscle activations (Berger et al., 1984). Treadmill acceleration during contralateral stance (single limb support), results in contralateral increases in plantarflexion and gastrocnemius activations. Concurrently, ipsilateral tibialis anterior activations increase as a result during swing phase. The same response in the swing limb was evoked by contralateral tibial nerve stimulation during single limb support. Our results suggest that these previous findings may be due in part to neural interlimb coordination with below-knee contralateral extensor muscles facilitating ipsilateral flexor muscle activation rather than merely a mechanical compensation to the perturbations applied during walking. Previous work has also demonstrated crossed limb increases in flexor muscle activation from cutaneous stimulation. High frequency contralateral skin stimulation consistently results in increased hindlimb flexion in deafferented cats (Gauthier and Rossignol, 1981). However the contralateral response is phase dependent, which increases in contralateral flexion only occurring during swing phase. It is important to note that the effects of cutaneous afferents are task (Duysens et al., 1993) and phase dependent (Gauthier and Rossignol, 1981; Haridas and Zehr, 2003; Yang and Stein, 1990). Given that increases in contralateral below-knee muscle and cutaneous afferent feedback can elicit increases in ipsilateral flexor activations, it is well within the realm of possibility that contralateral below-knee afferents could have a net facilitory effect on ipsilateral

flexors.

4.4.4 Alternative explanation for decreases in flexion-to-extension (Q1) tibials anterior and rectus femoris muscle activations

Reductions in ipsilateral flexor muscle activations could alternatively be explained by increases in contralateral afferent feedback proximal to the knee inhibiting the ipsilateral flexors. Despite no increase in contralateral crank torque (Fig. 23A), we did observe a significant increase in contralateral resultant force production (Fig. 23B) in Q1 beginning at IB0. Ting, et al. showed ipsilateral tibialis anterior and rectus femoris muscle activations decrease during flexion phase (Q4) of pedaling, when high rhythmic contralateral extensor force ($\sim$ 300N) is generated concomitantly in comparison to low rhythmic extensor force (just above leg weight)(1998, 2000). Studies in walking rats have indicated contralateral extensor muscle afferents (most likely force-dependent Ib afferents) presynaptically inhibit ipsilateral flexor muscle afferents (Hayes et al., 2012; Hochman et al., 2013). Inhibition of the ipsilateral flexor afferents could thus lead to a decrease in flexor muscle output. This provides an alternative, but less likely explanation for our results, as the operation of this circuit in isolation is not expressed in our findings. Nevertheless, the activation of this circuitry is not mutually exclusive from the proposed net facilitory effect of contralateral, below-knee afferents on ipsilateral flexor muscle activations.

Our observed increase in contralateral resultant force production could translate into increases in extensor afferent feedback above the knee, however the modulation of the ipsilateral tibialis anterior and rectus femoris muscle activations occurred during flexion-to-extension quadrant (Q3) (Fig. 22), not during the flexion quadrant (Q4) as reported by Ting and colleagues (1998, 2000). Additionally, timing and amplitude of effective force application also remained consistent on the contralateral side (Fig. 24) and Ting et als previous work. The inconsistent phasing of modulations to ipsilateral flexor muscle activations make it unlikely that our findings are due exclusively to

increases in contralateral extensor afferents.

There were also no significant changes in the contralateral extensor muscles proximal to the IB (vastus lateralis, and gluteus maximus) (Fig. 21B) during IB trials with respect to Baseline conditions. These muscles contribute to power production during leg extension in cycling and maintained afferent feedback during this study due to their proximal location with respect to the IB. However, increases in motor evoked potentials in muscles proximal to an ischemic block or following amputation are well documented in the literature, occurring in both the arms and legs (Brasil-Neto et al., 1992; Brasil-Neto et al., 1993; McNulty et al., 2002; Vallence et al., 2012; Ziemann et al., 1998). This is attributed to increases in cortico-spinal excitability, most likely at the cortical level, since H/M ratios (Hoffman-reflex/M-wave) measured proximal to an IB indicating spinal α-motor neuron pool excitability have remained unchanged despite the onset of IB (Brasil-Neto et al., 1993; Leukel et al., 2009; Vallence et al., 2012). Hence, the lack of increased proximal activations we observed is not consistent with the literature. This discrepancy could be attributed to the high variability of dynamic EMG in comparison to motor evoked potentials affecting our statistical power, as contralateral vastus lateralis activations appeared higher, but did not show significance during extension (0-180°, $p = 0.175$).

4.4.5 Intralimb response to ischemic deafferentation

There is also a within-limb response of significantly lower contralateral biceps femoris long head activations during the transition from extension to flexion (Q1) and lateral gastrocnemius activations during flexion (Q4). Sural nerve stimulation during stance elicits both an increase and decrease in biceps femoris long head activations during forward and backward pedaling, respectively (Hoogkamer et al., 2012). Since hamstring activation phasing in forward pedaling is similar to that of backward walking (Ting, 1997), it would not be surprising that a lack of cutaneous sensation during

forward pedaling would results in a subsequent drop in biceps femoris long head activation. The decrease we observed in lateral gastrocnemius activations after the onset of IB, could be explained by the significant reduction in plantarflexion (Fig. 22A) and/or a pressure-induced reduction in Ia afferents caused by the blood pressure cuff (Leukel et al., 2009). Previous work postulates the application of pressure to the muscles below the knee via blood pressure cuff, immediately reduces Ia afferent feedback by increasing the Achilles tendon contributions to stretch, thus limiting the actual plantarflexor fascicle stretch.

The increase in ipsilateral gluteus maximus muscle activations seen in Figure 19, could be an intralimb compensatory response to the decrease in tibialis anterior and rectus femoris muscles activations. The gluteus maximus muscle is a primary extensor in pedaling, normally active from 0-180 (Raasch, 2007; Zajac, 2003). The reduction in ipsilateral tibialis anterior and rectus femoris muscle activations (Fig. 18) leads to a lower crank torque (Fig. 23A) in the same flexion to extension pedaling phase (Q1). The gluteus maximus muscles significant increase in activation in the subsequent extension quadrant (Q2) is most likely to make up for insufficient power application in Q1 (Fig. 23A). Alternatively it could be an interlimb compensation for reduced afferent feedback from the contralateral plantarflexors. The average ipsilateral crank torque in Q2 trending towards increasing over that of Baseline, (Fig. 9B), and the significantly higher ipsilateral resultant force in Q2 and Q3 over Baseline (Fig. 23C), can most likely be attributed to the increased action of the gluteus maximus muscle.

4.4.6 Conclusions

We suspected an imbalance in the stance phase extensor afferent feedback and swing phase flexor muscle activations of the limbs may act to trigger the spontaneous transition from walking to running. Although our hypothesis that flexor motor output

would increase was not supported, we did observe contralateral afferent feedback dependent modulations of ipsilateral flexor motor output. To our knowledge, this study provides the first investigation into the net effects in humans of contralateral below-knee afferent feedback on ipsilateral muscle coordination, independent of ipsilateral mechanical compensations during locomotion. In conclusion, unilateral below-knee, ischemic deafferentation has significant effects on both inter and intra-limb motor output. The net interlimb effect is a significant decrease in flexor muscle activations (tibialis anterior and rectus femoris) during the transition from flexion to extension in pedaling (Q1). There is also a within-limb response of significantly lower biceps femoris long head activations during the transition from extension to flexion (Q3) and lateral gastrocnemius activations during flexion (Q4). Due to the rapid time course of these responses (within 0-4 minutes of IB onset), we speculate that cutaneous and/or Ia afferents may have a more substantial role in the interlimb coordination of the legs during locomotion than previously expected.

CHAPTER V

CONCLUSIONS

Afferent feedback is important for modulating locomotion and maintaining stability. Studying locomotor extremes and applying perturbations to normal locomotion allows us to probe the effects of afferent feedback on the control of normal gait. Investigating the walk-to-run gait transition specifically provides a unique locomotor event to investigate the fundamental determinants of legged locomotion (walking or running) and identify the sensory inputs important to the ongoing neuromuscular control of walking and running.

5.1 Major findings

The first goal of this dissertation was to investigate the contributions of plantarflexor muscles during stance (Aim 1) and flexor muscles during swing (Aim 2) to the walk-to-run transition. To accomplish this I used unilateral, transtibial amputee subjects as a means to assess the affects of unilaterally eliminating plantarflexor propulsive force production and below-knee flexor activation on the walk-to-run transition speed. The main objective of Aim 1 was to determine the preferred gait transition speeds of unilateral, transtibial amputee subjects, and the influence of kinetics on the walk-to-run gait transition speed. Unilateral, transtibial amputee subjects transition between gaits at a lower speed than able-bodied controls and are still able to generate higher propulsive forces walking at speeds above their preferred gait transition speed. This finding indicates that their walk-to-run transition is not likely dictated by the force-length-velocity characteristics of the intact plantarflexor muscles. Thus, as an experimental model, unilateral, transtibial amputee subjects can provide unique insights for decoupling the previously identified performance limit of plantarflexor muscles from

the preferred gait transition speed in order to probe other potential determinants. The main objective of Aim 2 was to quantify the muscle activation during walking and running gaits relative to the walk-to-run gait transition speed for unilateral, transtibial amputee subjects. The swing phase tibialis anterior muscle activation is a major determinant of the walk-to-run transitions in unilateral, transtibial amputee subjects. Swing phase dorsiflexion moments alone do not explain these results and additional work is necessary to probe potential mechanical and neural explanations. Furthermore, in unilateral, transtibial amputee subjects, swing-phase rectus femoris and biceps femoris long head activations and their respective joint moments are a function of changes in absolute speed and thus not indicative of their significantly lower gait transition speed.

The second goal of this dissertation was to probe the potential contributions of afferent feedback to the underlying neuromuscular mechanism ultimately responsible for the transition (Aim 3). The main objective of Aim 3 was to evaluate the effects of contralateral sensory loss on the motor output of the ipsilateral leg. Unilateral below-knee, ischemic deafferentation has significant effects on both inter- and intralimb motor output. The net effect of contralateral sensory loss below the knee is a significant decrease in ipsilateral flexor muscle activations during the transition from flexion to extension in pedaling (Q1). Due to the rapid time course of these responses, I speculate either i) contralateral below-knee afferents (most likely Ia and/or cutaneous) have a net excitatory effect on the ipsilateral flexor muscles or ii) contralateral above knee afferents (most likely Ib) have an inhibitory effect on the ipsilateral flexor muscles. I suspect Ia and cutaneous afferents may have a more substantial role in pedaling locomotion and potentially the walk-to-run gait transition than initially thought. As I did not explicitly test whether a discrepancy in the stance phase extensor afferent feedback and swing phase flexor muscle activations between the legs causes the walk-to-run gait transition, future investigations of this should consider

the individual effects of cutaneous, Ia, and Ib feedback from contralateral extensors onto ipsilateral flexors.

5.2 Implications to the investigations of walk-to-run gait transition

Per my investigations, it appears as though the walk-to-run transition is influenced differentially by variables depending on the dynamics of the system. Thus, I suspect the previously discussed Extensor hypothesis (Arnold et al., 2013; Farris and Sawicki, 2012a; Neptune and Sasaki, 2005)) and Flexor hypothesis (Ivanenko et al., 2008; Malcolm et al., 2009b; Prilutsky and Gregor, 2001), are not mutually exclusive. Pires, et al. proposed a mechanical cascade during stance influencing the gait transition, in that as walking speed increases, mechanical limits of the ankles cause subsequent unfavorable compensations at the hip (2014). I suspect that contralateral stance phase extensors and ipsilateral swing phase flexors may be tied together via a similar cascade, but neurally modulated via afferent feedback from the contralateral extensors affecting motor output of ipsilateral flexors.

Bartlett and Kram found that selectively perturbing the demand on dorsiflexors, plantarflexors, and hip flexors resulted in altered walk-to-run transition speeds, however perturbing multiple muscle groups at once did not produce a summative effect. They introduced the theoretical framework that a critical threshold of influence must be met in order for the walk-to-run transition to occur, in which an ultimate, underlying trigger can be influenced by various muscle groups, whose impact can change with walking conditions (e.g. incline walking). I suspect that the ultimate, underlying trigger for the walk-to-run transition is strongly influenced by the interlimb coordination of extensor afferent feedback and flexor muscle activations.

5.2.1 Aim 1 implications

Propulsive force production appears to always peak at ∼2.1 m/s regardless of the subject population and gait transition speed. I observed this in able-bodied subjects, unilateral, transtibial amputee subjects subjects (Aim 1), and a single bilateral amputee subject I collected pilot data from using the same protocol as in Aim 1 (Fig. 25A). I suspect that this is due to the pendular dynamics of walking (Kram et al., 1997). This is supported by ability of simplistic compass gait models to accurately predict changes in gait transition speeds with changes in incline (Hubel and Usherwood, 2013). However, modulations in afferent feedback from the plantarflexors at high walking speeds, due to their unique force-length-velocity characteristics may still affect the bilateral coordination and contribute to the walk-to-run gait transition. As my Aim 3 investigation demonstrated, unilateral manipulation of afferent feedback has a significant effect on interlimb muscle coordination and amplitude.

5.2.2 Aim 2 implications

Rectus femoris and biceps femoris long head muscle activations during swing phase also appeared to be tied to changes in absolute speed changes, as critical divergent points for both were identified at similar absolute speeds in able bodied controls and unilateral, transtibial amputee subjects (Aim 2). Tibialis anterior muscle activation was the only tested variable that significantly corresponded with the walk-to-run transition speed in both able-bodied controls and unilateral transtibial amputee subjects. However that does not mean that limits in plantarflexor force production and flexor muscles (those measured and unmeasured) did not substantially contribute to the able-bodied walk-to-run transition, and possibly the unilateral transtibial amputee walk-to-run transition.

Although I concluded that the tibialis anterior is of major importance in both unilateral transtibial amputee subjects and able-bodied subjects, that is not to say

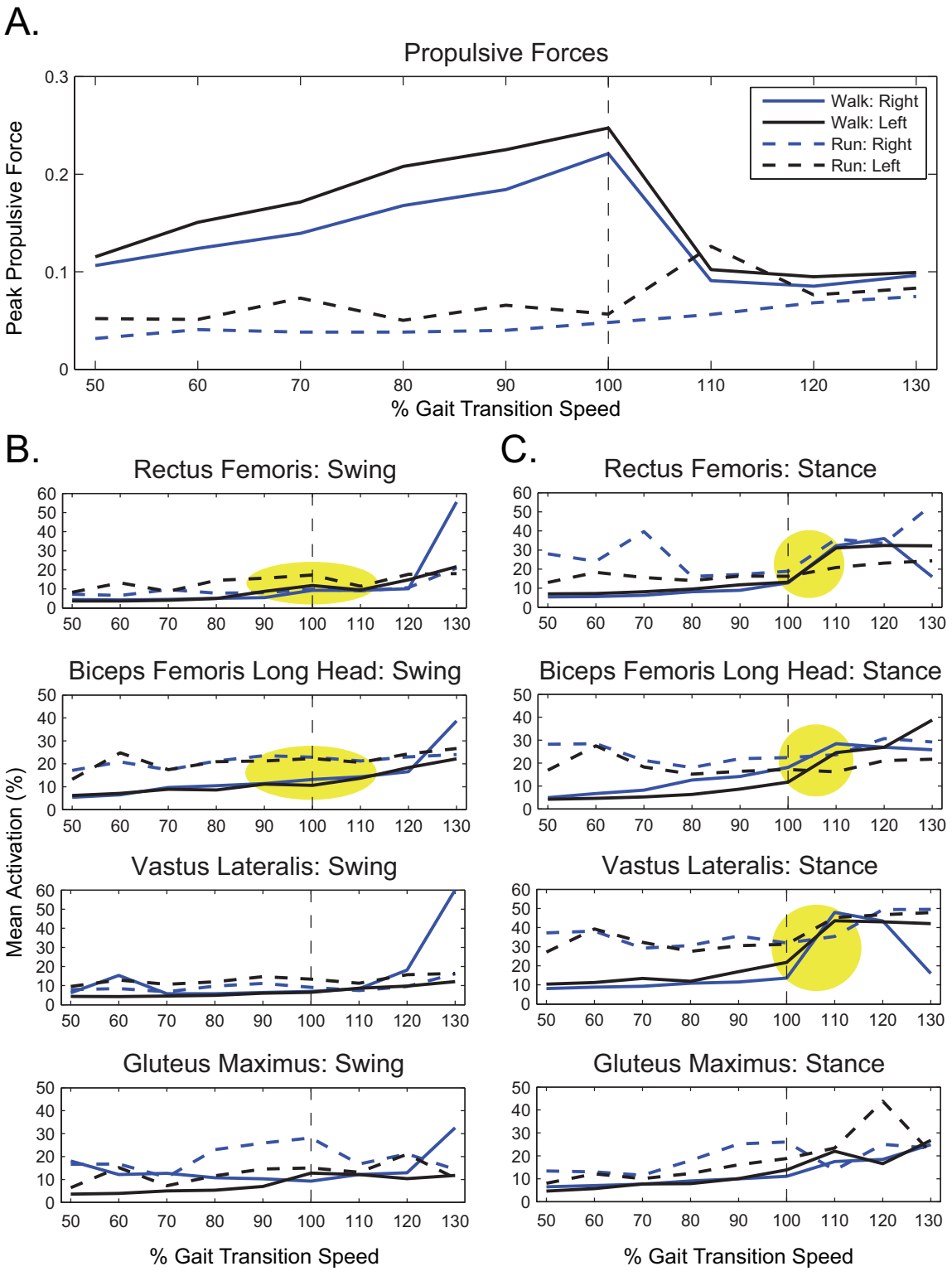

Figure 25: Bilateral, transtibial amputee pilot data (n=1). A)Peak propulsive force production normalized to body weight. B) Swing phase muscle activations. C) Stance phase muscle activations. Data presented is for the right (blue) and left (black) legs during walking (solid lines) and running (dashed lines). Yellow ovals and circles indicates areas on interest discussed in the text. 100% Gait transition speed indicates 2.1 m/s.

that the activation levels of one muscle is ultimately responsible for the walk-to-run gait transition. Work by Prilutsky and Gregor (2001) reported that total sums of stance- and swing-related muscle activations, exhibited the characteristics of a critical divergent point (as defined in Aim 2), and corresponded with previously reported changes in perceived exertion during walking and running (Hreljac et al., 2002; Noble et al., 1973). This was later corroborated by estimations of mean lumbosacral alpha motor neuron activations during walking and running with respect to the gait transition (Ivanenko et al., 2008). Additionally, the researchers found this pattern to hold true despite removing any one muscle from the mean of all activations. This is further corroborated by pilot data I collected from a bilateral, transtibial amputee, following the same protocol used in Aim 2. Despite the bilateral amputees complete lack of functional tibialis anterior muscles, he was still able to transition between a walk and a run.

5.2.2.1 Bilateral amputee pilot work

Cursory assessment of walking and running muscle activations of the bilateral, transtibial amputee, shows swing-phase rectus femoris and biceps femoris long head muscle activations do not have critical divergent points (Fig. 25B, yellow ovals). Despite similar gait transition speeds, this is not consistent with our findings in able-bodied control subjects (Aim 2). The stance-phase activations of rectus femoris, biceps femoris long heard, and vastus lateralis do exhibit a marked increase in activations during walking beginning at 110% GTS in comparison to 100% GTS (Fig 25C, yellow circles), however not so much so that it creates a critical divergent point with respect to running activations. Interestingly, the bilateral, transtibial amputee transitioned between gaits at 2.1 m/s, remarkably close to the average transition speed in able-bodied subjects in Aim 1 (2.09 m/s). Also consistent with able-bodied subjects, propulsive force production during walking peaked at 100% GTS (Fig. 25A). Given

that bilateral, transtibial amputee subjects do not have functional plantarflexor muscles, their propulsive force production at speeds above ∼2.1 m/s must be limited by something other than intrinsic architectural limits of the plantarflexors, as previously shown in able-bodied subjects (Arnold et al., 2013; Farris and Sawicki, 2012a; Lai et al., 2015; Neptune and Sasaki, 2005). Although, the bilateral, transtibial amputee results add an interesting element to this thesis work, ultimately the results from one subject must be interpreted cautiously and can not provide a basis for drawing final conclusions.

5.2.3 Aim 3 implications

In Aim 3 I assessed the effects of contralateral below-knee sensory loss on the motor output of the ipsilateral leg. The results from this investigation provide further support for the immediate and substantial effects that contralateral changes in afferent feedback can have on ipsilateral muscle activations, specifically the swing phase-flexor muscles. Ultimately I attempted to reconcile two major hypotheses in the literature regarding the walk-to-run transition by proposing the underlying neuromuscular mechanism involved a force feedback-dependent inhibition (from contralateral below-knee extensors) of swing phase flexor muscle activations. The findings that above-knee extensor afferents and below-knee extensor afferents may have a net inhibitory and facilitory effect on ipsilateral flexor muscles, respectively, does not clearly reconcile the aforementioned Extensor hypothesis & Flexor hypothesis of the walk-to-run transition. However, our investigations (Aim 2) support that a critical level of muscle activation, especially from the tibialis anterior (a flexor muscle) is very important to walk-to-run transition (Aim 2). Thus, any influence extensor afferents may have on flexor muscle activations will in turn have an effect on the walk-to-run transition.

5.3 Discussion of possible afferent effects on interlimb coordination

Previous ischemic nerve block studies have indicated approximately a 15-20 minute timeline necessary to induce suppressions of Ia and Ib afferent feedback with application of a blood pressure cuff (Berger et al., 1984; Dickey and Winter, 1992; Dietz et al., 1979; Laszlo, 1967). Our results surprisingly indicated immediate affects on afferent feedback after the application of the contralateral ischemic block (Aim 3). This is evident by the significant decrease in ipsilateral rectus femoris activations at IB0 (Fig 18). Quantification of cutaneous sensation with von Frey Filaments indicated reductions in feedback as soon as the first assessment after the ischemic block was applied (Fig. 16, pre-IB4). Reductions were significant for the L5 dermatome beginning at pre-IB4, and for the S1 and L4 dermatomes beginning at pre-IB12. However, due to the immediate (within $\sim$1 minute of application of the blood pressure cuff) changes in muscle activations I observed, it appears that our results could also be attributed to changes in feedback from afferents (most likely Ib) from muscles above the IB, (located above the knee) as well as other afferents below the knee (most likely Ia). Potential contributions of afferent types to my results are discussed in this section. It is important to remember that effects to afferent input are both task and phase dependent (Zehr, 1999), hence my extrapolating any functional relevance from responses observed during cycling onto other forms of locomotion (walking, running, etc) are done so speculatively.

5.3.1 Increase in afferent feedback of knee and hip extensors

Ting et al. previously identified reductions in ipsilateral tibialis anterior and rectus femoris activations due to increases in extensor force production during pedaling (1998; 2000). They proposed the spinal locomotor central pattern generator for pedaling included inhibitory crossed limb connection between contralateral extensor and

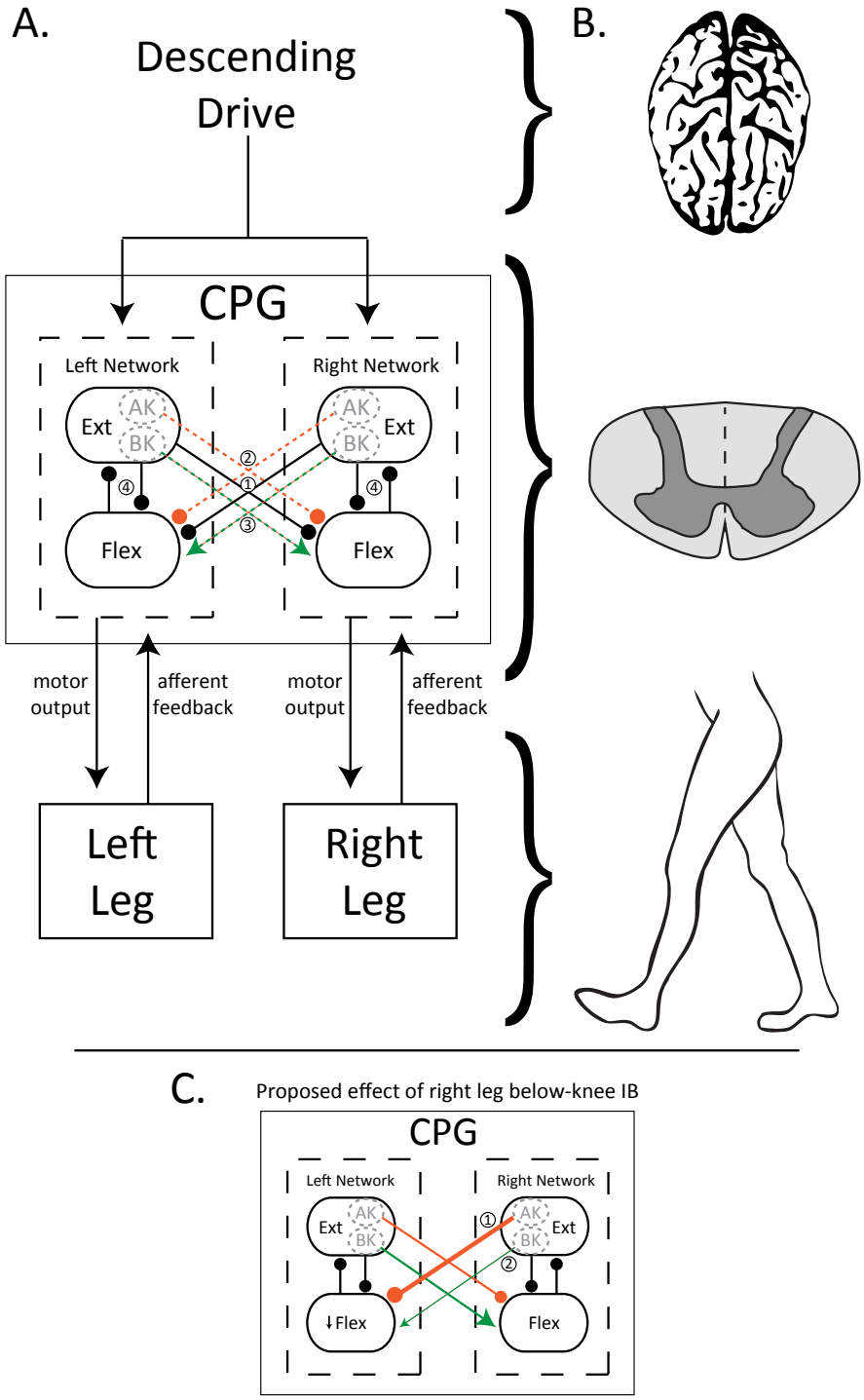

Figure 26: Proposed CPG organization. A) 1: Inhibitory interlimb coupling originally described by Ting et al., between extensor half centers (Ext) and contralateral flexor half centers (Flex)(organization of figure in black adapted from Ting et al.,, 1998). 2: Proposed crossed limb inhibition between above-knee (AK) Ext and contralateral Flex(orange); 3: Proposed crossed limb facilitation between below-knee (BK) Ext and contralateral Flex(green); 4: Ipsilateral inhibition of Ext and Flex half centers B) Graphical representation of location for each component of the control model. From top to bottom: brain/ cortical level; spinal level; left and right legs C. Proposed effect of right leg below-knee IB as in Aim 3. 1: Increased AK inhibition; 2: Decreased BK facilitation.

ipsilateral flexor half centers (Fig. 26A, black,1). The immediate changes I observed may also have been due to an increase in afferent feedback of knee and hip extensors (most likely from force-dependent Ib afferents). Resultant force production increased significantly after the onset of the ischemic block (Fig. 23B, beginning at IB0). Although this significant increase was relatively small in comparison to the magnitude of total force proxduction, it cannot be dismissed. In line with the increase in resultant force production, I anecdotally observed increases in vastus lateralis muscle activations, which act to direct force during extension (Zajac et al., 2003), however the differences observed were not significant ($p = 0.175$). Increases in cortico-spinal excitability of muscles proximal to the IB, could also have contributed to the increase in force production and thus Ib afferent feedback (Brasil-Neto et al., 1992; Brasil-Neto et al., 1993; McNulty et al., 2002; Vallence et al., 2012; Ziemann et al., 1998). The afferent feedback below the knee was substantially degraded by an ischemic nerve block during my Aim 3 investigation. Thus, I propose a crossed limb inhibition pathway between Ext and contralateral Flex is mainly due to extensor afferents from muscles above the knee (AK) (Fig. 26C, orange,1).

5.3.2 Reduction in afferent feedback below the knee

The below-knee (BK) contralateral afferent feedback (most likely Ia and/ or cutaneous), was reduced by the ischemic block in Aim 3. A crossed limb facilitation pathway between below-knee Ext and contralateral Flex could also account for the decrease in ipsilateral flexor activation we observed (Fig. 26C, green,2). I speculate the immediate changes observed in motor output may be due to a reduction in Ia afferent feedback as a result of the pressure applied to the plantarflexors by the cuff, rather than ischemic deafferentation. Background EMG from tibialis anterior and soleus muscles do not increase with the onset of an ischemic block, indicating that

the ischemic block itself does not alter their respective motor neuron pool excitabilities (Leukel, 2009). Simply applying and inflating a blood pressure cuff below the knee, shows an immediate (within 5 seconds of cuff application) reduction in short latency response (SLR) to stretch in the soleus muscle (Leukel et al., 2009). The SLR is thought to be mediated by Ia afferents (Eccles et al., 1962; Gillies et al., 1969; Hagbarth et al., 1973), thus a reduction in SLR implies a reduction in Ia afferent feedback. Leukel et. al proposed a mechanism to explain this immediate response (2009). Before the blood pressure cuff is inflated below the knee, dorsiflexion elicits normal muscle-tendon complex dynamics. However, upon inflation of the cuff, the underlying muscles (plantarflexors) may be restricted and dorsiflexion could result in an increased lengthening of the Achilles tendon. This would result in a reduction in actual muscle stretch and subsequent Ia afferent feedback.

Previous literature has indicated manipulating cutaneous afferent feedback can effect muscle activations during locomotion. Looking across the limbs, contralateral sural nerve stimulation during stance- phase of walking causes an increase in ipsilateral tibialis anterior activation (Hoogkamer et al., 2012). A reduction in contralateral sural nerve feedback at onset of ischemic block could have relevance to the subsequent decrease I observed in ipsilateral tibialis anterior muscle activations. As reductions in cutaneous afferent feedback were directly observed in Aim 3, I am confident a loss of cutaneous feedback had an effect. The magnitude of that effect however, cannot be determined and may have been overpowered by changes in other afferents.

5.3.2.1 Proposed functional relevance of below-knee extensor muscles facilitating ipsilateral flexor muscles

I postulate this facilitation from below-knee extensors onto contralateral flexors could have functional relevance in gait for an anticipatory activation of flexor muscles preceding heel-strike to increase ankle joint stiffness. Our results of Aim 3 show a

significant reduction in the ipsilateral tibialis anterior and rectus femoris muscle activations during quadrant 1 (the flexion to extension transition), which can be likened to terminal swing/early stance in walking. The below-knee afferent feedback from the contralateral limb during stance may cause an excitation of ipsilateral flexor muscles during terminal swing phase. Appropriate joint stiffness upon heel strike and weight acceptance is important to energy absorption (Ogawa et al., 2014). It is important to note that as walking speed increases, generally so does the collisional force (Aim 1). Interestingly, in a simulation study of a bipedal model with compliant joints, adjusting ankle stiffness during walking induced gait transitions between other forms of compliant walking (walking with altered mechanics) (Huang and Wang, 2012). This research indicated that ankle stiffness is important to gait selection in bipeds. Whether or not plantarflexor Ia afferent feedback increases with walking speed is not clear in the literature (Cronin et al., 2009; Sinkjaer et al., 1996; van der Krogt et al., 2009). Regardless, the probability of changes in Ia feedback being due to changes in the soleus muscle lengthening during level walking is unlikely, as modeling and in vivo investigations have confirmed it is mainly isometric during stance phase of walking to exploit elastic energy storage in the tendon (Ishikawa et al., 2005; Lai et al., 2015; Zajac et al., 2003). However, during down slope walking in cats, soleus and medial gastrocnemius muscle fascicles significantly increase length and velocity (Maas et al., 2009), resulting in an increase of Ia afferent feedback (Abelew et al., 2000; Gregor et al., 2006; Sabatier et al., 2015). Thus our results could be pertinent to aiding interlimb coordination during downslope walking.

5.4 Limitations & future directions

5.4.1 Prosthetic componentry

The prosthetic componentry of subjects in Aim 1 and Aim 2 was not standardized. Variability of stiffness in prosthetic feet can alter muscle activations in both the

intact and residual limbs (Fey et al., 2013). Although standardizing prosthetic foot componentry would be ideal, providing the necessary hardware and clinical services, as well as waiting the lengthy adaptation period to a new device made this approach unreasonable and unnecessary to test our hypothesis. Instead, I limited our inclusion and exclusion criteria to pick a relatively homogenous subject pool with respect to prosthetic device type (included passively-elastic; excluded Solid-Ankle Cushion Heel (SACH) and powered ankle feet) and activity level(recreationally or competitively fit) to minimize intersubject variability. I am confident only including passively-elastic prosthetic devices maintained the homogeneity of the subject pool, as the variability in our amputee EMG and kinematic data was comparable to that of our control subjects.

5.4.2 Anterior-posterior propulsive force production as an analog to plantarflexor force production

In Aim 1, I make the assumption that anterior-posterior propulsive force production is indicative of the intact side plantarflexor force production in unilateral, transtibial amputee subjects. This is a very reasonable assumption for able-bodied subjects, as plantarflexor muscles have been shown to be the major source of propulsive force production during walking (Anderson and Pandy, 2003; Kepple et al., 1997; Neptune et al., 2001; Neptune et al., 2004; Silverman and Neptune, 2012; Zajac et al., 2002, 2003). Additionally, modeling and experimental studies indicate that decreases in anterior-posterior propulsive force production at higher than normal walking speeds is due to limitations of the force-length-velocity characteristics of the plantarflexors (Arnold et al., 2013; Farris and Sawicki, 2012a; Lai et al., 2015; Neptune and Sasaki, 2005). I was not able to directly assess changes in intact side plantarflexor muscles' contractile behavior at high walking speeds in the unilateral transtibial amputee subjects. Thus, despite their intact side increases in propulsive force production during walking at higher than normal speeds (Fig. 3A), I did not directly observe

that the force-length-velocity characteristics of the intact side plantarflexors were not a limiting factor resulting in their lower gait transition speed. In comparing able-bodied subjects to unilateral, transtibial amputee subjects intact side, previous modeling work indicates similar contributions of the soleus and gastrocnemius muscles to propulsion (Silverman and Neptune, 2012). However to our knowledge no one has quantified the series elastic element and muscle fascicle contributions to plantarflexor force production in AMP subjects. Future investigations of unilateral, transtibial amputee subjects should dissociate the contributions of the plantarflexor muscle-tendon complex (series elastic element and muscle fascicle) to force production, specifically during increasing walking speeds. This could be accomplished with the use of at musculoskeletal model or an in vivo assessment with ultrasonography during walking at constant velocities above preferred walking speed and above the walk-to-run transition speed.

5.4.3 Deciphering contributions of afferent feedback to interlimb coordination

Although the results of Aim 3 are intriguing, the conclusions that can be drawn from them are limited due to ambiguity in the exact source of the contralateral afferent feedback affecting the ipsilateral side. I have identified methodological considerations that should be accounted for in future studies using the mechanically decoupled cycle ergometer to pin point the underlying circuitry responsible for our results.

One of the major limitations of our investigation was the increase in contralateral force production after the ischemic block was applied. Future investigations need to account for or prevent this from occurring. Providing real-time visual feedback of resultant force output to subjects, specifically in the flexion-to-extension and extension phases (Q1 and Q3, respectively) during pedaling could account for this. An additional investigation to verify the mechanism of immediate Ia feedback suppression via application of a blood pressure cuff below the knee is necessary if I plan on

utilizing it in future investigations. The proposed mechanism by Leukel et al. (2009), is that the reduction in Ia feedback is due to decreased plantarflexor muscle fascicle lengthening. This could be verified by in vivo assessments of muscle fascicle shortening by ultrasonography during dorsiflexion. Additionally all of our collections once the ischemic block was applied were during bilateral pedaling. This prevents us from knowing whether the changes in motor output we saw were locomotor dependent. All future investigations should include unilateral pedaling trials for each condition.

Previous work by Ting et al., has demonstrated that increases in contralateral force output during extension results in ipsilateral reductions in flexor motor output. Future investigations should focus on systematically assessing the effects of modulating Ib, Ia, and cutaneous afferents individually and in tandem. Potential conditions to accomplish this include: load manipulation (Ib), Achilles tendon vibrations and/or blood pressure cuff application (Ia), and lidocaine injections (cutaneous). Furthermore assessment of Hoffman-reflex and/or plantarflexor muscle fascicle shortening (via ultrasonography) during each condition would be ideal to verify changes in Ia excitability and plantarflexor mechanics. Defining the afferent inputs that contribute to the excitability of swing phase flexors muscles will provide insights into the neural interlimb connections of the legs. Subsequent investigations of the walk-to-run gait transition speed should use these insights in developing conditions to unilaterally and bilaterally perturb extensor afferents and flexor muscle demands.

5.5 Clinical relevance

This research presented in this dissertation has clinical applications to prosthetic device development and gait rehabilitation strategies.

Currently, the field of prosthetics is attempting to advance technology and design of lower extremity prosthetic devices to most accurately and efficiently mimic able-bodied human gait. A key facet to this is the ability for amputee subjects to both

walk and run with the same device. However, this is being attempted with limited information due to the paucity of scientific knowledge regarding gait transitions in amputee subjects. Due to high cost and insurance restrictions, most lower limb amputee subjects are restricted to only one device (per amputation) (Mitka, 2008): an everyday walking prosthesis with a heel component and foot covering for daily ambulation. J-shaped, carbon fiber blades characteristic of running-specific prostheses are ideal for running, as they significantly lower heart rate and oxygen consumption when compared to walking prosthesis, to levels consistent with those of able-bodied controls (Brown et al., 2009). Presently, prosthetic design is migrating toward powered biomimetic components, which have also been shown to decrease oxygen consumption as compared to traditional walking prostheses (Herr and Grabowski, 2012). However, these powered prosthetic foot-ankle components currently only allow for walking, which is not surprising since the gait transition has long been a stumbling block in the field of legged robotics (Aoi et al., 2012). Furthermore, sensory feedback and interlimb coordination have been completely neglected in prosthetic devices. Currently neuromechanics-based orthotic exoskeletons are being developed for use in the stroke population (Takahashi et al., 2015). These exoskeletons utilize myoelectrical control via the stroke patients' paretic soleus muscle to proportionally modulate timing and magnitude of plantarflexor assistance as needed during the propulsive phase of the gait cycle. To my knowledge, my work in Aim 1 is the first study to characterize the gait transitions in unilateral transtibial amputee subjects. In Aim 2 I identified the tibialis anterior muscle activations as a key determinant of the gait selection of unilateral, transtibial amputee subjects and able-bodied controls. These findings provide foundational data for the development of more robust lower limb prosthetic devices to include both walking and running. Given my results, I propose a possible way to account for interlimb coordination and facilitate smooth transitions between gaits would be to use intact leg tibialis anterior activations as a reference input to a

powered ankle-foot devices control algorithm.

To strategize appropriate gait rehabilitation strategies, understanding the interaction between mechanical compensations and neural pathways that govern intra- and interlimb coordination during locomotion is of great importance. Pinpointing how deficits or abundance of specific afferent signals effect motor output uni- and bi-laterally can improve our understanding of biomechanical gait compensations in pathological populations. My work is especially pertinent to pathologies that manifest with unilateral deficits, such as in hemiparesis resulting from stroke, cerebral palsy, and spinal cord injury, as well as musculoskeletal trauma. Although my work has not identified specific connections per say, it provides a foundational basis for future investigations. Specifically, my results in Aim 3 are most likely due to an increase in Ib afferent feedback from muscles proximal to the ischemic block or a decrease in Ia and/or cutaneous afferent below the knee and require additional investigation.

Another interesting finding of potential clinical importance was the increase in ipsilateral gluteus maximus muscle activations after ischemic block (Aim 3). As this could be indicative of an interlimb pathway affected by the contralateral side below-knee deafferentation, providing a neural mechanism to explain pathological gait compensations. Previous studies have found that energy lost during the heel strike collision, must be made up in order to continue steady walking (Garcia et al., 1998; Kuo, 2002). The most energy efficient strategies to accomplish this is through either increased hip joint torque during single limb support or increased propulsive force production during double limb support. The proposed explanation of an interlimb pathway between contralateral side below-knee afferents and ipsilateral hip extensors could be functionally relevant to gait in persons with unilateral below-knee below-knee deficits such as in persons with amputation, stroke, or paralysis. As in unilateral, below-knee amputee subjects the lack of an effective foot-ankle complex limits both propulsive force production and afferent feedback. Compared to controls,

amputee subjects have higher positive hip work (Grumillier et al., 2008; Silverman et al., 2008) and hip extensor moments (Bateni and Olney, 2002; Grumillier et al., 2008) during early stance in walking, when the intact limb is leading (amputated side trailing). This increased hip extensor action is considered a compensatory response to aid propulsion due to the insufficient propulsion on the amputated side. Simulation studies have shown increases in gluteus maximus activations, during early stance as a contributor to this compensation (Silverman and Neptune, 2012; Zmitrewicz et al., 2007). Walking with a contralateral total ischemic block above the knee, also shows an increase in gluteus maximus activation on the ipsilateral side (Dickey and Winter, 1992). Thus, deficits in contralateral afferent feedback from the action of propulsion could elicit an increase in contralateral hip extensors (gluteus maximus). This is possible through either excitation (via an excitatory connection) or facilitation (via the release on an inhibitory connection). Suggesting that under normal locomotor circumstances contralateral below-knee afferent feedback could have an inhibitory effect on the ipsilateral hip extensors. Thus providing a neural basis for the development of rehabilitation strategies for populations exhibiting this compensation.

5.6 Final thoughts

The goals of this dissertation were to investigate the contributions of plantarflexor muscles during stance and flexor muscles during swing to the walk-to-run transition and probe the potential contributions of afferent feedback to the underlying neuromuscular mechanism ultimately responsible for the transition. In line with my goal, this research ultimately contributes four major findings to the field: i) unilateral transtibial amputees transition from a walk to a run at significantly slower speeds than able bodied individuals, ii) the walk-to-run transition speed is not limited by propulsive force production in unilateral, transtibial amputees, iii) the tibialis anterior muscle is of major importance in the walk-to-run transition in both unilateral

transtibial amputee subjects and able-bodied individuals, and iv) contralateral below-knee extensor afferents may have a net facilitory effect on ipsilateral tibialis anterior and rectus femoris muscles during locomotion.

APPENDIX A

MECHANICALLY DECOUPLED CYCLE ERGOMETER

A.1 Index of effectiveness

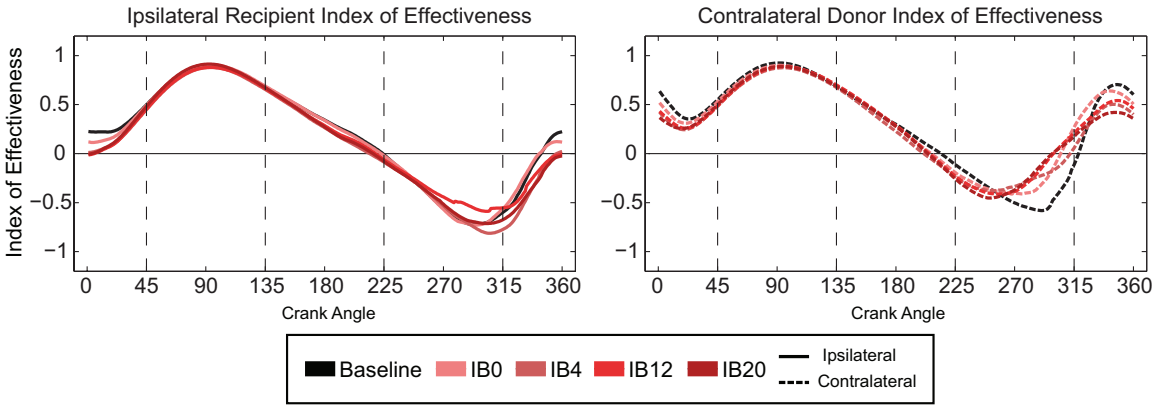

Figure 27: Index of Effectiveness

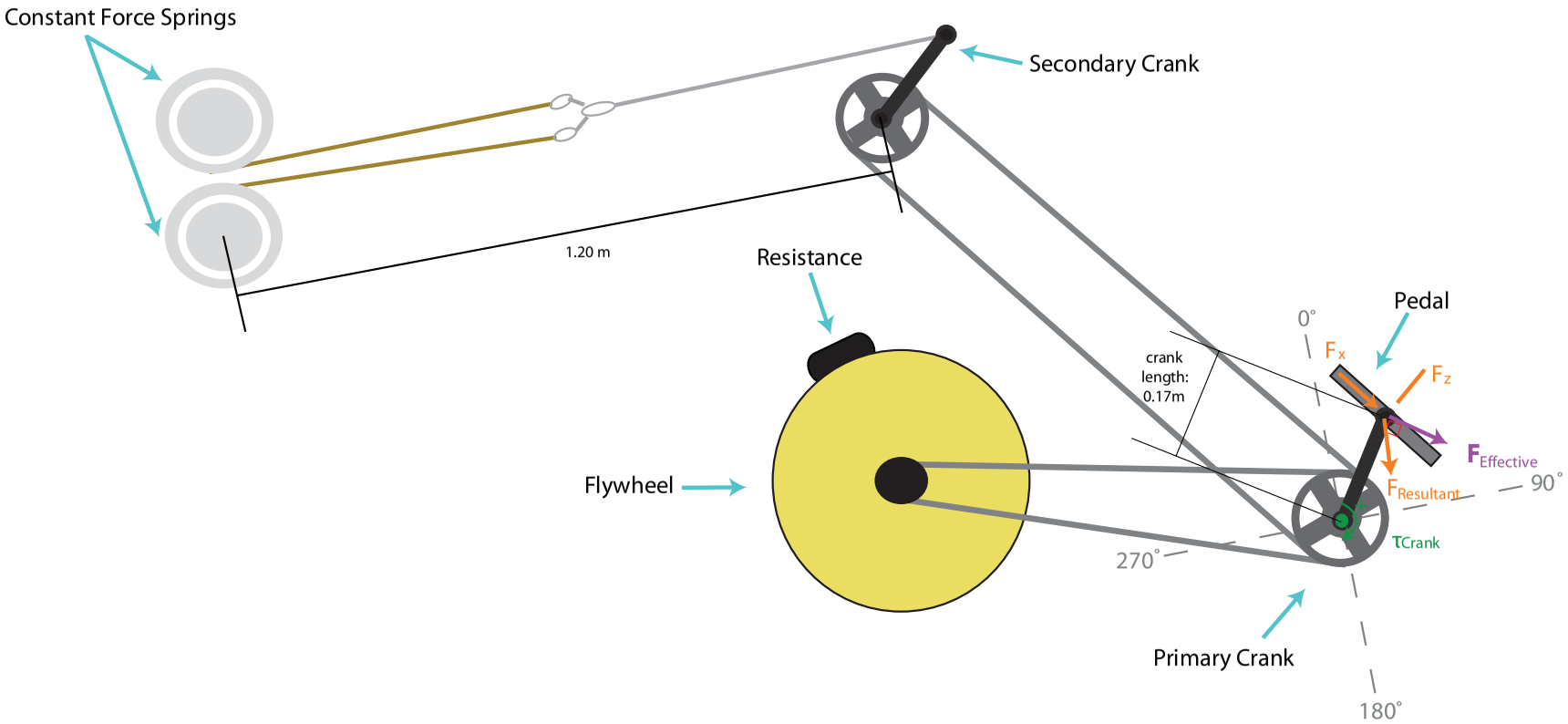

Figure 28: Schematic of the mechanically decoupled cycle ergometer.

A.2 Force pedal calibration

The force pedals each used two Kistler type 9251 piezoelectric load cells. Voltage was amplified through a Kistler 5010 amplifier. The voltage conversion for the pedal Z direction was 100 N/V and 40 N/V for the pedal X direction. Sensitivity (V/Cu) was determined through multiple calibration trials

A.2.1 To calibrate in the Z direction (See Fig. 27):

- Secured force pedal in a clamp in the upright position
- Verified force pedal was completely level
- Placed 58.8lbs. of weight (265.55N) on the force pedal to calibrate the voltage output
- Measured voltage output collected through Vicon as well as directly out of the Kistler 5010 Amplifier with a voltmeter.
- The output N/V was calculated
- The sensitivity (V/Cu) of the amplifier was adjusted such that 100N = 1 V
- This process repeated and a minimum of three consistent trials were obtained.

A.2.2 To calibrate in the X direction (See Fig. 27):

The process described above was completed with two exceptions:
- The force pedal was placed in the clamp such that the X direction faced upwards
- Placed 10.0lbs. of weight (44.48N) on the plate to calibrate the voltage output
- The sensitivity (V/Cu) of the amplifier was adjusted such that 40N = 1 V

A.3 Mechanically decoupled cycle ergometer vs. Lode

A.3.1 Contributions of constant force springs

The 28.8 lbs of force was applied from the constant force spring (Stainless Steel Constant-Force Spring, Item 9293K25, McMaster Carr) to each 0.17m secondary

crank arm over a distance of 1.2m. It was estimated that the addition of the constant force springs applied a maximum resistive torque of -21.83Nm at 98° and a maximum assistive torque 21.83Nm at 262° (Fig. 28).

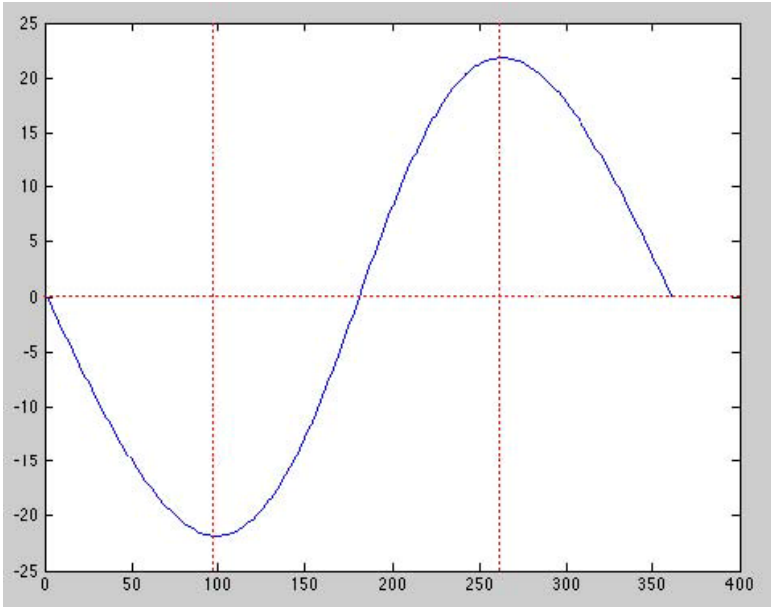

Figure 29: Calculated trace of the crank torque generated by the constant force spring applied to one crank. Vertical red dashed lines indicate maximum resistive and assistive torque).

An electromagnetically braked ergometer (Lode)(Excaliber Sport, Groningen, Netherlands) was utilized to assess the differences in crank torque profiles with and without the constant force spring applied (Fig. 29).

It should be noted that all watts calculations were made with respect to time not crank angle.

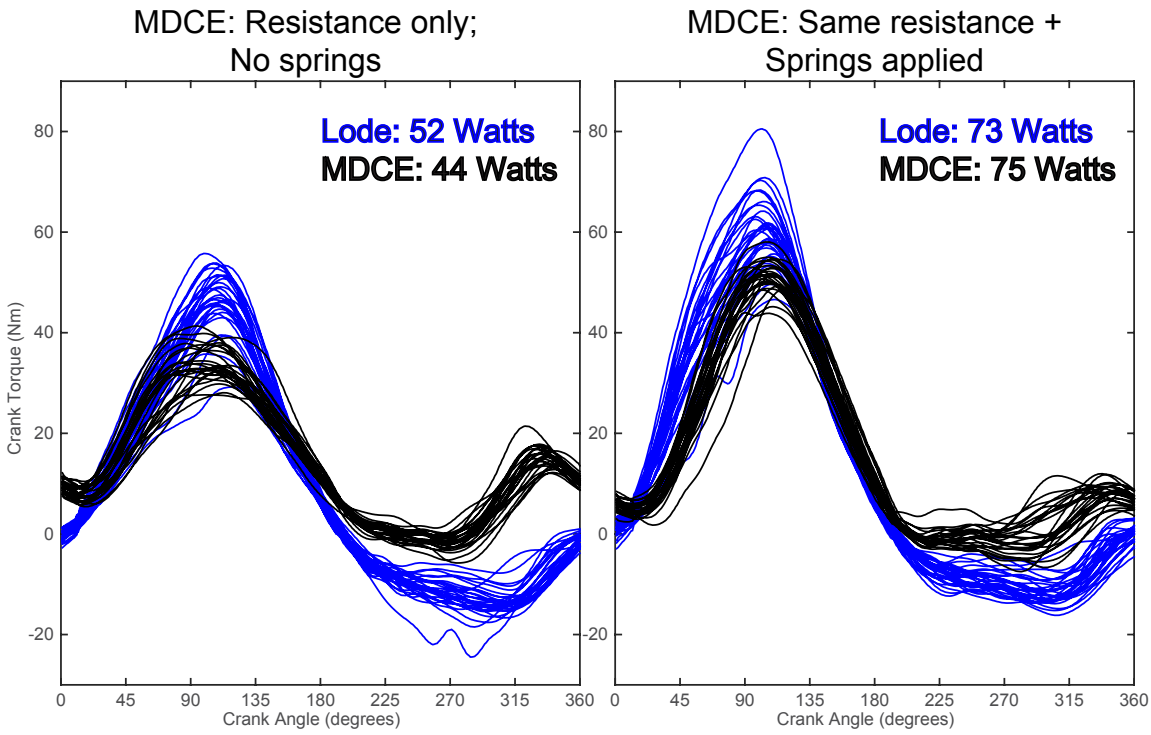

Figure 30: Effects of of the constant force springs on crank torque (MDCE: mechanically decoupled cycle ergometer).

A.4 Calculations

A.4.1 Resultant force

θpedal = Pedal Angle (degree) PHEX = horizontal (x) component of pedal heel trajectory in coordinate plane

PTOX = horizontal (x) component of pedal toe trajectory in coordinate plane

PHEZ = vertical (z) component of pedal heel trajectory in coordinate plane

PTOZ = vertical (z) component of pedal toe trajectory in coordinate plane

Resultant Fx = horizontal (x) component of resultant force on pedal

Resultant Fz = vertical (z) component of resultant force on pedal

Fx = horizontal (x) component of force produced by foot on the pedal

Fz = vertical (z) component of force produced by foot on the pedal

$$\theta\text{pedal} = \tan^{(}-1)((PHEX - PTOX)/(PHEZ - PTOZ)) - 0.9$$

Resultant Fx = [Fz sin(θpedal)] + [Fx cos(θpedal)]

Resultant Fz = [Fz cos(θpedal)] + [Fx sin(θpedal)]

A.4.2 Crank Torque

crank = crank torque

Fz = vertical (z) component of force produced by foot on the pedal

Fx = horizontal (x) component of force produced by foot on the pedal

θcrank = crank angle (degree)

Crank length = 0.17m

crank = [(-Fz cos(θcrank)) + (Fx sin(θcrank))] * 0.17

A.4.3 Effective force

crank = crank torque

Crank length = 0.17m

Feffective = crank 0.17

A.4.4 Crank Offset

SIMPLE CALCULATIONS:

θcrank difference = angle between primary and secondary cranks

θcrank offset = crank offset = deviation from 180 degree θcrank difference (perfect pedaling)

θcrank offset = θcrank difference 180

DETAILED CALCULATIONS FOR CODING PURPOSES:

θcrank primary = primary crank angle (L crank); crank offset is calculated with respect to the primary crank in the forward direction

θcrank secondary = secondary crank angle (R crank)

θcrank difference = angle between primary and secondary cranks

θcrank offset = crank offset = deviation from 180 degree θcrank difference (perfect pedaling)

θcrank difference = (360 - θcrank secondary) + θcrank primary

if θcrank difference $>$ 360

θcrank offset = θcrank difference 540

else

θcrank offset = θcrank difference 180

A.4.5 Angular velocity

ωpedal = angular velocity of pedal

C = cadence

ωpedal = C(revolutions/minute(1 minute)/(60 seconds) 2)

A.4.6 Power (watts)

P = power (watts)

τcrank = crank torque

pedal = angular velocity of pedal

$$P = \tau \text{crank} \ \ \omega \text{pedal}$$

References

Abelew, T.A., Miller, M.D., Cope, T.C., Nichols, T.R., 2000. Local loss of proprioception results in disruption of interjoint coordination during locomotion in the cat. J Neurophysiol 84, 2709-2714.

Adamczyk, P.G., Kuo, A.D., 2014. Mechanisms of gait asymmetry due to push-off deficiency in unilateral amputees. IEEE transactions on neural systems and rehabilitation engineering : a publication of the IEEE Engineering in Medicine and Biology Society.

Alexander, R.M.N., 1977. Mechanics and scaling of terrestrial locomotion, in: Pedley, T.J. (Ed.), Scale Effects in Animal Locomotion. Academic Press, New York, NY, pp. 93-110.

Alibiglou, L., Brown, D.A., 2011. Relative temporal leading or following position of the contralateral limb generates different aftereffects in muscle phasing following adaptation training post-stroke. Exp Brain Res 211, 37-50.

Alibiglou, L., Lopez-Ortiz, C., Walter, C.B., Brown, D.A., 2009. Bilateral limb phase relationship and its potential to alter muscle activity phasing during locomotion. J Neurophysiol 102, 2856-2865.

Anderson, F.C., Pandy, M.G., 2003. Individual muscle contributions to support in normal walking. Gait & Posture 17, 159-169.

Andersson, O., Forssberg, H., Grillner, S., Lindquist, M., 1978. Phasic gain control of the transmission in cutaneous reflex pathways to motoneurones during 'fictive' locomotion. Brain research 149, 503-507.

Aoi, S., Egi, Y., Sugimoto, R., Yamashita, T., Fujiki, S., Tsuchiya, K., 2012. Functional Roles of Phase Resetting in the Gait Transition of a Biped Robot From Quadrupedal to Bipedal Locomotion. Ieee T Robot 28, 1244-1259.

Arnold, E.M., Hamner, S.R., Seth, A., Millard, M., Delp, S.L., 2013. How muscle fiber lengths and velocities affect muscle force generation as humans walk and run at different speeds. J Exp Biol 216, 2150-2160.

Baron, G.C., Irving, G.A., 2002. Effects of tourniquet ischemia on current perception thresholds in healthy volunteers. Pain practice : the official journal of World Institute of Pain 2, 129-133.

Bartlett, J.L., Kram, R., 2008. Changing the demand on specific muscle groups affects the walk-run transition speed. J Exp Biol 211, 1281-1288.

Bateni, H., Olney, S.J., 2002. Kinematic and kinetic variations of below-knee amputee gait. Journal of Prosthetics and Orthotics 12, 7.

Berger, W., Dietz, V., Quintern, J., 1984. Corrective reactions to stumbling in man: neuronal co-ordination of bilateral leg muscle activity during gait. The Journal of physiology 357, 109-125.

Bickley, L.S., 2009. Bates Guide to Physical Examination and History Taking

10th ed. Lippincott-Raven Publishers.

Black, K.J., Bevan, C.A., Murphy, N.G., Howard, J.J., 2013. Nerve blocks for initial pain management of femoral fractures in children. The Cochrane database of systematic reviews 12, CD009587.

Blickhan, R., 1989. The spring-mass model for running and hopping. J Biomech 22, 1217-1227.

Brasil-Neto, J.P., Cohen, L.G., Pascual-Leone, A., Jabir, F.K., Wall, R.T., Hallett, M., 1992. Rapid reversible modulation of human motor outputs after transient deafferentation of the forearm: a study with transcranial magnetic stimulation. Neurology 42, 1302-1306.

Brasil-Neto, J.P., Valls-Sole, J., Pascual-Leone, A., Cammarota, A., Amassian, V.E., Cracco, R., Maccabee, P., Cracco, J., Hallett, M., Cohen, L.G., 1993. Rapid modulation of human cortical motor outputs following ischaemic nerve block. Brain : a journal of neurology 116 (Pt 3), 511-525.

Broker, J.P., Gregor, R.J., 1990. A dual piezoelectric element force pedal for kinetic analysis of cycling. Int J Sport Biomech 6, 10.

Brown, M.B., Millard-Stafford, M.L., Allison, A.R., 2009. Running-specific prostheses permit energy cost similar to nonamputees. Med Sci Sports Exerc 41, 1080-1087.

Burden, A., 2010. How should we normalize electromyograms obtained from

healthy participants? What we have learned from over 25 years of research. Journal of electromyography and kinesiology : official journal of the International Society of Electrophysiological Kinesiology 20, 1023-1035.

Caldwell, G.E., Li, L., 2000. How strongly is muscle activity associated with joint moments? Motor control 4, 53-59; discussion 97-116.

Cappellini, G., Ivanenko, Y.P., Poppele, R.E., Lacquaniti, F., 2006. Motor patterns in human walking and running. J Neurophysiol 95, 3426-3437.

Cavagna, G.A., Heglund, N.C., Taylor, C.R., 1977. Mechanical work in terrestrial locomotion: two basic mechanisms for minimizing energy expenditure. The American journal of physiology 233, R243-261.

Choi, J.T., Bastian, A.J., 2007. Adaptation reveals independent control networks for human walking. Nat Neurosci 10, 1055-1062.

Christensen, M.S., Lundbye-Jensen, J., Geertsen, S.S., Petersen, T.H., Paulson, O.B., Nielsen, J.B., 2007. Premotor cortex modulates somatosensory cortex during voluntary movements without proprioceptive feedback. Nat Neurosci 10, 417-419.

Collins, J.J., 2003. The handbook of brain theory and neural networks, 2nd ed. The MIT Press, Cambridge, MA.

Cordo P., Gurfinkel V.S., Bevan L., Kerr G.K., 1995. Proprioceptive consequences of tendon vibration during movement. J Neurophysiol. 74, 1675-1688.

Cronin, N.J., Ishikawa, M., Grey, M.J., af Klint, R., Komi, P.V., Avela, J., Sinkjaer, T., Voigt, M., 2009. Mechanical and neural stretch responses of the human soleus muscle at different walking speeds. The Journal of Physiology 587, 3375-3382.

Delcomyn, F., 1980. Neural basis of rhythmic behavior in animals. Science 210, 492-498.

Dickey, J.P., Winter, D.A., 1992. Adaptations in gait resulting from unilateral ischaemic block of the leg. Clinical biomechanics 7, 215-225.

Diedrich, F.J., Warren, W.H., 1995. Why change gaits - Dynamics of the walk run transition. J Exp Psychol Human 21, 183-202.

Diedrich, F.J., Warren, W.H., 1998. The dynamics of gait transitions: Effects of grade and load. Journal of Motor Behavior 30, 60-78.

Dietz, V., Harkema, S.J., 2004. Locomotor activity in spinal cord-injured persons. J Appl Physiol (1985) 96, 1954-1960.

Dietz, V., Muller, R., Colombo, G., 2002. Locomotor activity in spinal man: significance of afferent input from joint and load receptors. Brain : a journal of neurology 125, 2626-2634.

Dietz, V., Schmidtbleicher, D., Noth, J., 1979. Neuronal mechanisms of human locomotion. J Neurophysiol 42, 1212-1222.

Duysens, J., Pearson, K.G., 1980. Inhibition of flexor burst generation by loading

ankle extensor muscles in walking cats. Brain research 187, 321-332.

Duysens, J., Tax, A.A., Trippel, M., Dietz, V., 1993. Increased amplitude of cutaneous reflexes during human running as compared to standing. Brain research 613, 230-238.

Eccles, J.C., Schmidt, R.F., Willis, W.D., 1962. Presynaptic inhibition of the spinal monosynaptic reflex pathway. The Journal of physiology 161, 282-297.

Eidelberg, E., Story, J.L., Meyer, B.L., Nystel, J., 1980. Stepping by chronic spinal cats. Exp Brain Res 40, 241-246.

Falls, H.B., Humphrey, L.D., 1976. Energy cost of running and walking in young women. Medicine and science in sports 8, 9-13.

Farley, C.T., Taylor, C.R., 1991. A mechanical trigger for the trot-gallop transition in horses. Science 253, 306-308.

Farris, D.J., Sawicki, G.S., 2012a. Human medial gastrocnemius force-velocity behavior shifts with locomotion speed and gait. Proceedings of the National Academy of Sciences of the United States of America 109, 977-982.

Farris, D.J., Sawicki, G.S., 2012b. The mechanics and energetics of human walking and running: a joint level perspective. J R Soc Interface 9, 110-118.

Fey, N.P., Klute, G.K., Neptune, R.R., 2013. Altering prosthetic foot stiffness influences foot and muscle function during below-knee amputee walking: A modeling

and simulation analysis. J Biomech 46, 637-644.

Fey, N.P., Silverman, A.K., Neptune, R.R., 2010. The influence of increasing steady-state walking speed on muscle activity in below-knee amputees. J Electromyogr Kines 20, 155-161.

Gailey, R.S., Wenger, M.A., Raya, M., Kirk, N., Erbs, K., Spyropoulos, P., Nash, M.S., 1994. Energy-Expenditure of Trans-Tibial Amputees during Ambulation at Self-Selected Pace. Prosthetics and Orthotics International 18, 84-91.

Ganley, K.J., Stock, A., Herman, R.M., Santello, M., Willis, W.T., 2011. Fuel oxidation at the walk-to-run-transition in humans. Metabolism: clinical and experimental 60, 609-616.

Garcia, M., Chatterjee, A., Ruina, A., Coleman, M., 1998. The simplest walking model: stability, complexity, and scaling. Journal of biomechanical engineering 120, 281-288.

Gatesy, S.M., Biewener, A.A., 1991. Bipedal Locomotion - Effects of Speed, Size and Limb Posture in Birds and Humans. J Zool 224, 127-147.

Gauthier, L., Rossignol, S., 1981. Contralateral hindlimb responses to cutaneous stimulation during locomotion in high decerebrate cats. Brain research 207, 303-320.

Geisser, S., Greenhouse, S.W., 1959. On methods in the analysis of profile data. Psychoometrika 24, 10.

Genin, J.J., Bastien, G.J., Franck, B., Detrembleur, C., Willems, P.A., 2008. Effect of speed on the energy cost of walking in unilateral traumatic lower limb amputees. Eur J Appl Physiol 103, 655-663.

Gillies, J.D., Lance, J.W., Neilson, P.D., Tassinari, C.A., 1969. Presynaptic inhibition of the monosynaptic reflex by vibration. The Journal of Physiology 205, 329-339.

Giuliani, C.A., Smith, J.L., 1987. Stepping behaviors in chronic spinal cats with one hindlimb deafferented. J Neurosci 7, 2537-2546.

Gregor, R.J., Smith, D.W., Prilutsky, B.I., 2006. Mechanics of slope walking in the cat: quantification of muscle load, length change, and ankle extensor EMG patterns. J Neurophysiol 95, 1397-1409.

Grillner, S., Rossignol, S., 1978. On the initiation of the swing phase of locomotion in chronic spinal cats. Brain research 146, 269-277.

Grillner, S., Zangger, P., 1979. On the central generation of locomotion in the low spinal cat. Exp Brain Res 34, 241-261.

Grillner, S., Zangger, P., 1984. The effect of dorsal root transection on the efferent motor pattern in the cat's hindlimb during locomotion. Acta Physiol Scand 120, 393-405.

Grumillier, C., Martinet, N., Paysant, J., Andre, J.M., Beyaert, C., 2008. Compensatory mechanism involving the hip joint of the intact limb during gait in unilateral trans-tibial amputees. J Biomech 41, 2926-2931.

Hagbarth, K.E., Wallin, G., Lofstedt, L., 1973. Muscle spindle responses to stretch in normal and spastic subjects. Scandinavian journal of rehabilitation medicine 5, 156-159.

Hagio, S., Fukuda, M., Kouzaki, M., 2015. Identification of muscle synergies associated with gait transition in humans. Frontiers in human neuroscience 9, 48.

Haridas, C., Zehr, E.P., 2003. Coordinated interlimb compensatory responses to electrical stimulation of cutaneous nerves in the hand and foot during walking. J Neurophysiol 90, 2850-2861.

Harischandra, N., Knuesel, J., Kozlov, A., Bicanski, A., Cabelguen, J.M., Ijspeert, A., Ekeberg, O., 2011. Sensory feedback plays a significant role in generating walking gait and in gait transition in salamanders: a simulation study. Frontiers in neurorobotics 5, 3.

Hassid, E., Rose, D., Commisarow, J., Guttry, M., Dobkin, B.H., 1997. Improved gait symmetry in hemiparetic stroke patients induced during body weight-supported treadmill stepping. J Neurol Rehabil 11, 21-26.

Hayes, H.B., Chang, Y.H., Hochman, S., 2012. Stance-phase force on the opposite limb dictates swing-phase afferent presynaptic inhibition during locomotion. J Neurophysiol 107, 3168-3180.

Herr, H.M., Grabowski, A.M., 2012. Bionic ankle-foot prosthesis normalizes walking gait for persons with leg amputation. P Roy Soc B-Biol Sci 279, 457-464.

Hesse, S., Herrmann, C., Bardeleben, A., Holzgraefe, M., Werner, C., Wingendorf, L., Kirker, S.G.B., 2013. A new orthosis for subluxed, flaccid shoulder after stroke facilitates gait symmetry: A preliminary study. J Rehabil Med 45, 623-629.

Hochman, S., Hayes, H.B., Speigel, I., Chang, Y.H., 2013. Force-sensitive afferents recruited during stance encode sensory depression in the contralateral swinging limb during locomotion. Ann Ny Acad Sci 1279, 103-113.

Hohne, A., Ali, S., Stark, C., Bruggemann, G.P., 2012. Reduced plantar cutaneous sensation modifies gait dynamics, lower-limb kinematics and muscle activity during walking. Eur J Appl Physiol 112, 3829-3838.

Holm, S., 1979. A simple sequentially rejective multiple test procedure. Scandanavian Journal of Statistics 6, 5.

Hoogkamer, W., Massaad, F., Jansen, K., Bruijn, S.M., Duysens, J., 2012. Selective bilateral activation of leg muscles after cutaneous nerve stimulation during backward walking. J Neurophysiol 108, 1933-1941.

Houdijk, H., Pollmann, E., Groenewold, M., Wiggerts, H., Polomski, W., 2009. The energy cost for the step-to-step transition in amputee walking. Gait & Posture 30, 35-40.

Hoyt, D.F., Taylor, C.R., 1981. Gait and the energetics of locomotion in horses. Nature 292, 2.

Hreljac, A., 1993a. Determinants of the Gait Transition Speed during Human Locomotion - Kinetic Factors. Gait & Posture 1, 217-223.

Hreljac, A., 1993b. Preferred and Energetically Optimal Gait Transition Speeds in Human Locomotion. Med Sci Sport Exer 25, 1158-1162.

Hreljac, A., 1995. Determinants of the Gait Transition Speed during Human Locomotion - Kinematic Factors. J Biomech 28, 669-677.

Hreljac, A., Arata, A., Ferber, R., Mercer, J.A., Row, B.S., 2001. An electromyographical analysis of the role of dorsiflexors on the gait transition during human locomotion. Journal of Applied Biomechanics 17, 287-296.

Hreljac, A., Limamura, R.T., Escamilla, R.F., Edwards, W.B., MacLeod, T., 2008. The relationship between joint kinetic factors and the walk-run gait transition speed during human locomotion. Journal of Applied Biomechanics 24, 149-157.

Hreljac, A., Parker, D., Quintana, R., Abdala, E., Patterson, K., SIson, M., 2002. Physical Education and Sport. Energetics and perceived exertion of low speed running and high speed walking 1, 27.

Huang, Y., Wang, Q., 2012. Gait selection and transition of passivity-based bipeds with adaptable ankle stiffness. International Journal of Advanced Robotic Systems 9, 1.

Hubel, T.Y., Usherwood, J.R., 2013. Vaulting mechanics successfully predict decrease in walk-run transition speed with incline. Biol Lett 9, 20121121.

Ishikawa, M., Komi, P.V., Grey, M.J., Lepola, V., Bruggemann, G.P., 2005. Muscle-tendon interaction and elastic energy usage in human walking. J Appl Physiol (1985) 99, 603-608.

Ivanenko, Y.P., Cappellini, G., Poppele, R.E., Lacquaniti, F., 2008. Spatiotemporal organization of alpha-motoneuron activity in the human spinal cord during different gaits and gait transitions. The European journal of neuroscience 27, 3351-3368.

Jeng, C.L., Torrillo, T.M., Rosenblatt, M.A., 2010. Complications of peripheral nerve blocks. British journal of anaesthesia 105 Suppl 1, i97-107.

Kepple, T.M., Siegel, K.L., Stanhope, S.J., 1997. Relative contributions of the lower extremity joint moments to forward progression and support during gait. Gait & Posture 6, 8.

Kopka, L., Serpell, M.G., 2005. Distal nerve blocks of the lower limb. Continuing Education in Anaesthesia, Critical Care & Pain 5, 5.

Kram, R., Domingo, A., Ferris, D.P., 1997. Effect of reduced gravity on the preferred walk-run transition speed. J Exp Biol 200, 821-826.

Kram, R., Griffin, T.M., Donelan, J.M., Chang, Y.H., 1998. Force treadmill for measuring vertical and horizontal ground reaction forces. J Appl Physiol 85, 764-769.

Kuo, A.D., 2002. Energetics of actively powered locomotion using the simplest walking model. J Biomech Eng-T Asme 124, 113-120.

Labini, F.S., Ivanenko, Y.P., Cappellini, G., Gravano, S., Lacquaniti, F., 2011. Smooth changes in the EMG patterns during gait transitions under body weight unloading. J Neurophysiol 106, 1525-1536.

Lai, A., Lichtwark, G.A., Schache, A.G., Lin, Y.C., Brown, N.A., Pandy, M.G., 2015. In vivo behavior of the human soleus muscle with increasing walking and running speeds. J Appl Physiol (1985) 118, 1266-1275.

Lajoie, Y., Teasdale, N., Cole, J.D., Burnett, M., Bard, C., Fleury, M., Forget, R., Paillard, J., Lamarre, Y., 1996. Gait of a deafferented subject without large myelinated sensory fibers below the neck. Neurology 47, 6.

Laszlo, J.I., 1967. Training of fast tapping with reduction of kinaesthetic, tactile, visual and auditory sensations. The Quarterly journal of experimental psychology 19, 344-349.

Leukel, C., Lundbye-Jensen, J., Gruber, M., Zuur, A.T., Gollhofer, A., Taube, W., 2009. Short-term pressure induced suppression of the short-latency response: a new methodology for investigating stretch reflexes. J Appl Physiol 107, 1051-1058.

Li, L., 2000. Stability landscapes of walking and running near gait transition speed. Journal of Applied Biomechanics 16, 428-435.

Li, L., Ogden, L.L., 2012. Muscular activity characteristics associated with preparation for gait transition. J Sport Health Sci 1, 27-35.

Lundberg A., Phillips, C.G., 1973. T. Graham Brown's film on locomotion in the decerebrate cat. J Physiol. 231 90P-91P.

Maas, H., Gregor, R.J., Hodson-Tole, E.F., Farrell, B.J., Prilutsky, B.I., 2009. Distinct muscle fascicle length changes in feline medial gastrocnemius and soleus muscles during slope walking. J Appl Physiol 106, 1169-1180.

MacKay-Lyons, M., 2002. Central pattern generation of locomotion: a review of the evidence. Phys Ther 82, 69-83.

MacLeod, T.D., Hreljac, A., Imamura, R., 2014. Changes in the preferred transition speed with added mass to the foot. J Appl Biomech 30, 95-103.

Malcolm, P., Fiers, P., Segers, V., Van Caekenberghe, I., Lenoir, M., De Clercq, D., 2009a. Experimental study on the role of the ankle push off in the walk-to-run transition by means of a powered ankle-foot-exoskeleton. Gait & Posture 30, 322-327.

Malcolm, P., Segers, V., Van Caekenberghe, I., De Clercq, D., 2009b. Experimental study of the influence of the m. tibialis anterior on the walk-to-run transition by means of a powered ankle-foot exoskeleton. Gait & Posture 29, 6-10.

Margaria, R., 1938. Sulla fisiologia e specialmente sul consumo energetico della marcia e della corsa a varie velocita ed inclinazioni del terreno. Atti Accad. Naz. Lincei Memorie/ Biomechanics and Energetics of Muscular Exercise (1976), pp. 6975., 9.

Mattes, S.J., Martin, P.E., Royer, T.D., 2000. Walking symmetry and energy

cost in persons with unilateral transtibial amputations: matching prosthetic and intact limb inertial properties. Arch Phys Med Rehabil 81, 561-568. Mauritz, K.H., 2002. Gait training in hemiplegia. Eur J Neurol 9, 23-29.

Mazzaro, N., Grey, M.J., Sinkjaer, T., 2005a. Contribution of afferent feedback to the soleus muscle activity during human locomotion. J Neurophysiol 93, 167-177.

Mazzaro, N., Grey, M.J., Sinkjaer, T., Andersen, J.B., Pareyson, D., Schieppati, M., 2005b. Lack of on-going adaptations in the soleus muscle activity during walking in patients affected by large-fiber neuropathy. J Neurophysiol 93, 3075-3085.

McGeer, T., 1990a. Passive bipedal running. Proceedings of the Royal Society of London. Series B, Biological sciences 240, 107-134.

McGeer, T., 1990b. Passive dynamic walking. The International Journal of Robotics Research 9, 62.

McNulty, P.A., Macefield, V.G., Taylor, J.L., Hallett, M., 2002. Cortically evoked neural volleys to the human hand are increased during ischaemic block of the forearm. The Journal of physiology 538, 279-288.

Mercier, J., Legallais, D., Durand, M., Goudal, C., Micallef, J.P., Prefaut, C., 1994. Energy-Expenditure and Cardiorespiratory Responses at the Transition between Walking and Running. Eur J Appl Physiol O 69, 525-529.

Minetti, A.E., Ardigo, L.P., Saibene, F., 1994. The Transition between Walking and Running in Humans - Metabolic and Mechanical Aspects at Different Gradients.

Acta Physiol Scand 150, 315-323.

Mitka, M., 2008. Advocates seek better insurance coverage for amputees needing limb prostheses. Jama 299, 2138-2140.

Mochon, S., Mcmahon, T.A., 1980. Ballistic walking. J Biomech 13, 49-57.

Neptune, R.R., Kautz, S.A., Zajac, F.E., 2001. Contributions of the individual ankle plantarflexors to support, forward progression and swing initiation during walking. J Biomech 34, 1387-1398.

Neptune, R.R., Sasaki, K., 2005. Ankle plantarflexor force production is an important determinant of the preferred walk-to-run transition speed. J Exp Biol 208, 799-808.

Neptune, R.R., Zajac, F.E., Kautz, S.A., 2004. Muscle mechanical work requirements during normal walking: the energetic cost of raising the body's center-of-mass is significant. J Biomech 37, 817-825.

Netter, F.H., Craig, J.A., Perkins, J., 2002. Atlas of Neuroanatomy and Neurophysiology Icon Custom Communications, U.S.A.

Noble, B.J., Metz, K.F., Pandolf, K.B., Bell, C.W., Cafarelli, E., Sime, W.E., 1973. Perceived exertion during walking and running. II. Medicine and science in sports 5, 116-120.

Nolan, L., Wit, A., Dudzinski, K., Lees, A., Lake, M., Wychowanski, M., 2003.

Adjustments in gait symmetry with walking speed in trans-femoral and trans-tibial amputees. Gait & Posture 17, 142-151.

Novacheck, T.F., 1998. The biomechanics of running. Gait Posture 7, 77-95.

Ogawa, T., Kawashima, N., Ogata, T., Nakazawa, K., 2014. Predictive control of ankle stiffness at heel contact is a key element of locomotor adaptation during split-belt treadmill walking in humans. J Neurophysiol 111, 722-732.

Orlovsky, G.N., Feldman, A.G., 1972. On the role of afferent signals in generation of stepping movements. Neurophysiology 4, 7.

Ortqvist, A., Grillner, L., Olofsson, I., Nordin, A., 1984. [Chlamydia infections in a clinic for adolescents in Stockholm]. Lakartidningen 81, 3929-3931.

Pearson, K.G., 2004. Generating the walking gait: role of sensory feedback. Progress in brain research 143, 123-129.

Pearson, K.G., Rossignol, S., 1991. Fictive motor patterns in chronic spinal cats. J Neurophysiol 66, 1874-1887.

Pires, N.J., Lay, B.S., Rubenson, J., 2014. Joint-level mechanics of the walk-to-run transition in humans. J Exp Biol 217, 3519-3527.

Powers, C.M., Rao, S., Perry, J., 1998. Knee kinetics in trans-tibial amputee gait. Gait & Posture 8, 1-7.

Prilutsky, B.I., Gregor, R.J., 2001. Swing- and support- related muscle activations differentially trigger human walk-run and run-walk transitions. The Journal of Experimental Biology, 2277-2287.

Prilutsky, B.I., Gregor, R.J., Ryan, M.M., 1998. Coordination of two-joint rectus femoris and hamstrings during the swing phase of human walking and running. Exp Brain Res 120, 479-486.

Raynor, A.J., Yi, C.J., Abernethy, B., Jong, Q.J., 2002. Are transitions in human gait determined by mechanical, kinetic or energetic factors? Hum Movement Sci 21, 785-805.

Roll J.P., Vedel J.P., Ribot E., 1989. Alteration of proprioceptive messages induced by tendon vibration in man: a microneurographic study. Exp Brain Res. 76,213-222.

Rotstein, A., Inbar, O., Berginsky, T., Meckel, Y., 2005. Preferred transition speed between walking and running: effects of training status. Med Sci Sports Exerc 37, 1864-1870.

Sabatier, M.J., Wedewer, W., Barton, B., Henderson, E., Murphy, J.T., Ou, K., 2015. Slope walking causes short-term changes in soleus H-reflex excitability. Physiological reports 3.

Sagawa, Y., Jr., Turcot, K., Armand, S., Thevenon, A., Vuillerme, N., Watelain, E., 2011. Biomechanics and physiological parameters during gait in lower-limb amputees: a systematic review. Gait Posture 33, 511-526.

Sanderson DJ, Martin PE. (1997) Lower extremity kinematic and kinetic adaptations in unilateral below-knee amputees during walking. Gait and Posture. 6:126-136.

Schieppati, M., 1987. The Hoffmann reflex: a means of assessing spinal reflex excitability and its descending control in man. Progress in neurobiology 28, 345-376.

Schlee, G., Milani, T.L., Sterzing, T., Oriwol, D., 2009. Short-time lower leg ischemia reduces plantar foot sensitivity. Neuroscience letters 462, 286-288.

Segers, V., Aerts, P., Lenoir, A., De Clercq, D., 2006. Spatiotemporal characteristics of the walk-to-run and run-to-walk transition when gradually changing speed. Gait & Posture 24, 247-254.

Segers, V., Aerts, P., Lenoir, M., De Clerq, D., 2007a. Dynamics of the body centre of mass during actual acceleration across transition speed. J Exp Biol 210, 578-585.

Segers, V., Lenoir, M., Aerts, P., De Clercq, D., 2007b. Influence of M. tibialis anterior fatigue on the walk-to-run and run-to-walk transition in non-steady state locomotion. Gait & Posture 25, 639-647.

Sentija, D., Rakovac, M., Babic, V., 2012. Anthropometric characteristics and gait transition speed in human locomotion. Hum Movement Sci 31, 672-682.

Shapiro, D.C., Zernicke, R.F., Gregor, R.J., 1981. Evidence for generalized motor programs using gait pattern analysis. J Mot Behav 13, 33-47.

Shiavi, R., Frigo, C., Pedotti, A., 1998. Electromyographic signals during gait: criteria for envelope filtering and number of strides. Medical & biological engineering & computing 36, 171-178.

Shik, M.L., Severin, F.V., Orlovskii, G.N., 1966. [Control of walking and running by means of electric stimulation of the midbrain]. Biofizika 11, 659-666.

Shik, M.L., Severin, F.V., Orlovsky, G.N., 1969. Control of walking and running by means of electrical stimulation of the mesencephalon. Electroencephalography and clinical neurophysiology 26, 549.

Silverman, A.K., Fey, N.P., Portillo, A., Walden, J.G., Bosker, G., Neptune, R.R., 2008. Compensatory mechanisms in below-knee amputee gait in response to increasing steady-state walking speeds. Gait & Posture 28, 602-609.

Silverman, A.K., Neptune, R.R., 2012. Muscle and prosthesis contributions to amputee walking mechanics: A modeling study. J Biomech 45, 2271-2278.

Sinclair, D.C., 1948. Observations on sensory paralysis produced by compression of a human limb. J Neurophysiol 11, 75-92.

Sinkjaer, T., Andersen, J.B., Ladouceur, M., Christensen, L.O., Nielsen, J.B., 2000. Major role for sensory feedback in soleus EMG activity in the stance phase of walking in man. The Journal of physiology 523 Pt 3, 817-827.

Sinkjaer, T., Andersen, J.B., Larsen, B., 1996. Soleus stretch reflex modulation

during gait in humans. J Neurophysiol 76, 1112-1120.

Snyder, R.D., Powers, C.M., Fontaine, C., Perry, J., 1995. The effect of five prosthetic feet on the gait and loading of the sound limb in dysvascular below-knee amputees. J Rehabil Res Dev 32, 309-315.

Steeves, J.D., Sholomenko, G.N., Webster, D.M., 1987. Stimulation of the pontomedullary reticular formation initiates locomotion in decerebrate birds. Brain research 401, 205-212.

Stevenson, A.J., Geertsen, S.S., Andersen, J.B., Sinkjaer, T., Nielsen, J.B., Mrachacz-Kersting, N., 2013. Interlimb communication to the knee flexors during walking in humans. The Journal of physiology 591, 4921-4935.

Takahashi, K.Z., Lewek, M.D., Sawicki, G.S., 2015. A neuromechanics-based powered ankle exoskeleton to assist walking post-stroke: a feasibility study. J Neuroeng Rehabil 12, 23.

Thorstensson, A., Roberthson, H., 1987. Adaptations to changing speed in human locomotion: speed of transition between walking and running. Acta Physiol Scand 131, 211-214.

Ting, L.H., 1997. Neural strategies for control of locomotion elucidated by novel pedaling paradigms. Stanford University.

Ting, L.H., Kautz, S.A., Brown, D.A., Zajac, F.E., 2000. Contralateral movement and extensor force generation alter flexion phase muscle coordination in pedaling. J

Neurophysiol 83, 3351-3365.

Ting, L.H., Raasch, C.C., Brown, D.A., Kautz, S.A., Zajac, F.E., 1998. Sensorimotor state of the contralateral leg affects ipsilateral muscle coordination of pedaling. J Neurophysiol 80, 1341-1351.

Torburn, L., Perry, J., Ayyappa, E., Shanfield, S.L., 1990. Below-knee amputee gait with dynamic elastic response prosthetic feet: a pilot study. J Rehabil Res Dev 27, 369-384.

Turvey, M.T., Holt, K.G., LaFiandra, M.E., Fonseca, S.T., 1999. Can the transitions to and from running and the metabolic cost of running be determined from the kinetic energy of running? Journal of Motor Behavior 31, 265-278.

Vallence, A.M., Hammond, G.R., Reilly, K.T., 2012. Increase in flexor but not extensor corticospinal motor outputs following ischemic nerve block. J Neurophysiol 107, 3417-3427.

Van Caekenberghe, I., Segers, V., De Smet, K., Aerts, P., De Clercq, D., 2010. Influence of treadmill acceleration on actual walk-to-run transition. Gait & Posture 31, 52-56.

van der Krogt, M.M., Doorenbosch, C.A., Becher, J.G., Harlaar, J., 2009. Walking speed modifies spasticity effects in gastrocnemius and soleus in cerebral palsy gait. Clinical biomechanics 24, 422-428.

Voller, B., Floel, A., Werhahn, K.J., Ravindran, S., Wu, C.W., Cohen, L.G., 2006.

Contralateral hand anesthesia transiently improves poststroke sensory deficits. Annals of neurology 59, 385-388.

Waters, R.L., Perry, J., Antonelli, D., Hislop, H., 1976. Energy cost of walking of amputees: the influence of level of amputation. Journal of Bone and Joint Surgery 58, 42-46.

Weiss, P.L., Kearney, R.E., Hunter, I.W., 1986. Position dependence of ankle joint dynamics–I. Passive mechanics. J Biomech 19, 727-735.

Winter, D.A., 2005. Biomechanics and motor control of human movement, 3rd ed. John Wiley & Sons, Hoboken, New Jersey.

Winter, D.A., Sienko, S.E., 1988. Biomechanics of below-knee amputee gait., J Biomech, pp. 361-367.

Yakovenko, S., McCrea, D.A., Stecina, K., Prochazka, A., 2005. Control of locomotor cycle durations. J Neurophysiol 94, 1057-1065.

Yang, J.F., Stein, R.B., 1990. Phase-dependent reflex reversal in human leg muscles during walking. J Neurophysiol 63, 1109-1117.

Zajac, F.E., Neptune, R.R., Kautz, S.A., 2002. Biomechanics and muscle coordination of human walking - Part I: Introduction to concepts, power transfer, dynamics and simulations. Gait & Posture 16, 215-232.

Zajac, F.E., Neptune, R.R., Kautz, S.A., 2003. Biomechanics and muscle coordination of human walking Part II: Lessons from dynamical simulations and clinical implications. Gait & Posture 17, 1-17.

Zakutansky, D.W., Kitano, K., Wallace, J.P., Koceja, D.M., 2005. H-reflex and motor responses to acute ischemia in apparently healthy individuals. Journal of clinical neurophysiology : official publication of the American Electroencephalographic Society 22, 210-215.

Zehr, E.P., Collins, D.F., Chua, R., 2001a. Human interlimb reflexes evoked by electrical stimulation of cutaneous nerves innervating the hand and foot. Exp Brain Res 140, 495-504.

Zehr, E.P., Hesketh, K.L., Chua, R., 2001b. Differential regulation of cutaneous and H-reflexes during leg cycling in humans. J Neurophysiol 85, 1178-1184.

Zehr, E.P., Komiyama, T., Stein, R.B., 1997. Cutaneous reflexes during human gait: electromyographic and kinematic responses to electrical stimulation. J Neurophysiol 77, 3311-3325.

Ziemann, U., Corwell, B., Cohen, L.G., 1998. Modulation of plasticity in human motor cortex after forearm ischemic nerve block. J Neurosci 18, 1115-1123.

Zmitrewicz, R.J., Neptune, R.R., Sasaki, K., 2007. Mechanical energetic contributions from individual muscles and elastic prosthetic feet during symmetric unilateral transtibial amputee walking: a theoretical study. J Biomech 40, 1824-1831.

VITA

Tracy Lynn Norman was born in Jacksonville, FL and grew up outside Gettysburg, PA. She attended Penn State University where she earned her undergraduate degree in Kinesiology. Upon graduation she joined Teach for America, and committed two years to teaching 7th and 8th grade science in a Title 1 school in Charlotte, NC. She is very excited to complete her PhD so she can get a dog.